Exact solutions of a Dirac equation with a varying CP-violating mass profile and coherent quasiparticle approximation

Olli Koskivaara

UNIVERSITY OF JYVÄSKYLÄ
DEPARTMENT OF PHYSICS

Master's thesis
Supervisor: Kimmo Kainulainen
November 30, 2015

Preface

This thesis was written during the year 2015 at the Department of Physics at the University of Jyväskylä. I would like to express my utmost gratitude to my supervisor Professor Kimmo Kainulainen, who guided me through the subtle path laid out by this intriguing subject, and provided me with my first glimpses of research in theoretical physics.

I would also like to thank my fellow students for the countless number of versatile conversations on physics and beyond.

Finally, I wish to thank my family and Ida-Maria for their enduring and invaluable support during the entire time of my studies in physics.

Abstract

In this master's thesis the phase space structure of a Wightman function is studied for a temporally varying background. First we introduce coherent quasiparticle approximation (cQPA), an approximation scheme in finite temperature field theory that enables studying non-equilibrium phenomena. Using cQPA we show that in non-translation invariant systems the phase space of the Wightman function has in general structure beyond the traditional mass-shell particle- and antiparticle-solutions. This novel structure, describing nonlocal quantum coherence between particles, is found to be living on a zero-momentum $k_0 = 0$ -shell.

With the knowledge of these coherence solutions in hand, we take on a problem in which such quantum coherence effects should be prominent. The problem, a Dirac equation with a complex and time-dependent mass profile, is manifestly non-translation invariant due to the temporal variance of the mass, and is in addition motivated by electroweak baryogenesis.

The Dirac equation is solved analytically, with no reference to the cQPA-formalism. The exact mode function solutions of the problem are then used to study the phase space of the system. We use the exact solutions to construct the Wightman function of the system, and Wigner transform it to get a picture of the phase space structure. This structure is found to match well with the one predicted by cQPA, containing particles, antiparticles and coherence. It is also noted that for weakly interacting systems the phase space near the mass wall may contain also coherence structures corresponding to correlations coming from different sides of the wall. These correlations are seen to be largely suppressed by interactions, and their existence is therefore limited to the vicinity of the wall. Further away from the wall only the cQPA-structure exists.

Tiivistelmä

Tässä pro gradu -tutkielmassa tarkastellaan aikariippuvan taustan omaavan Wightmanin funktion faasiavaruuden rakennetta. Aluksi esittelemme koherentin kvasihiukkasapproksimaation (cQPA), joka on epätasapainoilmiöiden tutkimiseen soveltuva lähestymistapa äärellisen lämpötilan kenttäteoriaan. Osoitamme cQPA:n avulla, että jos tarkastelemme systeemiä, joka ei ole translaatioinvariantti, sen faasiavaruudessa on perinteisten massakuoria vastaavien hiukkas- ja antihiukkasratkaisujen lisäksi uudenlaista rakennetta. Tämä hiukkasten välistä epälokaalia kvanttikoherenssia kuvaava rakenne ilmenee nollaliikemääräkuorella $k_0 = 0$.

Seuraavaksi otamme tarkasteltavaksemme ongelman, jossa koherenssirakenteen tulisi näkyä. Valitsemamme systeemi, Diracin yhtälö kompleksisella aikariippuvalla massalla, ei ole translaatioinvariantti aikariippuvan massan vuoksi, minkä takia faasiavaruuden rakenne voi olla epätriviaali. Motivaationa ongelmalle on sähköheikko baryogeneesi.

Ratkaisemme kyseisen Diracin yhtälön analyyttisesti ilman cQPA-tekniikoita. Tuloksena saatavia eksakteja moodifunktioita käytämme systeemin faasiavaruuden tutkimiseen. Konstruoimme eksakteista ratkaisuista systeemin Wightmanin funktion, ja Wigner-muuntamalla sen pääsemme käsiksi faasiavaruuden rakenteeseen. Rakenne vastaa hyvin cQPA:n ennustuksia, sisältäen kuorirakennetta vastaten hiukkasia, antihiukkasia ja niiden välistä koherenssia. Lisäksi havaitsemme, että heikosti vuorovaikuttavien systeemien tapauksessa faasiavaruudessa voi olla massavallin lähellä koherenssirakenteita vastaten vallin eri puolilta tulevia korrelaatioita. Vuorovaikutukset heikentävät näitä pitkän matkan korrelaatioita voimakkaasti, ja rakennetta ilmeneekin vain massavallin läheisyydessä. Kauempana massamuutoksesta havaitaan vain cQPA-rakennetta.

Contents

1 Introduction **1**

2 Electroweak baryogenesis **4**

3 Coherent quasiparticle approximation (cQPA) **9**

3.1 Finite temperature field theory 9

3.1.1 Imaginary-time formalism 9

3.1.2 Real-time formalism 10

3.2 Schwinger–Keldysh formalism 10

3.3 Basics of cQPA 14

3.3.1 Generalities 14

3.3.2 Formalism 16

4 Dirac equation with a varying mass **25**

4.1 General case 25

4.2 Gauss' hypergeometric functions 31

4.3 Kink-wall 34

4.4 Normalization 38

4.5 Solutions 47

5 Phase space structure of the Wigner function **51**

5.1 Wightman function 51

5.2 Wigner function 53

5.2.1 Step-function correlator with a finite Fourier transform 53

5.2.2 Step-function correlator with a damped Fourier transform 57

5.2.3 Wigner function for the kink-potential 59

6 Conclusions **71**

Appendix A Conventions **76**

Appendix B Constant mass solutions **77**

1 Introduction

Modern particle physics studies the fundamental interactions and properties of the known subatomic particles. The most notable particle physics theory is the Standard Model, which very successfully describes a major part of observed particle phenomena. Despite its success, the Standard model also leaves phenomena unexplained, and theories reaching outside it and trying to fill its deficiencies are commonly called *beyond Standard Model theories*. Whether one consider the Standard model or one of its extensions, one is usually dealing with some kind of a *quantum field theory*.

Essentially quantum field theories are collections of calculational techniques that have turned out to be overwhelmingly suitable for describing the physics of fundamental particles. They can be also applied to many phenomena outside particle physics; for example certain condensed matter systems can be elegantly studied in a quantum field theoretical setting. Different situations require different techniques and correspondingly different quantum field theories. Most of these are however zero-temperature theories, i.e. the energy of the system being studied is assumed to be so high that the temperature of the surroundings can be neglected. When one is studying situations where the energy of the system is comparable to temperature, one needs techniques from *finite temperature field theory*.

Finite temperature field theory has also many different approaches to it but, regardless of the chosen method, calculations are fairly tedious. In order to be able to study sensible physical situations one has to, as in general in physics, choose a set of approximations and assumptions that simplify the problem while maintaining its important properties. A common assumption is that the system under consideration is translation invariant, i.e. its properties do not change if it is translated in space-time. This assumption is in general well justified, but it does not hold in situations where the system is out of thermal equilibrium.

The coherent quasiparticle approximation (cQPA) provides an approximation scheme in finite temperature field theory that does not assume the system to be nearly translation invariant. Abandoning this assumption gives rise to completely new solutions in the phase space of the system. The phase space of a system is the space where all possible states of the system reside. Usually in particle physics the phase space consists

of two kinds of solutions: particles and antiparticles. In addition to these usual solutions cQPA predicts the existence of solutions describing *nonlocal quantum coherence*. To be more precise, these novel solutions consist of quantum mechanical interaction between e.g. particles and antiparticles with the same helicity and opposite momenta.

The existence of these coherence-solutions is the principal motivation behind this thesis. The main goal is to find these solutions by using an approach different from cQPA. This is done by choosing a problem that is expected to exhibit the coherence-structure and by studying the problem with techniques outside cQPA.

The problem studied in this thesis is a fermionic particle with a mass that is complex and affected by the background. This kind of a system is definitely not translation invariant because of the altering mass. Such a situation is physically motivated by electroweak baryogenesis, which is a proposed mechanism trying to explain the matter-antimatter asymmetry of the universe. The mechanism includes particles acquiring their masses during a phase transition in the early universe, which gives rise to a system with an effectively space-time-dependent mass. The mass is also required to be complex, because this permits CP-violation, which is one of the vital ingredients for a successful baryogenesis.

Mathematically the aforementioned problem is expressed as a Dirac equation with a space-time-dependent mass. In this thesis such a Dirac equation is solved analytically for a certain mass profile. The so-obtained solutions are then used to construct an object, the so-called Wigner function, that carries information about the phase space structure of the system. The Wigner function is analyzed numerically to obtain illustrations of the possible phase space structures, and these results are compared to the predictions made by cQPA.

The structure of this thesis is as follows. Chapter 2 gives a short review of electroweak baryogenesis as a model for explaining the matter-antimatter asymmetry of the universe. Chapter 3 introduces finite temperature field theory and especially a certain approach to it called the Schwinger–Keldysh formalism. It also includes an introduction to coherent quasiparticle approximation, containing a derivation of the coherence-structure in a certain case. In Chapter 4 we lay aside cQPA and solve the Dirac equation for a complex time-dependent mass profile. These exact solutions are then used in Chapter 5 to construct the Wigner function and

to analyze the phase space structure of the system. Finally, Chapter 6 is devoted to conclusions, discussion and summary.

2 Electroweak baryogenesis

The Standard Model of particle physics very successfully describes the structure of the matter we are used to seeing in everyday life. Its particle content is also capable of dealing with not-so-familiar phenomena such as supernovae and superfluidity. One of the basic predictions of the Standard Model is the existence of antiparticles, which annihilate with particles into radiation or are correspondingly born from it as particle-antiparticle pairs. One especially speaks of *antimatter*, which consists of antibaryons as opposed to ordinary matter consisting of baryons. Yet all the matter we see around us seems to consist of, well, matter. Why do we not see clumps of antimatter around us?

The previous question can be easily extended outside Earth. A famous argument states that Moon does not consist of antimatter since Neil Armstrong did not annihilate when laying his foot on its surface. This naïve reasoning is supported by firm observational data: the observable universe consists almost entirely of ordinary matter instead of a more balanced mixture of antimatter and matter. The amount of baryonic matter is usually described by the *baryon-to-photon ratio* η, which is measured to be [1]

$$\eta = \frac{n_B}{n_\gamma} = (6.05 \pm 0.07) \times 10^{-10}.$$

This dominance of ordinary matter is intriguing, since all usual particle physics processes create (or destroy) an equal amount of baryons and antibaryons. Of course one could just argue that this was how things started in the first place: the universe was born with more matter than antimatter. This argument however meets a dead end in the light of inflation theory. According to inflation, the universe went through an epoch of exponential expansion right after the Big Bang. This expansion was so fierce, that any abundances and disproportions existing in the usual particle content before it would have been wiped out to nonexistent. Due to its many triumphs, the theory of inflation is well-established in the modern theory of cosmology, and hence the observed matter content cannot be taken as an initial condition.

We are then facing a fundamental question: where did all this matter come from? This question remains among the most important unsolved problems of modern physics. According to the above reasoning, there

has to exist a post-inflationary process that produces more baryons than antibaryons. This hypothetical process is called *baryogenesis*. Although we do not have a correct model for baryogenesis, we do know what it should look like. In his 1967 paper [2] the Russian physicist Andrei Sakharov outlined three necessary conditions that every model trying to explain the observed matter-antimatter asymmetry has to fulfil:

1. ***Baryon number violation.***
2. ***C- and CP-violation.***
3. ***Interactions out of thermal equilibrium.***

Condition 1 is obvious; in order to create a net baryon number out of nothing, there has to be a physical process in which baryon number is not conserved. The second condition deals with the symmetry operations C (charge-conjugation) and CP (charge-conjugation and parity). A system with an equal amount of particles and antiparticles is invariant under C- and CP-transformations, unlike a system with more baryons than antibaryons. Hence both C- and CP-symmetry have to violated during a baryogenesis process. However, CPT-symmetry (CP combined with time reversal T) is an exact symmetry of every relativistic quantum field theory. This implies that, even though C- and CP-symmetry may not be conserved, the masses of the produced particles and antiparticles have to match precisely. This brings us to Condition 3; in thermal equilibrium particles and antiparticles would have the same distribution functions, and therefore any excess of baryons would be compensated by processes decreasing the baryon number.

Remarkably, all the three Sakharov conditions are satisfied by the Standard Model. Even though the Standard Model Lagrangian density conserves baryon number at a classical level (and indeed all observed particle physics processes seem to conserve it too), there are anomalies rising from non-perturbative effects that allow it to be violated. The baryonic current can be shown to be non-vanishing as [3]

$$\partial_\mu J^\mu_B = \frac{n_g g^2}{32\pi^2} \epsilon^{\mu\nu\alpha\beta} W^a_{\mu\nu} W^a_{\alpha\beta},$$

where n_g is the number of generations, g the $SU(2)$ coupling and $W^a_{\mu\nu}$ the $SU(2)$ field strength. Therefore Condition 1 can indeed be met within the

Standard Model. Condition 2 is fulfilled due to the electroweak sector, where both C- and CP-symmetry are violated, as also experiments have verified. The third condition, out of equilibrium conditions, is offered by the expansion and cooling of the universe. A particularly interesting epoch where Condition 3 can be satisfied occurs when the universe had cooled down to approximately 100 GeV. This is when the universe went through the electroweak phase transition (EWPT), and particles acquired their masses. This situation will be described in more detail when we introduce electroweak baryogenesis.

Since the Standard Model indeed seems to lay down suitable conditions for production of matter-antimatter asymmetry, why is there need for new baryogenesis scenarios? Because the Sakharov conditions are *necessary*, but not *sufficient*. Even with the right ingredients, there is no guarantee that a matter-antimatter asymmetry will be produced. In addition, a successful baryogenesis has to produce the right number of baryons. This is exactly where the Standard Model baryogenesis falters; it fails to produce enough baryons. There is need for beyond-Standard-Model physics.

Numerous models have been proposed to solve the baryogenesis problem. *Leptogenesis* tries to tackle the problem by first creating a lepton-antilepton asymmetry, which could then be mediated by Standard Model processes into a baryon-antibaryon asymmetry. One is then led to search for mechanisms that would produce a lepton-antilepton asymmetry in the first place. The *Affleck–Dine Mechanism* is a baryogenesis model involving a scalar field with a non-zero baryon number. This mechanism is mostly interesting in supersymmetric settings. *GUT-scale baryogenesis* proposes that the baryon excess was created right after the Big Bang at Grand Unified Theory (GUT) temperatures $T \sim 10^{15}$ GeV. In a GUT-scenario baryon number violation is a built-in feature, since quarks and leptons are coupled by massive GUT-bosons. Models like this however suffer from the fact that they are practically impossible to test experimentally due to the enormous energies. The same is true with *Planck-scale baryogenesis* models, which indeed operate at the Planck scale $T \sim 10^{19}$ GeV. At those energies quantum gravity has to be taken into account, and the basic conservation laws for particle numbers do not hold anymore. In addition to being untestable, Planck- and GUT-scale baryogeneses are assumed to be pre-inflationary processes, and hence their contributions to baryon-antibaryon asymmetry would probably have been washed out during inflation.

By far the most popular model has been *electroweak baryogenesis* (EWBG). This model will lay down a motivation for the main topic of this thesis, and will therefore be now considered in more detail. As mentioned earlier, the Standard Model does contain processes which violate baryon number. One such process is mediated by a non-perturbative field configuration called *sphaleron*. The vacuum of the electroweak theory is infinitely degenerate, with the ground states separated by energy barriers. Sphalerons are field solutions living at the tops of these barriers, i.e. saddle points of the electroweak potential energy. Different ground states have in general different baryon numbers, and hence moving from one ground state to another could produce a baryon-antibaryon asymmetry. At low temperatures this transition would have to occur via quantum tunneling. This tunneling is however suppressed by a factor of the order

$$\mathrm{e}^{-8\pi^2/g^2} \sim 10^{-162},$$

where g is again the $SU(2)$ coupling. This tiny barrier penetration factor makes it impossible to obtain the baryon-antibaryon asymmetry of the universe from quantum tunnelings. At very high temperatures the situation changes. Instead of tunneling, the field can go from one ground state to another by surpassing the barrier with the help of thermal fluctuations. This *sphaleron process* could have produced baryon number violation in the hot early universe.

In order to create a net baryon excess, sphaleron processes themselves are not enough. At high temperatures they violate the baryon number constantly, and any net baryon excess would have been also wiped off. This is why the hypothetical electroweak baryogenesis takes place at the electroweak phase transition, which broke the electroweak symmetry. If this phase transition was strongly first order, the new phases with broken symmetry would have emerged and expanded as bubbles in the old symmetric phase. With time these bubbles would collide and amalgamate, eventually filling the whole space. During this process, particles in the plasma would collide and scatter with the bubble walls. These phase transition domain walls create out-of-equilibrium conditions together with C- and CP-violation, and therefore the Sakharov conditions are satisfied. The key to a baryon excess is that, while sphaleron processes still proceed without restraint in the symmetric phase, they are very rare in the broken phase. A net baryon number created at the bubble wall will not be wiped out in the broken phase, and therefore at the end of the phase transition a baryon-antibaryon asymmetry remains.

The popularity of EWBG arises from the fact that it can, unlike many of its cousin models, be tested with man-made particle accelerators. EWBG in the Standard Model has already been ruled out. The electroweak phase transition in the Standard Model is a smooth crossover [4] instead of being strongly first order, and hence all baryon-antibaryon asymmetry would have been washed out by sphalerons. EWBG still remains a plausible model for many theories reaching beyond the Standard Model.

The main topic of this thesis involves solving the equation of motion of a fermion with a time-dependent mass. Exactly his kind of a situation occurs in EWBG, as particles obtain their masses during the phase transition. In Chapter 4 the analysis is performed for a general complex mass (even though the mass profile corresponding to the bubble wall has to be specified), which is significant because CP-violation is directly related to the change in the real and imaginary parts of the mass during the bubble transition. The derived mode functions will give valuable information about the behaviour of the particle in the vicinity of the bubble wall. They will especially be used to investigate coherence phenomena near the domain wall. In the next chapter we will present another technique that is of great use in studying EWBG-scenarios.

3 Coherent quasiparticle approximation (cQPA)

3.1 Finite temperature field theory

Usually when referring to quantum field theory (QFT), one is considering calculations performed at zero temperature. In most cases these techniques work, since the energy scale of the system under consideration is often large compared to its temperature. There are however also situations in which the zero-temperature approximation is not valid, e.g. many phenomena of the early universe. In such situations one has to employ new techniques, and these techniques constitute what is commonly called *finite temperature field theory* or *thermal field theory* (TFT).

TFT has to for example take into account the fact that propagating particles interact with their surroundings, when the energy of the particle and the temperature of its surroundings are comparable. Particles are also often short-lived due to a large number of interactions, and hence the usual asymptotic in- and out-states familiar from zero-temperature QFT are ill-defined. This eventually leads one to consider temporal expectation values instead of transition amplitudes.

There are two main formulations of TFT: the real-time and the imaginary-time formalisms. We will now describe the main features of both of these briefly. These short reviews are based mainly on [5] and [6], which the reader is guided to consult for more detailed and thorough treatment of finite temperature field theory. Some ideas are taken from [7], which offers a modern and more mathematical exposition.

3.1.1 Imaginary-time formalism

As the name suggests, this formalism is based on performing calculations with the help of an imaginary time parameter. One starts by Wick-rotating the time parameter t as $t \to -\mathrm{i}\tau$, $\tau \in \mathbb{R}$.[1] Similarly in momentum space one replaces $k^0 \to -\mathrm{i}\tilde{k}^0$. As a result the notions of conventional quantum mechanics, probability amplitudes (with imaginary time arguments) can be written as path integrals. This further enables one to

[1] Note that this also corresponds to a change between the Minkowski and the Euclidean space: $t^2 - \vec{x}^2 \to -(\tau^2 + \vec{x}^2)$.

express (quantum) partition functions, describing the properties of systems at non-zero temperature, as path integrals too. The step to finite temperature field theory is then just a matter of defining a generating functional by adding a source to the partition function. This allows one to use the tools familiar from zero-temperature QFT, such as functional differentiation and diagrammatic techniques.

Even though introducing an imaginary time parameter might feel questionable and obscure, it is still just a certain parametrization. All real-time physical observables are in the end retained by an analytic continuation.

All in all, the imaginary-time formalism is the one most frequently used in TFT, and it is indeed a powerful toolbox able to deal with many kinds of phenomena. It however lacks the ability to cope with a certain situation that plays a crucial role in this thesis. When considering systems out of equilibrium, the partition function needed in the imaginary-time formalism cannot be generally constructed. Hence, there is a need for a theory capable of treating non-equilibrium phenomena.

3.1.2 Real-time formalism

One can also perform TFT calculations without expressing the results in terms of an imaginary time parameter. There are a couple of ways to do this. One way is to introduce a closed time path (CTP) in the complex plane and study Green's functions along it. In the next section we will consider a specific CTP formalism of TFT, which will hopefully clarify this method a bit and which will be essential in understanding the basics of cQPA.

Another way to avoid imaginary time is to use the so called thermo field dynamics. This method, which we will not consider here (see [7] for an introduction to the subject), is based on doubling the states in the Hilbert space of the system.

3.2 Schwinger–Keldysh formalism

The coherent quasiparticle approximation, the subject of the next chapter, is based on the *Schwinger–Keldysh formalism*, a certain variant of the

real-time formalism of TFT. The basics of this formalism were laid out by J. S. Schwinger [8] and L. V. Keldysh [9]. Instead of the usual "in-out" calculations one is interested in "in-in" calculations, and hence it is convenient to introduce a closed time path going from some initial time t to some future time t_0 and then back to t again. This enables one to calculate expectation values instead of transition amplitudes.

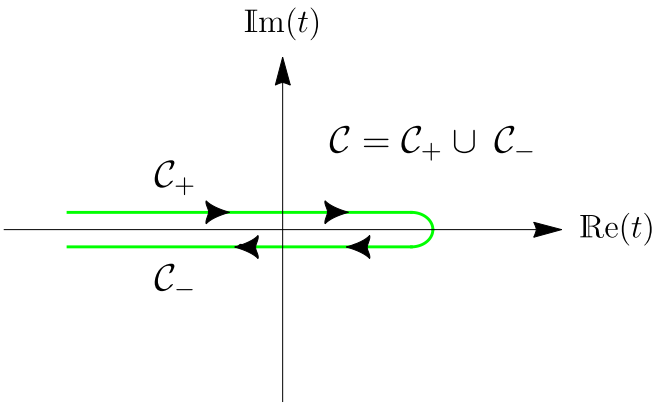

Figure 1: The Schwinger–Keldysh contour in the complex time plane, running from some initial time to an arbitrary future time and back again.

Consider the contour $\mathcal{C}$ in Figure 1, which starts from some initial value $t + \mathrm{i}\varepsilon$, travels to some t_0 along the upper half-plane and then returns to $t - \mathrm{i}\varepsilon$ in the lower half-plane (in the end one may set $\varepsilon \to 0, t \to -\infty, t_0 \to \infty$).[2] We define n-particle propagators (also called n-point Green's functions and correlators) as time-ordered expectation values of the fields $\Theta(x_i)$,

$$\begin{aligned} G^{(n)}(x_1, x_2, \ldots, x_n) &\doteq \langle \Omega \,|\mathcal{T}_{\mathcal{C}}\{\Theta(x_1)\Theta(x_2)\cdots\Theta(x_n)\}|\,\Omega\rangle \\ &\doteq \mathrm{Tr}\,[\hat{\rho}\,\Theta(x_1)\Theta(x_2)\cdots\Theta(x_n)] \end{aligned}$$

where $\mathcal{T}_{\mathcal{C}}$ denotes time-ordering *along* the path $\mathcal{C}$ (one can think of time flowing along $\mathcal{C}$) and $\hat{\rho}$ is an unknown quantum density matrix describing the system. We are especially interested in 2-point Green's functions, for which we define the propagator

$$\mathrm{i}\Delta(u, v) \doteq \langle \mathcal{T}_{\mathcal{C}}\{\phi(u)\phi^{\dagger}(v)\}\rangle$$

[2] One could complain that we are using imaginary time after all, but this is just a real integral performed in the complex plane. All results are in the end expressed in terms of real time, and there is no need for any analytic continuations.

for scalar fields ϕ and

$$\mathrm{i}S_{\alpha\beta}(u,v) \doteq \langle \mathcal{T}_{\mathcal{C}}\{\psi_\alpha(u)\overline{\psi}_\beta(v)\}\rangle$$

for fermionic fields ψ. Note that we omitted the ground state Ω from the notation for the expectation value. Since the object of interest for us will be the fermionic propagator S (from which we shall suppress the Dirac indices unless they are explicitly needed), we shall, in what follows, state all results in terms of it. The bosonic propagator Δ can be dealt with in a similar fashion, the only difference being in the commutation relations.

Due to the nature of the path $\mathcal{C}$, a propagator splits in general to four pieces. We define

$$\begin{cases} \mathrm{i}S^{++}(u,v) \doteq \mathrm{i}S^{\mathrm{F}}(u,v) = \langle \mathcal{T}\{\psi(u)\overline{\psi}(v)\}\rangle, & \text{(1a)} \\ \mathrm{i}S^{+-}(u,v) \doteq \mathrm{i}S^{<}(u,v) = \langle \overline{\psi}(v)\psi(u)\rangle, & \text{(1b)} \\ \mathrm{i}S^{-+}(u,v) \doteq \mathrm{i}S^{>}(u,v) = \langle \psi(u)\overline{\psi}(v)\rangle, & \text{(1c)} \\ \mathrm{i}S^{--}(u,v) \doteq \mathrm{i}S^{\overline{\mathrm{F}}}(u,v) = \langle \overline{\mathcal{T}}\{\overline{\psi}(u)\psi(v)\}\rangle. & \text{(1d)} \end{cases}$$

A few comments on the above definitions (1a)–(1d) are now in order.

- The plus and minus signs as superscripts indicate how the time-like components of u and v are oriented on $\mathcal{C}$. For example $\mathrm{i}S^{-+}(u,v)$ refers to the case where $u_0 \in \mathcal{C}_-$ and $v_0 \in \mathcal{C}_+$ (see Figure 1).
- F and $\overline{\mathrm{F}}$ refer to the usual chronological (Feynman) and anti-chronological (anti-Feynman) Green's functions, respectively.
- $S^<$ and $S^>$, the "mixed" cases, are related to the self-correlation of the fermionic field ψ between the space-time points u and v. They are called *Wightman functions*, and will later be our main interest.
- The Wightman function $S^<$ in (1b) is often defined with an additional minus sign, which is just a mere convention arising from the anticommutation of the fermionic fields.
- $\mathcal{T}$ is the regular time-ordering (not along $\mathcal{C}$) and $\overline{\mathcal{T}}$ denotes the "anti-time-ordering":

$$\overline{\mathcal{T}}\{\overline{\psi}(u)\psi(v)\} = \begin{cases} \psi(v)\overline{\psi}(u), & v_0 < u_0 \\ \overline{\psi}(u)\psi(v), & u_0 < v_0. \end{cases}$$

The propagators (1a)–(1d) are not all linearly independent of each other. Using the explicit form of the time-ordering

$$\mathcal{T}\{\psi(u)\psi(v)\} = \theta(u_0 - v_0)\psi(u)\psi(v) + \theta(v_0 - u_0)\psi(v)\psi(u)$$

(and also that of the anti-time-ordering) we can write

$$\begin{cases} S^{\mathrm{F}}(u,v) = \theta(u_0 - v_0)S^{>}(u,v) + \theta(v_0 - u_0)S^{<}(u,v), & \text{(2a)} \\ S^{\overline{\mathrm{F}}}(u,v) = \theta(v_0 - u_0)S^{>}(u,v) + \theta(u_0 - v_0)S^{<}(u,v). & \text{(2b)} \end{cases}$$

We shall further define a couple of interesting quantities. The *advanced propagator* is given by

$$S^{\mathrm{a}} \doteq S^{\mathrm{F}} - S^{>} = S^{<} - S^{\overline{\mathrm{F}}} = \theta(v_0 - u_0)(S^{<} - S^{>}), \tag{3}$$

where the last two equalities follow from the definitions and equation (2a). Similarly the *retarded propagator* is

$$S^{\mathrm{r}} \doteq S^{\mathrm{F}} - S^{<} = S^{>} - S^{\overline{\mathrm{F}}} = \theta(u_0 - v_0)(S^{>} - S^{<}). \tag{4}$$

The definitions (1b) and (1c) imply the following hermiticity relation for the Wightman functions $S^{<,>}$:

$$\left[\mathrm{i}S^{<,>}(u,v)\gamma^0\right]^{\dagger} = \mathrm{i}S^{<,>}(v,u)\gamma^0. \tag{5}$$

This hermitian version of the Wightman function is often denoted by $\overline{S}^{<,>}(u,v) \doteq \mathrm{i}S^{<,>}(u,v)\gamma^0$. Using this together with equations (3) and (4) gives

$$\left[\mathrm{i}S^{\mathrm{a,r}}(u,v)\gamma^0\right]^{\dagger} = -\mathrm{i}S^{\mathrm{r,a}}(v,u)\gamma^0,$$

which encourages us to decompose S^{a} and S^{r} into their hermitian and skew-hermitian parts. Indeed we define

$$\begin{aligned} S_{\mathrm{H}} &\doteq \frac{1}{2}\left(S^{\mathrm{r}} + S^{\mathrm{a}}\right), \\ S_{\mathrm{SH}} &\doteq \frac{\mathrm{i}}{2}\left(S^{\mathrm{r}} - S^{\mathrm{a}}\right) = \frac{\mathrm{i}}{2}\left(S^{>} - S^{<}\right) \doteq \mathcal{A}, \end{aligned}$$

where the second part $\mathcal{A}$ is called the *spectral function*. One can then write

$$S^{\mathrm{a,r}} = S_{\mathrm{H}} \pm \mathrm{i}S_{\mathrm{SH}}.$$

3.3 Basics of cQPA

3.3.1 Generalities

A *quasiparticle* is "*a disturbance, in a medium, that behaves as a particle and that may conveniently be regarded as one*", according to Encyclopædia Britannica [10]. This encapsulates quite well what physicists usually mean by a quasiparticle: something that is not quite a particle but can still be, at least mathematically, treated as one. Such situations often occur in many-body systems, where particles interact with their surroundings forming different kind of collective structures. These structures can adopt particle-like properties, like effective masses. One example is a charged particle moving amidst a sea of other charged particles, both of the same and opposite charge than the particle under consideration. Under appropriate circumstances the moving particle will attract a "cloud" of particles of the opposite charge around it, and the whole clump can be considered as a quasiparticle moving in the system (see Figure 2 for an enlightening illustration of the situation). Another example of a quasiparticle is the electron we observe in experiments. According to quantum electrodynamics, it is actually a system consisting of the bare electron surrounded by a cloud of virtual photons.[3]

In literature the term "quasiparticle" is sometimes used interchangeably with the term "collective excitation". Some authors (cf. [13]) prefer to conjoin quasiparticles to fermionic systems and collective excitations to bosonic systems. Generally speaking collective excitations describe usually phenomena where many particles act in a similar way to form a bigger structure, instead of there being a single source at the core of the structure, as is usually the case with quasiparticles. Examples of such phenomena include phonons, plasmons and magnons.

Using a *quasiparticle approximation* (QPA) means basically assuming that a part of our system can be, to a reasonable approximation, considered as a quasiparticle. This can for example mean that the Green's function related to this quasiparticle is close to that of a free particle, i.e. it is strongly enough peaked around its (effective) mass shell [14]. In any case, a traditional QPA usually has to assume weak interactions (the quasiparticles are screened by the clouds surrounding them) and a slowly varying back-

[3] See Chapter 6.5 in [12] for a discussion on how the whole concept of a "free electron" is questionable.

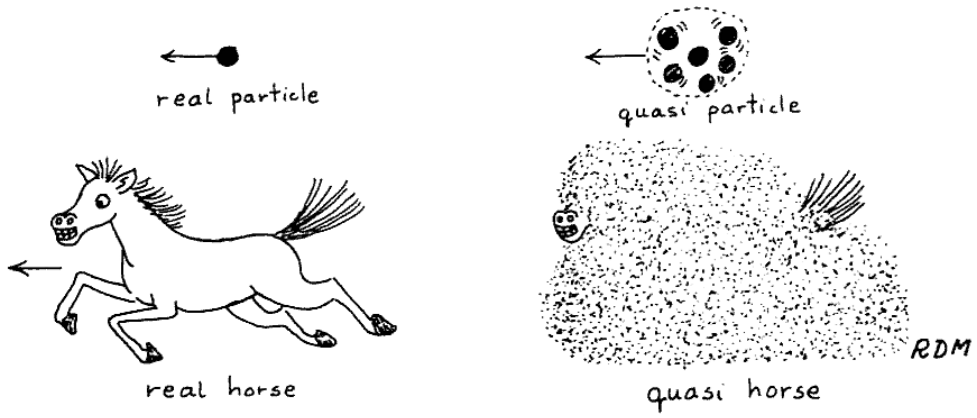

Figure 2: A quasiparticle consisting of a bare particle and a cloud of surrounding particles, compared with a quasihorse consisting of a real horse surrounded by a dust cloud following it. The picture is taken from [11] which contains many similar amusing analogies (such as the propagation of a drunken man, which is worth seeing).

ground (otherwise there would be no time for the quasiparticle to form, or it would be very short-lived). Furthermore, it is usually assumed that the system under consideration is close to thermal equilibrium, i.e. nearly translation invariant [15].

The *coherent quasiparticle approximation* (cQPA) is a certain approximation scheme that relinquishes one of the above mentioned assumptions, namely that of translation invariance. It was first introduced in [16] and has since been developed in [15] and [17–23]. The major property of this formalism is that in addition to the ordinary mass-shell solutions it includes completely new singular shell solutions that are absent in the translation invariant case. These solutions have been deduced to carry the information of nonlocal quantum coherence between e.g. particle- and antiparticle-solutions. This makes cQPA a valuable tool when one is interested in non-equilibrium phenomena where coherence-effects may also play a role, for example electroweak baryogenesis where also the mass is space-time-dependent. Other possible applications of the formalism include inflation and preheating, neutrino flavour oscillation in an inhomogeneous background, decoherence, thermalization and leptogenesis.

3.3.2 Formalism

In this thesis we will only need cQPA for fermions with no flavour mixing. Notations will mainly follow those of [16]; a different formulation can be found in [23] where also flavour mixing is taken into account. For our purposes the objects of interest are the fermionic 2-point Wightman functions $S^{<,>}(u,v)$ defined in (1b) and (1c). These functions describe the most interesting properties of out-of-equilibrium systems; they are for example related to the particle density and density of states of the system [24].

In order to get our hands on the Wightman functions, we must first specify the underlying setting in terms of the fermion spinors ψ. We will start with a Lagrangian density of the form,

$$\mathcal{L} = \overline{\psi}(\mathrm{i}\partial\!\!\!/ - P_{\mathrm{R}}m - P_{\mathrm{L}}m^*)\psi, \tag{6}$$

where $P_{\mathrm{R}} = \frac{1}{2}\left(1+\gamma^5\right)$ and $P_{\mathrm{L}} = \frac{1}{2}\left(1-\gamma^5\right)$ are the standard projection operators, and the mass is allowed to be space-time-dependent and complex. The origin of this Lagrangian density is explained in more detail in Chapter 4, for now we will just take it as a model describing e.g. EWBG-scenarios where the mass is effectively varying. The Dirac equation implied by (6) is

$$\left(\mathrm{i}\partial\!\!\!/_u - P_{\mathrm{R}}m - P_{\mathrm{L}}m^*\right)\psi(u) = 0. \tag{7}$$

Multiplying equation (7) from the right hand side by $\overline{\psi}(v)$ and taking an expectation value yields an equation for one of the Wightman functions:

$$\left(\mathrm{i}\partial\!\!\!/_u - P_{\mathrm{R}}m - P_{\mathrm{L}}m^*\right)\langle\psi(u)\overline{\psi}(v)\rangle = 0.$$

The corresponding equation for the other Wightman function is obtained by multiplying equation (7) by $\overline{\psi}(v)$ from the left, and the results can be compactly written as

$$\left(\mathrm{i}\partial\!\!\!/_u - P_{\mathrm{R}}m - P_{\mathrm{L}}m^*\right)S^{<,>}(u,v) = 0. \tag{8}$$

Another useful form is

$$\left(\mathrm{i}\partial\!\!\!/_u - m_{\mathrm{R}} - \mathrm{i}m_{\mathrm{I}}\gamma^5\right)S^{<,>}(u,v) = 0, \tag{9}$$

where we have decomposed the mass as $m \doteq m_{\mathrm{R}} + \mathrm{i}m_{\mathrm{I}}$.

It turns out to be useful to separate the internal (microscopic) degrees of freedom of the system from the external (macroscopic) ones, i.e. work in a mixed representation. In order to do this, we first define the relative coordinate $r \doteq u - v$ and the average coordinate $X \doteq \frac{1}{2}(u+v)$, which correspond to microscopic and macroscopic scales, respectively. Then we perform a Fourier-transform with respect to the average coordinate r, i.e. introduce the so-called *Wigner transformation*

$$S^{<,>}(k,X) \doteq \int \mathrm{d}^4 r\, \mathrm{e}^{\mathrm{i}k\cdot r} S^{<,>}\left(X + \frac{r}{2}, X - \frac{r}{2}\right), \tag{10}$$

where k is the internal conjugate momentum related to r. We shall refer to this Wigner-transformed Wightman function as the *Wigner function*. It is often credited as being the closest phase space representation one can obtain of a quantum mechanical system. It will be of particular importance to us, since a system that is not translation invariant will depend on both the internal and the external coordinate.[4] The relative coordinate r is related to the coherence of the system between different points, basically measuring the nonlocality of the coherence. The average coordinate X gives the average position of the two points whose mutual coherence r is measuring; it will be related to macroscopic distances.

Our next task is then to correspondingly Wigner-transform the Dirac equation (9). The first step is to write the equation as a sort of a convolution:

$$\int \mathrm{d}^4 w \left[\mathrm{i}\not{\partial}_u - m_{\mathrm{R}}(u) - \mathrm{i}\gamma^5 m_{\mathrm{I}}(u)\right] \delta^{(4)}(u-w) S^{<,>}(w,v) = 0. \tag{11}$$

The point in doing this is that there is a known formula for the Wigner transformation of this kind of an object. It is given by [25]

$$\int \mathrm{d}^4(u-v) \mathrm{e}^{\mathrm{i}k\cdot(u-v)} \int \mathrm{d}^4 w f(u,w) g(w,v) = \mathrm{e}^{-\mathrm{i}\lozenge} \{f(k,X)\} \{g(k,X)\}, \tag{12}$$

where the diamond operator $\lozenge$ acting on a pair of functions is defined as[5]

$$\lozenge\{f\}\{g\} \doteq \frac{1}{2}\left[(\partial_X f)\cdot(\partial_k g) - (\partial_k f)\cdot(\partial_X g)\right]. \tag{13}$$

[4]For translation invariant propagators we can write $S^{<,>}(u,v) = S^{<,>}(u-v,0) = S^{<,>}(r)$, i.e. they only depend on the relative coordinate.

[5]The diamond operator bears a resemblance to the Poisson bracket of two functions. Using equation (13) one can define $\lozenge^n$ for every $n \in \mathbb{N}$, and furthermore $\mathrm{e}^{-\mathrm{i}\lozenge}$.

Transforming equation (11) with respect to the relative coordinate $r = u - v$ and using equation (12) allows us to write the Dirac equation as

$$\mathrm{e}^{-\mathrm{i}\diamondsuit}\left\{F(k,X)\right\}\left\{S^{<,>}(k,X)\right\} = 0, \tag{14}$$

where we are left to compute the Wigner transformation of

$$F(u,v) \doteq \left[\mathrm{i}\not{\partial}_u - m_{\mathrm{R}}(u) - \mathrm{i}\gamma^5 m_{\mathrm{I}}(u)\right]\delta^{(4)}(u-v).$$

This can be done by writing the delta function as a Fourier transformation, resulting in

$$F(k,X) = \not{k} - m_{\mathrm{R}}(X) - \mathrm{i}m_{\mathrm{I}}(X)\gamma^5.$$

Note that in obtaining the above result we also shifted the variables inside the integral as $u \to u - \frac{r}{2}$ to get the mass parameters as functions of X.

Now we will turn our attention to the diamond exponential. It can be formally rearranged as

$$\begin{aligned}
\mathrm{e}^{-\mathrm{i}\diamondsuit} &\doteq \sum_{n=0}^{\infty}\frac{1}{n!}(-\mathrm{i}\diamondsuit)^n = 1 - \mathrm{i}\diamondsuit + \frac{1}{2!}(-\mathrm{i}\diamondsuit)^2 + \frac{1}{3!}(-\mathrm{i}\diamondsuit)^3 + \ldots \\
&= 1 - \frac{\mathrm{i}}{2}(\partial_X\cdot\partial_k) + \frac{1}{2!}\left(-\frac{i}{2}\,\partial_X\cdot\partial_k\right)^2 + \frac{1}{3!}\left(-\frac{i}{2}\,\partial_X\cdot\partial_k\right)^3 + \ldots \\
&\quad + \frac{\mathrm{i}}{2}(\partial_k\cdot\partial_X) + \frac{1}{2!}\left(\frac{i}{2}\,\partial_k\cdot\partial_X\right)^2 + \frac{1}{3!}\left(\frac{i}{2}\,\partial_k\cdot\partial_X\right)^3 + \ldots \\
&\quad + \{\text{mixed terms}\} \\
&= \mathrm{e}^{-\frac{\mathrm{i}}{2}\partial_X\cdot\partial_k} + \mathrm{e}^{\frac{\mathrm{i}}{2}\partial_k\cdot\partial_X} - 1 + \{\text{mixed terms}\}.
\end{aligned}$$

So equation (14) can then be written as

$$\begin{aligned}
\left(\mathrm{e}^{-\frac{\mathrm{i}}{2}\partial_X\cdot\partial_k} + \mathrm{e}^{\frac{\mathrm{i}}{2}\partial_k\cdot\partial_X} - 1 + \{\text{mixed terms}\}\right)\{\not{k} - m_{\mathrm{R}}(X) \\
-\mathrm{i}m_{\mathrm{I}}(X)\gamma^5\}\left\{S^{<,>}(k,X)\right\} = 0,
\end{aligned} \tag{15}$$

where the pairs of derivatives operate on the objects inside the brackets as dictated by the diamond operator. The first thing to notice in equation (15) is that operating with the mixed terms gives no contribution. This is due to the fact that the object inside the first brackets is linear in k, and all the mixed terms differentiate it with respect to k and X. Similarly the

terms with $(\partial_k \cdot \partial_X)^n$, $n > 1$, in the second exponential can be left out; the term inside the brackets goes to zero when differentiated with these higher order terms. All in all we can write the remaining equation as

$$\left\{ \not{k} + \frac{\mathrm{i}}{2}\not{\partial}_X - \left[m_{\mathrm{R}}(X) - \mathrm{i}m_{\mathrm{I}}\gamma^5 \right] \mathrm{e}^{-\frac{\mathrm{i}}{2}\overleftarrow{\partial}_X \cdot \partial_k} \right\} S^{<,>}(k,X) = 0, \tag{16}$$

where the arrow above the other partial derivative in the exponential indicates that these spatial derivatives only operate to the left on the mass functions, while the derivative with respect to k only operates on $S^{<,>}$. If we further define operators $\hat{m}_0$ and $\hat{m}_5$ such that

$$\hat{m}_{0,5} S(k,X) \doteq m_{\mathrm{R,I}} \mathrm{e}^{-\frac{\mathrm{i}}{2}\overleftarrow{\partial}_X \cdot \partial_k} S(k,X),$$

we can write the Wigner-transformed Dirac equation in a final compact form:

$$\left(\not{k} + \frac{\mathrm{i}}{2}\not{\partial}_X - \hat{m}_0 - \mathrm{i}\hat{m}_5\gamma^5 \right) S^{<,>}(k,X) = 0. \tag{17}$$

We shall proceed to work with hermitian Wightman functions. Applying the hermiticity condition (5) to equation (10) tells us that $\overline{S}^{<,>}(k,X)$ are hermitian:

$$\left[\mathrm{i}S^{<,>}(k,X)\gamma^0 \right]^\dagger = \mathrm{i}S^{<,>}(k,X)\gamma^0.$$

Multiplying equation (17) from the right by $\mathrm{i}\gamma^0$ results in an equation for the hermitian Wightman functions:

$$\left(\not{k} + \frac{\mathrm{i}}{2}\not{\partial}_X - \hat{m}_0 - \mathrm{i}\hat{m}_5\gamma^5 \right) \overline{S}^{<,>}(k,X) = 0 \tag{18}$$

If we further multiply equation (18) from the right by γ^0 and represent the Dirac gamma matrices as direct products in the chiral (Weyl) representation (see Appendix A), we find the following equation of motion for $\overline{S}^{<,>}(k,X)$:

$$\left\{ k_0 + \frac{\mathrm{i}}{2}\partial_t + \sigma^3 \otimes \left[\vec{\sigma} \cdot \left(\vec{k} - \frac{\mathrm{i}}{2}\vec{\nabla} \right) \right] - \left(\sigma^1 \hat{m}_0 - \sigma^2 \hat{m}_5 \right) \otimes \mathbb{1} \right\} \overline{S}^{<,>} = 0. \tag{19}$$

In the above equation $\vec{\sigma} = (\sigma^1, \sigma^2, \sigma^3)$ is a vector of the Pauli sigma matrices.

Due to the nature of the operators $\hat{m}_0$ and $\hat{m}_5$, equation (19) contains an infinite amount of derivatives and is therefore difficult to study in its most general form. Imposing different space-time symmetries can however reduce the equation to a more easily approached one. The two most simple choices are a static system and a system with spatial symmetry. In this cQPA-introduction we shall concentrate on spatial homogeneity, since it is related to our later studies of the Dirac equation. See for example [16] for a similar treatise of a static case with planar symmetry.

Assuming spatial homogeneity, $\overline{S}^{<,>}(k, X) = \overline{S}^{<,>}(k, t)$, allows us to drop spatial derivatives in equation (19), resulting in

$$\left[k_0 + \frac{\mathrm{i}}{2}\partial_t - \gamma^0\left(\vec{\gamma}\cdot\vec{k} - \hat{m}_0 - \mathrm{i}\gamma^5\hat{m}_5\right)\right]\overline{S}^{<,>}(k,t) = 0. \tag{20}$$

Also the mass operators contain only derivatives with respect to t and k_0, since three-momentum is now conserved. The amount of derivatives is still infinite, of course. A system with spatial homogeneity has another advantage. Let us consider the helicity operator $\hat{h}$ defined in terms of the spin operator $\hat{S} = \gamma^0\vec{\gamma}\gamma^5$ as

$$\hat{h} = \hat{k}\cdot\hat{S} = \frac{\vec{k}}{|\vec{k}|}\cdot\hat{S}.$$

In the chiral representation this becomes just

$$\hat{h} = \mathbb{1}\otimes\hat{k}\cdot\vec{\sigma},$$

from which it is easy to see that the helicity operator commutes with the differential operator (Hamiltonian)

$$\begin{aligned}\mathfrak{D} &= k_0 + \frac{\mathrm{i}}{2}\partial_t - \gamma^0\left(\vec{\gamma}\cdot\vec{k} - \hat{m}_0 - \mathrm{i}\gamma^5\hat{m}_5\right)\\ &= k_0 + \frac{\mathrm{i}}{2}\partial_t + \sigma^3\otimes\vec{\sigma}\cdot\vec{k} - \sigma^1\hat{m}_0\otimes\mathbb{1} + \sigma^2\hat{m}_5\otimes\mathbb{1}\end{aligned}$$

of equation (20). This guarantees that helicity is a good quantum number for our system, a conserved quantity. We are therefore encouraged to decompose the Wightman function into a block-diagonal helicity-conserving form, namely

$$\overline{S}^{<}_h = g^{<}_h\otimes\frac{1}{2}\left(\mathbb{1} + h\hat{k}\cdot\vec{\sigma}\right),$$

where $g_h^<$ is an unknown 2×2-matrix and our new object of interest. The point of this form is that now the Wightman function is an eigenstate of the helicity operator with an eigenvalue $h \in \{-1, 1\}$, i.e. $\hat{h}\overline{S}_h^< = h\overline{S}_h^<$. An exactly similar decomposition can of course be done for $\overline{S}^>$ too; for simplicity we shall from now on state our results for $\overline{S}^<$ only.

Substituting $\overline{S}_h^<$ into equation (20) allows us to write the following equation for $g_h^<$:

$$\left(k_0 + \frac{\mathrm{i}}{2}\partial_t + h|\vec{k}|\sigma^3 - \hat{m}_0\sigma^1 - \hat{m}_5\sigma^2\right) g_h^< = 0. \tag{21}$$

To analyze different properties of equation (21), we will first write $g_h^<$ in a vector form with a basis given by the Pauli spin matrices:

$$g_h^< = \frac{1}{2}\left(g_0^h + \sum_{i=1}^{3} g_i^h \sigma^i\right). \tag{22}$$

Plugging this representation into equation (21), multiplying the resulting equation individually by each σ^i and finally taking the trace of each of the remaining equations gives us four equations containing the four unknowns g_μ^h:

$$\begin{cases} \left(k_o + \frac{\mathrm{i}}{2}\partial_t\right) g_0^h + h|\vec{k}|g_3^h - \hat{m}_0 g_1^h + \hat{m}_5 g_2^h = 0, & \text{(23a)} \\ \left(k_o + \frac{\mathrm{i}}{2}\partial_t\right) g_1^h - \mathrm{i}h|\vec{k}|g_2^h - \hat{m}_0 g_0^h + \mathrm{i}\hat{m}_5 g_3^h = 0, & \text{(23b)} \\ \left(k_o + \frac{\mathrm{i}}{2}\partial_t\right) g_2^h + \mathrm{i}h|\vec{k}|g_1^h + \mathrm{i}\hat{m}_0 g_3^h + \hat{m}_5 g_0^h = 0, & \text{(23c)} \\ \left(k_o + \frac{\mathrm{i}}{2}\partial_t\right) g_3^h + h|\vec{k}|g_0^h - \mathrm{i}\hat{m}_0 g_2^h - \mathrm{i}\hat{m}_5 g_1^h = 0. & \text{(23d)} \end{cases}$$

These equations can further be divided into real and imaginary parts, resulting in a total of eight equations:

$$\begin{cases} \sum_{\beta=0}^{4} \hat{A}_{\alpha\beta}^h g_\beta^h = \partial_t g_\alpha^h, & \text{(24a)} \\ \sum_{\beta=0}^{4} \hat{B}_{\alpha\beta}^h g_\beta^h = 0. & \text{(24b)} \end{cases}$$

The matrices $\hat{A}$ and $\hat{B}$ in the above equations can be read from equations (23). Equation (24a) governs the time evolution of the $g_h^<$-functions, and is therefore called the *kinetic equation*. Equation (24b) on the other hand restricts the phase space structure of the Wightman functions, and is accordingly called the *constraint equation*. The infinite amount of derivatives however makes the situation still complicated, and we shall consequently introduce one more approximation.

We shall truncate the gradient expansion in the mass operators $\hat{m}_0$ and $\hat{m}_5$ to zeroth order, in which case the operators reduce to the real and imaginary part of the mass:

$$\hat{m}_{0,5} \longrightarrow m_{\mathrm{R,I}}.$$

This approximation actually corresponds to an expansion in $\hbar$, since in normal units we have $\partial \to \hbar\partial$. Formally the approximation holds when $\partial_X \ll k$, i.e. the changes in the background field (characterized by the macroscopic scale X) are small compared to the momenta of the particles. Let us now study what the constraint equation (24b) tells us under this assumption. The matrix $\hat{B}$ becomes just a constant matrix

$$\hat{B} = \begin{bmatrix} k_0 & -m_{\mathrm{R}} & m_{\mathrm{I}} & h|\vec{k}| \\ m_{\mathrm{I}} & 0 & k_0 & 0 \\ -m_{\mathrm{R}} & k_0 & 0 & 0 \\ h|\vec{k}| & 0 & 0 & k_0 \end{bmatrix},$$

and equation (24b) is thus in this case an algebraic one. In order to obtain non-trivial solutions for equation (24b), the determinant of $\hat{B}$ has to vanish. This requirement restricts the possible phase space structure of our system:

$$\det(\hat{B}) = k_0^2 \left(k^2 - |m|^2\right) = 0.$$

So in addition to the usual mass-shell solutions given by the standard dispersion relation $k_0 = \pm\omega_k \doteq \pm\sqrt{|\vec{k}|^2 + |m|^2}$, the constraint equation allows solutions living at $k_0 = 0$. The full solution of our system, acquiring a singular shell structure, is hence in general proportional to $\delta(k^2 - |m|^2)$ and $\delta(k_0)$. These novel $k_0 = 0$ -solutions are at the heart of cQPA, and they are the main motivation behind this thesis.

The constraint equation (24b) can be solved separately for the cases $k_0 \neq 0$ and $k_0 = 0$. Doing this and plugging the solutions to the decomposition

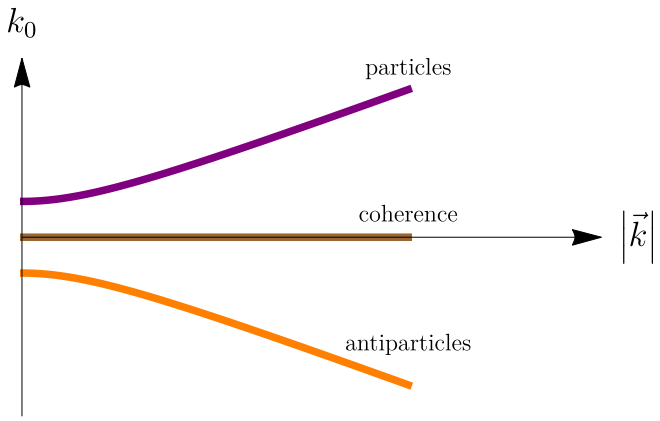

Figure 3: The shell structure of the Wightman function $S^<$ predicted by cQPA. Here we have chosen $|m| = 1$. For a given value of $|\vec{k}|$ one has the on-shell-solutions corresponding to particles (purple) and antiparticles (orange), and in addition solutions corresponding to coherence between them (brown), living at $k_0 = 0$.

(22) one finds that the full matrix solution is in general of the form

$$g_h^<(k_0, |\vec{k}|; t) = 2\pi |k_0| f^h_{s_{k_0}}(|\vec{k}|, t) \begin{bmatrix} 1 - \frac{h|\vec{k}|}{k_0} & \frac{m}{k_0} \\ \frac{m^*}{k_0} & 1 + \frac{h|\vec{k}|}{k_0} \end{bmatrix} \delta(k^2 - |m|^2)$$
$$+ \pi \left\{ f_2^h(|\vec{k}|, t) \begin{bmatrix} \frac{hm_{\mathrm{R}}}{|\vec{k}|} & 1 \\ 1 & -\frac{hm_{\mathrm{R}}}{|\vec{k}|} \end{bmatrix} + f_3^h(|\vec{k}|, t) \begin{bmatrix} -\frac{hm_{\mathrm{I}}}{|\vec{k}|} & -\mathrm{i} \\ \mathrm{i} & \frac{hm_{\mathrm{I}}}{|\vec{k}|} \end{bmatrix} \right\} \delta(k_0),$$

where f_i^h are unknown real functions parametrizing the solutions on different shells, and we have denoted $s_{k_0} \doteq \mathrm{sgn}(k_0)$. Here the full shell-structure of the system is apparent. The upper line describes the basic particle- and antiparticle-solutions living on the positive- and negative-energy shells $\pm\omega_k$. The second line contains the solutions living on the mysterious $k_0 = 0$ -shell. These zero-momenta solutions are interpreted to encode the information about *quantum coherence between particles and antiparticles with the same helicity h and opposite momenta* $\vec{k}$.[6] The complete shell structure predicted by cQPA is illustrated in Figure 3.

[6]The easiest way to see the coherence-nature of these solutions is to observe that the quantum interference of the particle- and antiparticle plane waves $\mathrm{e}^{\pm \mathrm{i}\omega_k t}$ contributes at zero momenta $k_0 = 0$. E.g. reference [16] contains many other discussions establishing this interpretation.

This is as far as we will go in this short introduction to cQPA. In this thesis we are more interested in the *existence* of these new spectral shells than in their *origin*. Now that we have seen how they emerge naturally in the cQPA-formalism, we shall leave the formalism aside and take another route towards these $k_0 = 0$ -solutions. In the next chapter we will take on a problem that should exhibit the coherence structure, namely a fermion whose mass changes as a function of time. This kind of problem most definitely is not translation invariant, and quantum mechanical coherence-effects will play a role since the changing mass will give rise to both particle- and antiparticle-solutions. In the end our goal is to construct the Wigner function out of the solutions to the given problem and use it to examine the whole phase space structure of the system, including the coherence structure predicted by cQPA.

As a final note let us point out, that this introduction to cQPA has been a narrow and in some sense primitive one. The approach adopted here follows the one used in the early cQPA-studies, and the formalism has since seen many refinements and generalizations. Rigorous transport equations have been studied, Feynman rules derived and flavour-coherence examined, to name a few. A major advance has been successfully adding interactions through a collision term, giving rise to decoherence and damping of the coherence solutions. The methods used here however serve well for our purposes, and are an equally correct way to reveal the somewhat hidden coherence structure.

4 Dirac equation with a varying mass

4.1 General case

We want to examine the motion of a fermionic particle with a space-time-dependent complex mass. The motivation for this kind of a situation was explained in Chapter 2. Basic quantum mechanics tells us that the motion of the particle is described by the Dirac equation. The complex and space-time-dependent mass however alters the situation, and one cannot just take the basic Dirac equation with the real mass replaced by a varying complex one. In order to find the correct Dirac equation for this situation, one has to mathematically specify the problem, i.e. write down an appropriate Lagrangian density.

The Lagrangian density that gives the familiar Dirac equation is the one describing a free fermion field ψ:

$$\mathcal{L}_{\text{Dirac}} = \overline{\psi}(\mathrm{i}\partial\!\!\!/ - m)\psi. \tag{25}$$

Indeed, the Euler–Lagrange equation with respect to $\overline{\psi}$ is

$$\begin{aligned} &\frac{\partial \mathcal{L}_{\text{Dirac}}}{\partial \overline{\psi}} - \partial_\mu \left[\frac{\partial \mathcal{L}_{\text{Dirac}}}{\partial(\partial_\mu \overline{\psi})} \right] = 0 \\ &\Rightarrow (\mathrm{i}\partial\!\!\!/ - m)\psi = 0. \end{aligned}$$

By using the projection operators P_{R} and P_{L} defined as

$$P_{\text{R}} = \frac{1}{2}\left(1 + \gamma^5\right), \qquad P_{\text{L}} = \frac{1}{2}\left(1 - \gamma^5\right),$$

we can divide the spinor ψ into left- and right-chiral components:

$$\psi = \left(P_{\text{R}} + P_{\text{L}}\right)\psi = P_{\text{R}}\psi + P_{\text{L}}\psi \doteq \psi_{\text{R}} + \psi_{\text{L}}.$$

The Lagrangian density (25) can then be written as

$$\mathcal{L}_{\text{Dirac}} = \mathrm{i}\overline{\psi}_{\text{R}}\partial\!\!\!/\psi_{\text{R}} + \mathrm{i}\overline{\psi}_{\text{L}}\partial\!\!\!/\psi_{\text{L}} - m\overline{\psi}_{\text{R}}\psi_{\text{L}} - m\overline{\psi}_{\text{L}}\psi_{\text{R}}. \tag{26}$$

Now it is evident why we cannot take this Lagrangian density as the one describing our model. We expect our Lagrangian density to be hermitian, because then its expectation values would be real, corresponding to

physical states. For a complex mass $m \in \mathbb{C}$ this condition is not fulfilled by $\mathcal{L}_{\text{Dirac}}$ due to the mass terms:

$$\begin{aligned}&\left(m\bar{\psi}_{\text{R}}\psi_{\text{L}} + m\bar{\psi}_{\text{L}}\psi_{\text{R}}\right)^{\dagger} = m^{*}\bar{\psi}_{\text{R}}\psi_{\text{L}} + m^{*}\bar{\psi}_{\text{L}}\psi_{\text{R}}\\ &\Rightarrow \mathcal{L}^{\dagger}_{\text{Dirac}} \neq \mathcal{L}_{\text{Dirac}}.\end{aligned}$$

This however gives us a clear clue on how the structure of $\mathcal{L}_{\text{Dirac}}$ should be altered. To retain hermiticity we take our effective free-field Lagrangian density to be

$$\mathcal{L} = \mathrm{i}\bar{\psi}_{\text{R}}\partial\!\!\!/\psi_{\text{R}} + \mathrm{i}\bar{\psi}_{\text{L}}\partial\!\!\!/\psi_{\text{L}} - m^{*}\bar{\psi}_{\text{R}}\psi_{\text{L}} - m\bar{\psi}_{\text{L}}\psi_{\text{R}}, \tag{27}$$

where the mass m is allowed to be space-time-dependent. The above Lagrangian density clearly satisfies $\mathcal{L}^{\dagger} = \mathcal{L}$. The space-time-dependence of the mass can be generated for example by an interaction of the fermion field ψ with a scalar field ϕ, i.e. through a Yukawa interaction

$$\mathcal{L}_{\text{Yukawa}} = -g\bar{\psi}\phi\psi,$$

where the coupling g is now complex. This can be approximated as

$$-g\bar{\psi}\phi\psi \approx -g\bar{\psi}\langle\phi(x)\rangle\psi = -m(x)\bar{\psi}\psi,$$

corresponding to complex and space-time-dependent mass-terms in (27).

Now that we have specified the Lagrangian density modeling our system, we are ready to bring up the Dirac equation associated with it. Using $\bar{\psi}_{\text{L,R}} = \bar{\psi}P_{\text{L,R}}$ together with other properties of the projection operators we can write $\mathcal{L}$ in (27) compactly as

$$\mathcal{L} = \bar{\psi}(\mathrm{i}\partial\!\!\!/ - P_{\text{R}}m - P_{\text{L}}m^{*})\psi, \tag{28}$$

which is what we already used in Chapter 3.3 when introducing the cQPA-formalism. Applying the Euler–Lagrange equations to equation (28) gives us straightforwardly the desired Dirac equation:

$$\begin{aligned}&\frac{\partial\mathcal{L}}{\partial\bar{\psi}} - \partial_{\mu}\underbrace{\left[\frac{\partial\mathcal{L}}{\partial(\partial_{\mu}\bar{\psi})}\right]}_{=0} = 0\\ &\Rightarrow (\mathrm{i}\partial\!\!\!/ - P_{\text{R}}m - P_{\text{L}}m^{*})\psi = \mathrm{i}\partial\!\!\!/\psi - m\psi_{\text{R}} - m^{*}\psi_{\text{L}} = 0.\end{aligned}$$

In this thesis, as in [26], we will for simplicity consider the case where the mass is time-dependent but spatially homogeneous. This will essentially lead to particle numbers while the space-dependent case is related to reflection problems. The underlying situation is the same in both cases: a fermionic particle in the presence of an altering mass profile. A space-dependent case with a real mass has been considered in [27], and the analysis was extended to a perturbatively imaginary space-dependent mass in [28]. The studies performed here and in [26] have the advantage of setting no restrictions for the magnitude of the mass parameters, resulting in more freedom for the amount of desired CP-violation.

To conclude these preliminaries, let us finally write the Dirac equation with the explicit space-time-dependences:

$$\left[\mathrm{i}\partial\!\!\!/ - P_{\mathrm{R}} m(t) - P_{\mathrm{L}} m^*(t)\right]\psi(t,\vec{x}) = 0. \tag{29}$$

This equation is the one we will proceed to solve. Our final goal is to use the exact solutions of the above equation to construct the Wigner function which we already examined using cQPA.

In order to get to the mode function solutions, we shall start by performing a canonical quantization of the spinor ψ. We will consider it as a spinor operator $\hat{\psi}$, which is assumed to obey the basic fermionic anti-commutation relations

$$\left\{\hat{\psi}_\alpha(t,\vec{x}_1), \hat{\psi}^\dagger_\beta(t,\vec{x}_2)\right\} = \delta^{(3)}(\vec{x}_1 - \vec{x}_2)\delta_{\alpha\beta},$$
$$\left\{\hat{\psi}_\alpha(t,\vec{x}_1), \hat{\psi}_\beta(t,\vec{x}_2)\right\} = 0.$$

The spinor is then expanded in terms of creation and annihilation operators. In the helicity basis this reads

$$\hat{\psi}(t,\vec{x}) = \int \frac{\mathrm{d}^3k}{(2\pi)^3} \sum_{h=\pm} \left[\hat{a}_{\vec{k}h}\mu_h(t,\vec{k})\mathrm{e}^{\mathrm{i}\vec{k}\cdot\vec{x}} + \hat{b}^\dagger_{\vec{k}h}\nu_h(t,\vec{k})\mathrm{e}^{-\mathrm{i}\vec{k}\cdot\vec{x}}\right], \tag{30}$$

where μ_h and ν_h are momentum-space spinors corresponding to particles and antiparticles, respectively. $\hat{a}^\dagger_{\vec{k}h}$ and $\hat{b}^\dagger_{\vec{k}h}$ denote creation operators creating fermions and antifermions, respectively, with momentum $\vec{k}$ and helicity h. Similarly $\hat{a}_{\vec{k}h}$ and $\hat{b}_{\vec{k}h}$ are the usual fermionic annihilation operators for particles and antiparticles. These operators satisfy the usual anticommutation algebra

$$\left\{\hat{a}_{\vec{k}_1 h_1}, \hat{a}^\dagger_{\vec{k}_2 h_2}\right\} = (2\pi)^3\delta^{(3)}(\vec{k}_1 - \vec{k}_2)\delta_{h_1 h_2} = \left\{\hat{b}_{\vec{k}_1 h_1}, \hat{b}^\dagger_{\vec{k}_2 h_2}\right\} \tag{31}$$

with all other anticommutators vanishing. The spinors μ and ν are assumed to be normalized according to the rule

$$\mu_h^\dagger(t,\vec{k})\mu_h(t,\vec{k}) = 1 = \nu_h^\dagger(t,\vec{k})\nu_h(t,\vec{k}). \tag{32}$$

In Chapter 3.3 we already noted that helicity is a conserved quantity in the cQPA-formalism. This is a similar case, and we shall in the same way separate helicity in our spinors from the time-dependent part. This is formally done by decomposing the spinors μ_h and ν_h as

$$\mu_h(t,\vec{k}) = \begin{bmatrix} \eta_h(t,\vec{k}) \\ \zeta_h(t,\vec{k}) \end{bmatrix} \otimes \xi_h(\vec{k}), \tag{33a}$$

$$\nu_h(t,\vec{k}) = \begin{bmatrix} \overline{\eta}_h(t,\vec{k}) \\ \overline{\zeta}_h(t,\vec{k}) \end{bmatrix} \otimes \xi_h(\vec{k}), \tag{33b}$$

where ξ_h is the helicity two-eigenspinor satisfying

$$\hat{h}\xi_h(\vec{k}) = h\xi_h(\vec{k}); \qquad h = \pm 1,$$

for the helicity operator $\hat{h} = \hat{k}\cdot\vec{\sigma}$. The new main objects of interest are the above introduced one-dimensional mode functions η_h, ζ_h, $\overline{\eta}_h$ and $\overline{\zeta}_h$. Applying the normalization condition (32) to the decompositions (33a) and (33b) gives us conditions for these new mode functions. For example:

$$1 = \mu_h^\dagger(t,\vec{k})\mu_h(t,\vec{k}) = \begin{bmatrix} \eta_h^*(t,\vec{k}) & \zeta_h^*(t,\vec{k}) \end{bmatrix} \begin{bmatrix} \eta_h(t,\vec{k}) \\ \zeta_h(t,\vec{k}) \end{bmatrix} \otimes \underbrace{\xi_h^\dagger(\vec{k})\xi_h(\vec{k})}_{=1}$$

$$\Rightarrow \quad \left|\eta_h(t,\vec{k})\right|^2 + \left|\zeta_h(t,\vec{k})\right|^2 = 1. \tag{34}$$

Similarly the normalization condition for ν_h implies

$$\left|\overline{\eta}_h(t,\vec{k})\right|^2 + \left|\overline{\zeta}_h(t,\vec{k})\right|^2 = 1. \tag{35}$$

Our next task is to substitute these decompositions with the expansion (30) into the Dirac equation (29). We will be again using the chiral representation of the Dirac matrices in which the projections operators become simply

$$P_{\mathrm{R}} = \begin{bmatrix} 0 & 0 \\ 0 & \mathbb{1} \end{bmatrix} = \frac{1}{2}(1-\sigma^3)\otimes\mathbb{1},$$

$$P_{\mathrm{L}} = \begin{bmatrix} \mathbb{1} & 0 \\ 0 & 0 \end{bmatrix} = \frac{1}{2}(1+\sigma^3)\otimes\mathbb{1}.$$

After substituting the decomposed spinor into the Dirac equation (29) one finds the following two equations:

$$\begin{aligned}
\mathrm{i}\partial_t \begin{bmatrix} \eta_h \\ \zeta_h \end{bmatrix} \otimes \xi_h + \sigma^3 \begin{bmatrix} \eta_h \\ \zeta_h \end{bmatrix} \otimes (\vec{k}\cdot\vec{\sigma})\xi_h - \frac{m^*}{2}(\sigma^1 - \mathrm{i}\sigma^2) \begin{bmatrix} \eta_h \\ \zeta_h \end{bmatrix} \otimes \xi_h \\
- \frac{m}{2}(\sigma^1 + \mathrm{i}\sigma^2) \begin{bmatrix} \eta_h \\ \zeta_h \end{bmatrix} \otimes \xi_h = 0, \\
\mathrm{i}\partial_t \begin{bmatrix} \overline{\eta}_h \\ \overline{\zeta}_h \end{bmatrix} \otimes \xi_h - \sigma^3 \begin{bmatrix} \overline{\eta}_h \\ \overline{\zeta}_h \end{bmatrix} \otimes (\vec{k}\cdot\vec{\sigma})\xi_h - \frac{m^*}{2}(\sigma^1 - \mathrm{i}\sigma^2) \begin{bmatrix} \overline{\eta}_h \\ \overline{\zeta}_h \end{bmatrix} \otimes \xi_h \\
- \frac{m}{2}(\sigma^1 + \mathrm{i}\sigma^2) \begin{bmatrix} \overline{\eta}_h \\ \overline{\zeta}_h \end{bmatrix} \otimes \xi_h = 0.
\end{aligned}$$

Using then $(\vec{k}\cdot\vec{\sigma})\xi_h = h|\vec{k}|\xi_h$ together with the explicit forms of the Pauli matrices, the above equations become

$$\begin{aligned}
\left\{ \mathrm{i}\partial_t \begin{bmatrix} \eta_h \\ \zeta_h \end{bmatrix} + h|\vec{k}| \begin{bmatrix} \eta_h \\ -\zeta_h \end{bmatrix} - m^* \begin{bmatrix} 0 \\ \eta_h \end{bmatrix} - m \begin{bmatrix} \zeta_h \\ 0 \end{bmatrix} \right\} \otimes \xi_h = 0, \\
\left\{ \mathrm{i}\partial_t \begin{bmatrix} \overline{\eta}_h \\ \overline{\zeta}_h \end{bmatrix} + h|\vec{k}| \begin{bmatrix} -\overline{\eta}_h \\ \overline{\zeta}_h \end{bmatrix} - m^* \begin{bmatrix} 0 \\ \overline{\eta}_h \end{bmatrix} - m \begin{bmatrix} \overline{\zeta}_h \\ 0 \end{bmatrix} \right\} \otimes \xi_h = 0.
\end{aligned}$$

All in all we have then four equations for each helicity h:

$$\begin{cases}
\mathrm{i}\partial_t \eta_h + h|\vec{k}|\eta_h = m\zeta_h & \text{(36a)} \\
\mathrm{i}\partial_t \zeta_h - h|\vec{k}|\zeta_h = m^*\eta_h & \text{(36b)} \\
\mathrm{i}\partial_t \overline{\eta}_h - h|\vec{k}|\overline{\eta}_h = m\overline{\zeta}_h & \text{(36c)} \\
\mathrm{i}\partial_t \overline{\zeta}_h + h|\vec{k}|\overline{\zeta}_h = m^*\overline{\eta}_h. & \text{(36d)}
\end{cases}$$

These equations could be decoupled into two second order equations by differentiating them with respect to time. Instead of doing this, we proceed by introducing yet another basis, because, as it turns out, this makes it easier to find analytic solutions for the problem we will be dealing with. We define the positive and negative frequency basis as the following linear combinations of the mode functions η_h, ζ_h, $\overline{\eta}_h$ and $\overline{\zeta}_h$:

$$\phi_{\pm h}(t,\vec{k}) \doteq \frac{1}{\sqrt{2}}\left[\eta_h(t,\vec{k}) \pm \zeta_h(t,\vec{k})\right], \tag{37a}$$

$$\overline{\phi}_{\pm h}(t,\vec{k}) \doteq \frac{1}{\sqrt{2}}\left[\overline{\eta}_h(t,\vec{k}) \pm \overline{\zeta}_h(t,\vec{k})\right]. \tag{37b}$$

According to equations (34) and (35) they obey the following normalization conditions:

$$\left|\phi_{+h}(t,\vec{k})\right|^2 + \left|\phi_{-h}(t,\vec{k})\right|^2 = 1 = \left|\overline{\phi}_{+h}(t,\vec{k})\right|^2 + \left|\overline{\phi}_{-h}(t,\vec{k})\right|^2. \tag{38}$$

A straightforward calculation shows that in this basis the equations (36a)–(36d) can be written as

$$(\mathrm{i}\partial_t \mp m_{\mathrm{R}})\,\phi_{\pm h} = -(h|\vec{k}| \pm \mathrm{i}m_{\mathrm{I}})\phi_{\mp h}, \tag{39a}$$

$$(\mathrm{i}\partial_t \mp m_{\mathrm{R}})\,\overline{\phi}_{\pm h} = (h|\vec{k}| \mp \mathrm{i}m_{\mathrm{I}})\overline{\phi}_{\mp h}, \tag{39b}$$

where the mass is written as $m(t) = m_{\mathrm{R}}(t) + \mathrm{i}m_{\mathrm{I}}(t)$.

Note that we still have four equations; the positive and negative frequency basis just permits a more compact notation. The two equations contained in (39a) can be however decoupled, as well as those in (39b). At this point it is useful to notice that switching $h \leftrightarrow -h$ in equation (39a) gives equation (39b) with $\overline{\phi}_{\pm h}$ replaced by $\phi_{\pm -h}$. Hence the mode functions $\overline{\phi}_{\pm h}$ will obey the same equations of motion as $\phi_{\pm -h}$, and it suffices to concentrate on $\phi_{\pm h}$, for example.

To decouple the equations (39a), one can start by solving for example ϕ_{-h} and its time derivative in terms of ϕ_{+h} and its derivative:

$$\phi_{-h} = \frac{m_{\mathrm{R}}\phi_{+h} - \mathrm{i}\partial_t\phi_{+h}}{h|\vec{k}| + \mathrm{i}m_{\mathrm{I}}}, \qquad \partial_t\phi_{-h} = \frac{\mathrm{i}\omega^2\phi_{+h} + m_{\mathrm{R}}\partial_t\phi_{+h}}{h|\vec{k}| + \mathrm{i}m_{\mathrm{I}}},$$

where $\omega^2(t) = \left|\vec{k}\right|^2 + \left|m(t)\right|^2$. Then taking the time derivative of equation (39a) with the upper signs, substituting the above expressions and manipulating the result, one finds the following second order differential equation for ϕ_{+h}:

$$\left[\partial_t^2 - \frac{\mathrm{i}(\partial_t m_{\mathrm{I}})}{h|\vec{k}| + \mathrm{i}m_{\mathrm{I}}}\,\partial_t + \omega^2 + \mathrm{i}(\partial_t m_{\mathrm{R}}) + \frac{m_{\mathrm{R}}(\partial_t m_{\mathrm{I}})}{h|\vec{k}| + \mathrm{i}m_{\mathrm{I}}}\right]\phi_{+h} = 0.$$

A similar analysis produces a corresponding equation of motion for ϕ_{-h}. These two equations can again be compactly expressed together as

$$\left[\partial_t^2 \mp \frac{\mathrm{i}(\partial_t m_{\mathrm{I}})}{h|\vec{k}| \pm \mathrm{i}m_{\mathrm{I}}}\,\partial_t + \omega^2 \pm \mathrm{i}(\partial_t m_{\mathrm{R}}) + \frac{m_{\mathrm{R}}(\partial_t m_{\mathrm{I}})}{h|\vec{k}| \pm \mathrm{i}m_{\mathrm{I}}}\right]\phi_{\pm h} = 0. \tag{40}$$

Let us emphasize that equation (40) is still completely general when it comes to the shape of the mass profile. This is as far as we are going to go with general arguments. In order to be able to search for solutions for equation (40), a mass profile has to be specified. The next step towards an exact solution is hence to choose an appropriate time-dependence for our mass function. Before specifying our choice, we shall introduce certain mathematical tools which we will need later on.

4.2 Gauss' hypergeometric functions

This section is based largely on [29] and [30]. Several other books on mathematical methods of physics provide a similar introduction to hypergeometric functions, and more mathematical expositions are of course numerous. Here the focus is on the basic properties of the functions and on relations that will be needed later on. Most of the identities given here are also presented in [26], and some have been taken from [31].

Definition. Let a, $b \in \mathbb{C}$ and $c \in \mathbb{C} \setminus \mathbb{Z}_{\leq 0}$. For all $z \in \mathbb{C}$, $|z| < 1$, *Gauss' hypergeometric function*[7] is defined as

$$ {}_2F_1(a,b,c;z) \doteq \sum_{n=0}^{\infty} \frac{(a)_n (b)_n}{(c)_n} \frac{z^n}{n!}, $$

where $(q)_n$ denotes the Pochhammer symbol

$$ (q)_n \doteq \begin{cases} 1, & n = 0, \\ \prod_{i=0}^{n-1} (q+i) = q(q+1)\cdots(q+n-1), & n > 0. \end{cases} $$

From the above definition one immediately sees that if either a or b is a negative integer, one of the Pochhammer symbol terminates the series and the result is just a polynomial. The three parameters a, b and c give a lot of room to play with. Indeed, many functions can be recognized as special cases of the hypergeometric function, as the following examples illustrate:

$$ \ln(1+z) = z \times {}_2F_1(1,1,2;-z), \tag{41} $$

[7] Also often called just the *hypergeometric function.*

$$\frac{1}{(1-z)^a} = {}_2F_1(a,1,1;z), \tag{42}$$

$$\arcsin(z) = z \times {}_2F_1\left(\frac{1}{2},\frac{1}{2},\frac{3}{2};z^2\right), \tag{43}$$

$$K(z) = \frac{\pi}{2} \times {}_2F_1\left(\frac{1}{2},\frac{1}{2},1;z^2\right), \tag{44}$$

$$T_n(z) = {}_2F_1\left(-n,n,\frac{1}{2};\frac{1-z}{2}\right), \tag{45}$$

where $K(z)$ is the complete elliptic integral of the first kind and $T_n(z)$ is the Chebyshev polynomial. The list could be continued readily; this is just to underline the versatility and generality of the hypergeometric function. It is not very far-fetched to think of it as the mother of all functions.[8]

The Pochhammer symbol can be written in terms of the gamma function as $(q)_n = \frac{\Gamma(q+n)}{\Gamma(q)}$. Using this we get another useful form for Gauss' hypergeometric function:

$${}_2F_1(a,b,c;z) = \sum_{n=0}^{\infty} \frac{\Gamma(a+n)\Gamma(b+n)\Gamma(c)}{\Gamma(c+n)\Gamma(a)\Gamma(b)} \frac{z^n}{n!}. \tag{46}$$

Note that even though we have only defined the hypergeometric function in the disc $|z| < 1$, it can be analytically continued to the region $|z| \geq 1$ too by avoiding the branch points of the function.

For us the most important feature of Gauss' hypergeometric function ${}_2F_1(a,b,c;z)$ is that it solves Euler's hypergeometic differential equation

$$\left\{ z(1-z)\frac{\mathrm{d}^2}{\mathrm{d}z^2} + [c-(1+a+b)z]\frac{\mathrm{d}}{\mathrm{d}z} - ab \right\} f(z) = 0. \tag{47}$$

This can be verified e.g. by substituting (46) into the differential equation and doing the differentiations and manipulating the sums and coefficients, or alternatively by searching for a solution via Frobenius method. Assuming that c is not an integer, the two independent solutions to equation (47) read

$$f_1(z) = C_1 \times {}_2F_1(a,b,c;z), \tag{48a}$$

[8] Yet it is itself a special case of the *generalized hypergeometric function* ${}_pF_q$, which is further generalized by the *Fox–Wright function*, which is a special case of the *Fox H-function*...

$$f_2(z) = C_2\, z^{1-c} \times {}_2F_1(1+a-c, 1+b-c, 2-c; z), \tag{48b}$$

where C_1 and C_2 are constants.

There are many relations concerning the hypergeometric function that will be needed later on. We will end this short section on hypergeometric functions by listing them here as identities. Some of these relations are obvious, while others would require a more elaborate treatment for a proof.

Identity 1 (Permutation symmetry)**.**

$${}_2F_1(a, b, c; z) = {}_2F_1(b, a, c; z)$$

Identity 2 (Euler's transformation)**.**

$${}_2F_1(a, b, c; z) = (1-z)^{c-a-b} \times {}_2F_1(c-a, c-b, c; z)$$

Identity 3.

$$\begin{aligned} {}_2F_1(a, b, c; z) = {} & \frac{\Gamma(c)\Gamma(c-a-b)}{\Gamma(c-a)\Gamma(c-b)} \times {}_2F_1(a, b, 1+a+b-c; 1-z) \\ & + \frac{\Gamma(c)\Gamma(a+b-c)}{\Gamma(a)\Gamma(b)} (1-z)^{c-a-b} \times {}_2F_1(c-a, c-b, 1-a-b+c; 1-z) \end{aligned}$$

Identity 4.

$$\frac{\mathrm{d}}{\mathrm{dz}} \Big[{}_2F_1(a, b, c; z) \Big] = \frac{ab}{c} \times {}_2F_1(1+a, 1+b, 1+c; z)$$

Identity 5.

$$\frac{abz}{c} \times {}_2F_1(1+a, 1+b, 1+c; z) = (c-1) \Big[{}_2F_1(a, b, c-1; z) - {}_2F_1(a, b, c; z) \Big]$$

Identity 6.

$$\begin{aligned} (c-b-1) \times {}_2F_1(a, b, c; z) = {} & (c-1) \times {}_2F_1(a, b, c-1; z) \\ & - b \times {}_2F_1(a, 1+b, c; z) \end{aligned}$$

Identity 7.

$$\begin{aligned} (c-b-1) \times {}_2F_1(a, b, c; z) = {} & (a-b-1)(1-z) \times {}_2F_1(a, 1+b, c; z) \\ & + (c-a) \times {}_2F_1(a-1, 1+b, c; z) \end{aligned}$$

Identity 8 (Mirror symmetry)**.**

$$[{}_2F_1(a,b,c;z)]^* = {}_2F_1(a^*,b^*,c^*;z^*),$$

where the asterisk denotes complex conjugation.

Identity 9 (Wronskian)**.**

$$\begin{aligned}&\mathcal{W}\left[{}_2F_1(a,b,c;z), z^{1-c}(1-z)^{c-a-b}\times {}_2F_1(1-a,1-b,2-c;z)\right]\\&\quad = (1-c)z^{-c}(1-z)^{c-a-b-1},\end{aligned}$$

where $\mathcal{W}$ computes the Wronskian, $\mathcal{W}[f_1,f_2] = f_1\frac{\mathrm{d}f_2}{\mathrm{d}z} - \frac{\mathrm{d}f_1}{\mathrm{d}z}f_2$ for two differentiable functions $f_1(z)$ and $f_2(z)$.

4.3 Kink-wall

We shall now return to equation (40) and proceed to solve it in a certain case. With applications to EWBG in mind, we choose the time-dependence of the mass to be

$$m(t) = m_1 + m_2\tanh\left(-\frac{t}{\tau_w}\right), \tag{49}$$

where m_1 and m_2 are complex time-independent mass parameters and τ_w is a parameter describing the time scale (or width) of the wall. This choice, known as the *kink profile*, is common in studies related to EWBG, and it is expected to describe different phase transition scenarios quite well [26, 27]. At early times ($t \to -\infty$) the mass becomes $m_1 + m_2$ and at late times ($t \to \infty$) $m_1 - m_2$. Choosing $m_1 = -m_2$ corresponds then to a situation where the mass changes continuously from a zero value to some finite value. We shall however keep the parameters unspecified for now. Figure 4 illustrates the shape of the mass function for certain parameters.

Before substituting our Ansatz (49) into our equations of motion, let us note that

$$\frac{m_{\mathrm{I}}(t)}{m_{\mathrm{R}}(t)} = \frac{m_{1\mathrm{I}} + m_{2\mathrm{I}}\tanh\left(-\frac{t}{\tau_w}\right)}{m_{1\mathrm{R}} + m_{2\mathrm{R}}\tanh\left(-\frac{t}{\tau_w}\right)},$$

where we have written $m_1 = m_{1\mathrm{R}} + \mathrm{i}m_{1\mathrm{I}}$ and $m_2 = m_{2\mathrm{R}} + \mathrm{i}m_{2\mathrm{I}}$. So the ratio of the imaginary and real parts of the mass is indeed time-dependent, and

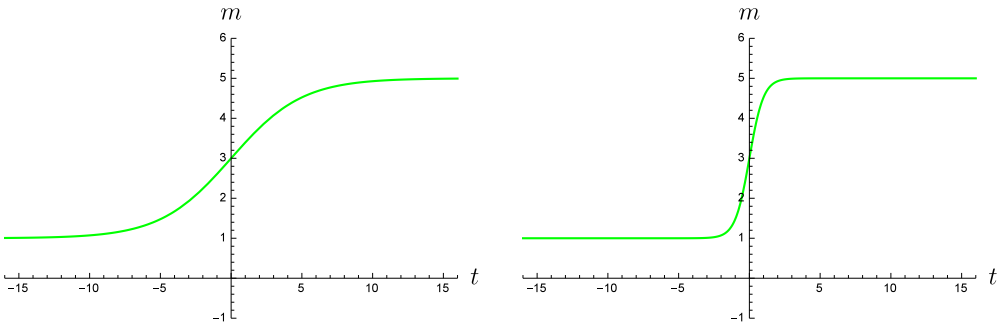

(a) **(b)**

Figure 4: The kink profile of equation (49), describing the change of the mass in time. The mass parameters in both figures are $m_1 = 3$ and $m_2 = -2$. Figure (a) has $\tau_w = 5$, while Figure (b) has $\tau_w = 1$ corresponding to a more abrupt mass change.

our model may involve CP-violation. Without affecting this CP-violation, we are free to perform global rotations on our spinors. It turns out that for the problem at hand it is suitable to perform a rotation that removes the imaginary part of the mass parameter multiplying the hyperbolic tangent. Such a rotation is given by

$$m(t) \longrightarrow m(t)\mathrm{e}^{\mathrm{i}\iota}; \qquad \iota = \arctan\left(-\frac{m_{2\mathrm{I}}}{m_{2\mathrm{R}}}\right).$$

Indeed, letting φ_1 and φ_2 be the phases of m_1 and m_2, respectively, the above rotation amounts to

$$\begin{aligned} m(t) &\longrightarrow \left[m_1 + m_2 \tanh\left(-\frac{t}{\tau_w}\right)\right] \mathrm{e}^{\mathrm{i}\iota} \\ &= \left[|m_1|\mathrm{e}^{\mathrm{i}\varphi_1} + |m_2|\mathrm{e}^{\mathrm{i}\varphi_2} \tanh\left(-\frac{t}{\tau_w}\right)\right] \mathrm{e}^{-\mathrm{i}\varphi_2} \\ &= |m_1|\mathrm{e}^{\mathrm{i}(\varphi_1-\varphi_2)} + |m_2| \tanh\left(-\frac{t}{\tau_w}\right) \\ &\doteq \hat{m}_1 + \hat{m}_2 \tanh\left(-\frac{t}{\tau_w}\right), \end{aligned}$$

where now $\hat{m}_1 \in \mathbb{C}$ and $\hat{m}_2 \in \mathbb{R}$. In what follows we shall for convenience drop the hats from these parameters and call them again $m_1 = m_{1\mathrm{R}} + \mathrm{i}m_{1\mathrm{I}}$ and $m_2 = m_{2\mathrm{R}}$. It should be kept in mind that these are not the parameters m_1 and m_2 we started with, but are related to them through the global rotation.

The main advantage of the rotation is that now our mass is of the form

$$m(t) = m_{1\mathrm{R}} + m_{2\mathrm{R}} \tanh\left(-\frac{t}{\tau_w}\right) + \mathrm{i}m_{1\mathrm{I}} = m_{\mathrm{R}}(t) + \mathrm{i}m_{\mathrm{I}}, \tag{50}$$

i.e. there is no time-dependence in the imaginary part of the mass. The two terms involving $\partial_t m_{\mathrm{I}}$ in equation (40) can then be dropped, and we are left with the following evidently simpler equation of motion:

$$\left[\partial_t^2 + \omega^2 \pm \mathrm{i}(\partial_t m_{\mathrm{R}})\right] \phi_{\pm h} = 0. \tag{51}$$

Despite the simple appearance of the above equation, it still is a second order differential equation containing also a derivative of the hyperbolic tangent, and its solutions are not obvious at first sight. The situation can be simplified by defining a new variable that factorizes the singularities:

$$z = \frac{1}{2}\left[1 - \tanh\left(-\frac{t}{\tau_w}\right)\right].$$

Now the limit $z \to 0$ corresponds to early times ($t \to -\infty$) and $z \to 1$ to late times ($t \to \infty$). With this new variable we can write the mass as $m = m_1 + (1-2z)m_2$. Let us now transform the quantities in equation (51) accordingly (for clarity we will from now on use total derivatives instead of partial ones, since they are in this case equivalent):

- $\dfrac{\mathrm{d}}{\mathrm{d}t} m_{\mathrm{R}} = \dfrac{\mathrm{d}}{\mathrm{d}t}\left[m_{2\mathrm{R}} \tanh\left(-\dfrac{t}{\tau_w}\right)\right] = -\dfrac{m_{2\mathrm{R}}}{\tau_w}\left[1 - \tanh^2\left(-\dfrac{t}{\tau_w}\right)\right]$
  $= \dfrac{4m_{2\mathrm{R}}}{\tau_w} z(z-1)$
- $\dfrac{\mathrm{d}}{\mathrm{d}t} = \dfrac{2}{\tau_w} z(1-z) \dfrac{\mathrm{d}}{\mathrm{dz}}$
- $\dfrac{\mathrm{d}^2}{\mathrm{d}t^2} = \left[\dfrac{2}{\tau_w} z(1-z)\right]^2 \dfrac{\mathrm{d}^2}{\mathrm{d}z^2} + \dfrac{4}{\tau_w^2} z(1-z)(1-2z) \dfrac{\mathrm{d}}{\mathrm{dz}}$
- $\omega^2 = \left|\vec{k}\right|^2 + m_{\mathrm{R}}^2 + m_{\mathrm{I}}^2$
  $= \left|\vec{k}\right|^2 + m_{\mathrm{I}}^2 + (m_{1\mathrm{R}} + m_{2\mathrm{R}})^2 - 4m_{1\mathrm{R}}m_{2\mathrm{R}}z - 4m_{2\mathrm{R}}^2 z(1-z).$

Equation (51) in terms of the z-coordinate is hence

$$\left\{ \left[\frac{2}{\tau_w} z(1-z)\right]^2 \frac{\mathrm{d}^2}{\mathrm{d}z^2} + \frac{4}{\tau_w^2} z(1-z)(1-2z) \frac{\mathrm{d}}{\mathrm{d}z} - 4m_{1\mathrm{R}} m_{2\mathrm{R}} z \right.$$
$$\left. - 4m_{2\mathrm{R}} z(1-z) \left(m_{2\mathrm{R}} \pm \frac{\mathrm{i}}{\tau_w} \right) + \left|\vec{k}\right|^2 + m_{\mathrm{I}}^2 + (m_{1\mathrm{R}} + m_{2\mathrm{R}})^2 \right\} \phi_{\pm h} = 0. \tag{52}$$

Next we redefine $\phi_{\pm h}$ in terms of yet new mode functions $\Xi_{\pm h}(z)$ as

$$\phi_{\pm h} = z^{\alpha}(1-z)^{\beta} \Xi_{\pm h}(z). \tag{53}$$

The parameters α and β are chosen to be

$$\alpha = -\frac{\mathrm{i}}{2} \tau_w \omega_-, \qquad \beta = -\frac{\mathrm{i}}{2} \tau_w \omega_+, \tag{54}$$

where ω_- and ω_+ are defined as the early- and late-time limits of the basic dispersion relation:

$$\omega_{\mp} \doteq \omega(t \to \mp\infty) = \sqrt{\left|\vec{k}\right|^2 + m_{\mathrm{I}}^2 + (m_{1\mathrm{R}} \pm m_{2\mathrm{R}})^2}.$$

This specific rescaling is chosen because it allows us to finally deform the equations of motion (52) into a form whose solutions are known. Substituting the rescaling (53) into equation (52) and performing a fair bit of algebra one ends up with the following equation for $\Xi_{\pm h}$:

$$\left\{ z(1-z) \frac{\mathrm{d}^2}{\mathrm{d}z^2} + [1 + 2\alpha - 2z(1+\alpha+\beta)] \frac{\mathrm{d}}{\mathrm{d}z} + \tau_w m_{2\mathrm{R}}^2 \right.$$
$$\left. \pm \mathrm{i}\tau_w^2 m_{2\mathrm{R}}^2 + (\alpha+\beta)(1+\alpha+\beta) \right\} \Xi_{\pm h}(z) = 0. \tag{55}$$

To make one last simplification, we define the following parameters:

$$\begin{cases} a_{\pm} \doteq 1 + \alpha + \beta \mp \mathrm{i}\tau_w m_{2\mathrm{R}} & \text{(56a)} \\ b_{\pm} \doteq \alpha + \beta \pm \mathrm{i}\tau_w m_{2\mathrm{R}} & \text{(56b)} \\ c \doteq 1 + 2\alpha. & \text{(56c)} \end{cases}$$

Straight from the above definitions one can verify that

$$c - (1 + a_{\pm} + b_{\pm})z = 1 + 2\alpha - 2z(1+\alpha+\beta),$$
$$a_{\pm} b_{\pm} = \tau_w m_{2\mathrm{R}}^2 \pm \mathrm{i}\tau_w^2 m_{2\mathrm{R}}^2 + (\alpha+\beta)(1+\alpha+\beta).$$

So with these parameters equation (55) can be finally written as

$$\left\{ z(1-z)\frac{\mathrm{d}^2}{\mathrm{d}z^2} + [c - (1 + a_\pm + b_\pm)z]\,\frac{\mathrm{d}}{\mathrm{d}z} - a_\pm b_\pm \right\} \Xi_{\pm h}(z) = 0. \quad (57)$$

Now it should be clear why we took the side road and talked about Gauss' hypergeometric functions in the previous section. Comparing equation (57) with equation (47) yields a rather satisfying fact: the equations of motion for the mode functions have reduced to Euler's hypergeometric differential equation, solutions of which are the previously considered Gauss' hypergeometric functions.

Since the parameter c is clearly not an integer, each of equations (57) has two independent solutions. These solutions are the ones given by equations (48):

$$\Xi^{(1)}_{\pm h}(z) = C^{(1)}_{\pm h} \times {}_2F_1(a_\pm, b_\pm, c; z), \quad (58a)$$

$$\Xi^{(2)}_{\pm h}(z) = C^{(2)}_{\pm h}\, z^{1-c} \times {}_2F_1(1 + a_\pm - c, 1 + b_\pm - c, 2 - c; z), \quad (58b)$$

where $C^{(1)}_{\pm h}$ and $C^{(2)}_{\pm h}$ are constants. The solutions to equations (51) are then obtained by simply multiplying the above expressions by $z^\alpha(1-z)^\beta$:

$$\phi^{(1)}_{\pm h} = C^{(1)}_{\pm h} z^\alpha (1-z)^\beta \times {}_2F_1(a_\pm, b_\pm, c; z), \quad (59a)$$

$$\phi^{(2)}_{\pm h} = C^{(2)}_{\pm h}\, z^{-\alpha} (1-z)^\beta \times {}_2F_1(1 + a_\pm - c, 1 + b_\pm - c, 2 - c; z), \quad (59b)$$

where we noticed that in the second solution we have $1 + \alpha - c = -\alpha$ in the exponent of z. Our next mission is to determine the constants $C^{(1,2)}_{\pm h}$ so that the modes $\phi_{\pm h}$ constructed suitably from the above solutions are normalized according to equation (38). Since this task will require some effort, a new chapter will be devoted to it.

4.4 Normalization

We shall start by looking at the asymptotic behaviours of the solutions (59). At early times ($z \to 0$) the hypergeometric functions ${}_2F_1$ approach unity, as is clear from their definition. For the prefactors we may use the observation that

$$z = \frac{1}{2}\left[1 - \tanh\left(-\frac{t}{\tau_w}\right)\right] = \frac{\mathrm{e}^{t/\tau_w}}{\mathrm{e}^{-t/\tau_w} + \mathrm{e}^{t/\tau_w}} \approx \mathrm{e}^{2t/\tau_w}$$

for small values of z (i.e. large negative values of t). From these we deduce that at early times the modes attain the following asymptotic forms:

$$\phi_{\pm h}^{(1)} \xrightarrow{t\to-\infty} C_{\pm h}^{(1)} \mathrm{e}^{2t\alpha/\tau_w} = C_{\pm h}^{(1)} \mathrm{e}^{-\mathrm{i}t\omega_-}, \tag{60a}$$

$$\phi_{\pm h}^{(2)} \xrightarrow{t\to-\infty} C_{\pm h}^{(2)} \mathrm{e}^{-2t\alpha/\tau_w} = C_{\pm h}^{(2)} \mathrm{e}^{\mathrm{i}t\omega_-}. \tag{60b}$$

This is certainly delightful: we obtain the basic positive and negative frequency plane-wave solutions (as we should, of course). From these we will only pick the positive frequency solution (60a) to represent our solution $\phi_{\pm h}$ (this is just choosing an initial condition). So from now on the mode function we will be normalizing is just $\phi_{\pm h}^{(1)} = \phi_{\pm h}$, and therefore we will for simplicity drop the upper indices from the constants too: $C_{\pm h} \doteq C_{\pm h}^{(1)}$.

At late times we expect to have a mixture of the positive and negative frequency solutions, and this indeed turns out to be the case. To establish this fact we may use Identity 3, which allows us to transform the arguments of the hypergeometric functions from z to $1-z$. Under this transformation our mode function becomes

$$\begin{aligned}\phi_{\pm h} = {} & C_{\pm h}\frac{\Gamma(c)\Gamma(c-a_\pm-b_\pm)}{\Gamma(c-a_\pm)\Gamma(c-b_\pm)} z^\alpha (1-z)^\beta \\ & \times {}_2F_1(a_\pm, b_\pm, 1+a_\pm+b_\pm-c; 1-z) \\ & + C_{\pm h}\frac{\Gamma(c)\Gamma(a_\pm+b_\pm-c)}{\Gamma(a_\pm)\Gamma(b_\pm)} z^\alpha (1-z)^{-\beta} \\ & \times {}_2F_1(c-a_\pm, c-b_\pm, 1-a_\pm-b_\pm+c; 1-z),\end{aligned} \tag{61}$$

where we used the fact that $\beta + c - a_\pm - b_\pm = -\beta$. Now the late-time limit $z \to 1$ ($t \to \infty$) is easy to consider since the hypergeometric functions approach again unity. For the prefactors we may now use

$$1 - z = \frac{\mathrm{e}^{-t/\tau_w}}{\mathrm{e}^{-t/\tau_w} + \mathrm{e}^{t/\tau_w}} \approx \mathrm{e}^{-2t/\tau_w}$$

for large values of t. Under these limits the expression (61) gives the following asymptotic form for the mode function at late times:

$$\begin{aligned}\phi_{\pm h} \xrightarrow{t\to\infty} {} & C_{\pm h}\frac{\Gamma(c)\Gamma(c-a_\pm-b_\pm)}{\Gamma(c-a_\pm)\Gamma(c-b_\pm)} \mathrm{e}^{-2t\beta/\tau_w} + C_{\pm h}\frac{\Gamma(c)\Gamma(a_\pm+b_\pm-c)}{\Gamma(a_\pm)\Gamma(b_\pm)} \mathrm{e}^{2t\beta/\tau_w} \\ = {} & C_{\pm h}\frac{\Gamma(c)\Gamma(c-a_\pm-b_\pm)}{\Gamma(c-a_\pm)\Gamma(c-b_\pm)} \mathrm{e}^{\mathrm{i}t\omega_+} + C_{\pm h}\frac{\Gamma(c)\Gamma(a_\pm+b_\pm-c)}{\Gamma(a_\pm)\Gamma(b_\pm)} \mathrm{e}^{-\mathrm{i}t\omega_+}.\end{aligned}$$

Indeed, we obtained a combination of the positive and negative frequency waves at late times.

In a similar fashion as we got the early-time positive and negative frequency modes (60), one can construct the corresponding positive and negative frequency solutions for late times. Since $\phi_{\pm h}$ are solutions to our equations of motion, so must be both parts of expression (61) *independently*, since the two are linearly independent. We can thus construct the following solutions applicable at late times:

$$\begin{aligned}\widetilde{\phi}^{(1)}_{\pm h} &= \widetilde{C}^{(1)}_{\pm h} z^{\alpha}(1-z)^{-\beta} \times {}_2F_1(c-a_{\pm}, c-b_{\pm}, 1-a_{\pm}-b_{\pm}+c; 1-z) \\ &= \widetilde{C}^{(1)}_{\pm h} z^{-\alpha}(1-z)^{-\beta} \times {}_2F_1(1-a_{\pm}, 1-b_{\pm}, 1-a_{\pm}-b_{\pm}+c; 1-z)\end{aligned} \tag{62a}$$

$$\widetilde{\phi}^{(2)}_{\pm h} = \widetilde{C}^{(2)}_{\pm h}\, z^{\alpha}(1-z)^{\beta} \times {}_2F_1(a_{\pm}, b_{\pm}, 1+a_{\pm}+b_{\pm}-c; 1-z), \tag{62b}$$

where we used Identities 1 and 2, and $\widetilde{C}^{(1)}_{\pm h}$ and $\widetilde{C}^{(2)}_{\pm h}$ are constants. As the earlier performed analysis shows, these indeed reduce to positive and negative frequency solutions at late times:

$$\widetilde{\phi}^{(1)}_{\pm h} \xrightarrow{t\to\infty} \widetilde{C}^{(1)}_{\pm h}\, \mathrm{e}^{-\mathrm{i}t\omega_+}, \tag{63a}$$

$$\widetilde{\phi}^{(2)}_{\pm h} \xrightarrow{t\to\infty} \widetilde{C}^{(2)}_{\pm h}\, \mathrm{e}^{\mathrm{i}t\omega_+}. \tag{63b}$$

Perhaps it should be stressed, that all the so far represented solutions are equally valid at all times. The above analysis merely distinguishes them by their behaviour at different times and therefore allows one to easily construct solutions suitable for different scenarios.

We shall proceed to work with $\phi_{\pm h}$ and the determination of the constants $C_{\pm h}$. First we will work out how the two constants C_{+h} and C_{-h} are related to each other. This relation is buried in equation (39a), relating ϕ_{+h} to ϕ_{-h}. Using $m_{\mathrm{R}} = m_{1\mathrm{R}} + (1-2z)m_{2\mathrm{R}}$ and writing (39a) in terms of the z-coordinate gives

$$\left\{ z(1-z)\,\frac{\mathrm{d}}{\mathrm{d}z} \pm \frac{\mathrm{i}\tau_w}{2}\left[m_{1\mathrm{R}} + (1-2z)m_{2\mathrm{R}}\right] \right\} \phi_{\pm h} = \frac{\mathrm{i}\tau_w}{2}(h\left|\vec{k}\right| \pm \mathrm{i}m_{\mathrm{I}})\phi_{\mp h}. \tag{64}$$

Remember that with the kink-profile for the mass we were able to rotate the time dependence of m_{I} away, and therefore m_{I} remains in the above equation as it is. The parameters $m_{1\mathrm{R}}$ and $m_{2\mathrm{R}}$ can be written in terms of

the parameters inside the hypergeometric functions $a_\pm$, $b_\pm$ and c. To see this, consider the following relations:

$$1) \qquad \pm \mathrm{i} m_{1\mathrm{R}} \tau_w = \frac{(a_\pm + b_\pm - 1)(1 + a_\pm + b_\pm - 2c)}{2(a_\pm - b_\pm - 1)},$$
$$2) \qquad \pm \mathrm{i} m_{2\mathrm{R}} \tau_w = \frac{1 - a_\pm + b_\pm}{2}.$$

These can be easily verified by straightforward calculations. Using them one can replace $m_{1\mathrm{R}}$ and $m_{2\mathrm{R}}$ in equation (64) by the parameters of the hypergeometric functions. Doing this and substituting $\phi_{\pm h}$ from equation (59a) to equation (64) gives, after a minor effort, the following result:

$$\left[z(1-z)\frac{\mathrm{d}}{\mathrm{dz}} + \alpha(1-z) - \beta z + \frac{(a_\pm + b_\pm - 1)(1 + a_\pm + b_\pm - 2c)}{4(a_\pm - b_\pm - 1)} \right.$$
$$\left. + \frac{1 - a_\pm + b_\pm}{4}(1 - 2z) \right] C_{\pm h} \times {}_2F_1(a_\pm, b_\pm, c; z) = \frac{\mathrm{i}\tau_w}{2}(h|\vec{k}| \pm \mathrm{i} m_{\mathrm{I}}) C_{\mp h}$$
$$\times {}_2F_1(a_\mp, b_\mp, c; z).$$

The left-hand side can be further simplified by using

$$\alpha = \frac{c-1}{2}, \qquad \beta = \frac{a_\pm + b_\pm - c}{2}.$$

The result is

$$\left[z(1-z)\frac{\mathrm{d}}{\mathrm{dz}} + \frac{b_\pm(a_\pm - c)}{a_\pm - b_\pm - 1} - b_\pm z \right] C_{\pm h} \times {}_2F_1(a_\pm, b_\pm, c; z)$$
$$= \frac{\mathrm{i}\tau_w}{2}(h|\vec{k}| \pm \mathrm{i} m_{\mathrm{I}}) C_{\mp h} \times {}_2F_1(a_\mp, b_\mp, c; z).$$

In order to relate the hypergeometric functions on both sides to each other, they should contain same parameters. To this end we can use the relations $a_\mp = b_\pm + 1$ and $b_\mp = a_\pm - 1$ together with Identity 1 to obtain

$$\left[z(1-z)\frac{\mathrm{d}}{\mathrm{dz}} + \frac{b_\pm(a_\pm - c)}{a_\pm - b_\pm - 1} - b_\pm z \right] C_{\pm h} \times {}_2F_1(a_\pm, b_\pm, c; z)$$
$$= \frac{\mathrm{i}\tau_w}{2}(h|\vec{k}| \pm \mathrm{i} m_{\mathrm{I}}) C_{\mp h} \times {}_2F_1(a_\pm - 1, 1 + b_\pm, c; z). \tag{65}$$

Let us now focus on the left-hand side and try to get the hypergeometric function match the one on the right-hand side. Identities 4 and 5 enable

us to write equation (65) as

$$\Big\{(1-z)(c-1)\times {}_2F_1(a_\pm,b_\pm,c-1;z)+\Big[\frac{b_\pm(a_\pm-c)}{a_\pm-b_\pm-1}+1-c$$
$$+(c-1-b_\pm)z\Big]\times {}_2F_1(a_\pm,b_\pm,c;z)\Big\}C_{\pm h}=\frac{\mathrm{i}\tau_w}{2}(h|\vec{k}|\pm \mathrm{i}m_\mathrm{I})C_{\mp h}$$
$$\times {}_2F_1(a_\pm-1,1+b_\pm,c;z).$$

This is already great since we have got rid of all the derivatives. Now applying Identity 6 to the left-hand side of the above equation results in

$$b_\pm(1-z)\times {}_2F_1(a_\pm,1+b_\pm,c;z)+\frac{b_\pm(1+b_\pm-c)}{a_\pm-b_\pm-1}\times {}_2F_1(a_\pm,b_\pm,c;z)$$
$$=\frac{\mathrm{i}\tau_w}{2}(h|\vec{k}|\pm \mathrm{i}m_\mathrm{I})\frac{C_{\mp h}}{C_{\pm h}}\times {}_2F_1(a_\pm-1,1+b_\pm,c;z).$$

The final identity to be used here is Identity 7 which is almost tailor-made for the situation at hand. Using it the above equation finally attains the form

$$\frac{b_\pm(a_\pm-c)}{a_\pm-b_\pm-1}\times {}_2F_1(a_\pm-1,b_\pm+1,c;z)=\frac{\mathrm{i}\tau_w}{2}(h|\vec{k}|\pm \mathrm{i}m_\mathrm{I})\frac{C_{\mp h}}{C_{\pm h}}$$
$$\times {}_2F_1(a_\pm-1,b_\pm+1,c;z).$$

Now the hypergeometric functions on both sides of the equation match. Since the equation has to hold for all values of z, we may deduce the following relation between the constants:

$$\frac{C_{\pm h}}{C_{\mp h}}=\frac{\mathrm{i}\tau_w(a_\pm-b_\pm-1)}{2b_\pm(a_\pm-c)}(h|\vec{k}|\pm \mathrm{i}m_\mathrm{I}). \tag{66}$$

Equation (66) is basically enough so that we could start to apply the normalization conditions for determining the constants. Let us first however write equation (66) completely in terms of physical parameters, i.e. remove the parameters $a_\pm$, $b_\pm$ and c. This can be done with the help of the following relations:

3) $(a_\pm-b_\pm-1)^2=-4m_{2\mathrm{R}}^2\tau_w^2$,

4) $b_\pm(a_\pm-c)=m_{2\mathrm{R}}\tau_w^2(m_{1\mathrm{R}}+m_{2\mathrm{R}}\mp\omega_-)$,

5) $(a_\pm-1)(1+b_\pm-c)=m_{2\mathrm{R}}\tau_w^2(m_{1\mathrm{R}}+m_{2\mathrm{R}}\pm\omega_-)$,

6) $\dfrac{b_\pm(a_\pm-1)(a_\pm-c)(1+b_\pm-c)}{(a_\pm-b_\pm-1)^2}=\dfrac{\tau_w^2}{4}(|\vec{k}|^2+m_\mathrm{I}^2)$.

Proofs of these relations are again direct calculations. Using the above relations one can write equation (66) as

$$\frac{C_{\pm h}}{C_{\mp h}} = -\frac{h\left|\vec{k}\right| \pm \mathrm{i}m_{\mathrm{I}}}{\sqrt{\left|\vec{k}\right|^2 + m_{\mathrm{I}}^2}} \sqrt{\frac{\omega_- \pm (m_{1\mathrm{R}} + m_{2\mathrm{R}})}{\omega_- \mp (m_{1\mathrm{R}} + m_{2\mathrm{R}})}}, \tag{67}$$

where the right-hand side indeed consists of only physical parameters.

Using the normalization condition (38) together with the solution (59a) and equation (66) we can write

$$\begin{aligned} 1 &= \left| C_{+h} z^{\alpha} (1-z)^{\beta} \times {}_2F_1(a_+, b_+, c; z) \right|^2 \\ &+ \left| C_{-h} z^{\alpha} (1-z)^{\beta} \times {}_2F_1(a_-, b_-, c; z) \right|^2 \\ &= |C_{+h}|^2 \left[|{}_2F_1(a_+, b_+, c; z)|^2 - \frac{b_+(a_+ - c)}{(a_+ - 1)(1 + b_+ - c)} \, |{}_2F_1(a_-, b_-, c; z)|^2 \right], \end{aligned} \tag{68}$$

where in the last step we used also the fact that α and β are, according to their definition (54), purely imaginary. In order to get to manipulate the moduli of the hypergeometric functions, we first note that $a_\pm^* = 2 - a_\pm$, $b_\pm^* = -b_\pm$ and $c^* = 2 - c$. Using this together with Identity 8 and the fact that z is real allows us to write

$$|{}_2F_1(a_\pm, b_\pm, c; z)|^2 = {}_2F_1(2 - a_\pm, -b_\pm, 2 - c; z) {}_2F_1(a_\pm, b_\pm, c; z).$$

Hence equation (68) can be written as

$$\begin{aligned} 1 = |C_{+h}|^2 \Bigg[& {}_2F_1(a_+, b_+, c; z) \times {}_2F_1(2 - a_+, -b_+, 2 - c; z) \\ & - \frac{b_+(a_+ - c)}{(a_+ - 1)(1 + b_+ - c)} \times {}_2F_1(a_+ - 1, 1 + b_+, c; z) \\ & \times {}_2F_1(1 - a_+, 1 - b_+, 2 - c; z) \Bigg], \end{aligned} \tag{69}$$

where we again used the relations $a_\mp = b_\pm + 1$ and $b_\mp = a_\pm - 1$ and Identity 1.

From the equation above it is clear that the difficulty in solving a meaningful form for the constants $C_{\pm h}$ is once more in the hypergeometric

functions. In order to get progress they should be somehow simplified, which is exactly what we are about to do. Combining equation (65) with equation (66) gives rise to the following relation:

$$\begin{aligned}&\left[\frac{a_+ - b_+ - 1}{b_+(a_+ - c)}\, z(1-z)\,\frac{\mathrm{d}}{\mathrm{dz}} + \frac{1 - a_+ + b_+}{a_+ - c}\, z + 1\right] \times {}_2F_1(a_+, b_+, c; z) \\ &= F_1(a_+ - 1, 1 + b_+, c; z).\end{aligned} \tag{70}$$

Upon interchanging $a_+ \to 1 - b_+$, $b_+ \to 1 - a_+$ and $c \to 2 - c$ in the above relation and using Identity 1 another useful relation comes out:

$$\begin{aligned}&\left[\frac{a_+ - b_+ - 1}{(1 - a_+)(c - b_+ - 1)}\, z(1-z)\,\frac{\mathrm{d}}{\mathrm{dz}} + \frac{1 - a_+ + b_+}{c - b_+ - 1}\, z + 1\right] \\ &\times {}_2F_1(1 - a_+, 1 - b_+, 2 - c; z) = {}_2F_1(2 - a_+, -b_+, 2 - c; z).\end{aligned} \tag{71}$$

The usefulness of these relations lies in the fact that the hypergeometric functions on the right-hand sides of equations (70) and (71) appear also in equation (69). Substituting the functions into equation (69) results in

$$\begin{aligned}1 = |C_{+h}|^2 \Bigg\{ &{}_2F_1(a_+, b_+, c; z) \left[\frac{a_+ - b_+ - 1}{(1 - a_+)(c - b_+ - 1)}\, z(1-z)\,\frac{\mathrm{d}}{\mathrm{dz}} + 1\right. \\ &\left. + \frac{1 - a_+ + b_+}{c - b_+ - 1}\, z\right] \times {}_2F_1(1 - a_+, 1 - b_+, 2 - c; z) \\ &- \frac{b_+(a_+ - c)}{(a_+ - 1)(1 + b_+ - c)} \left[\frac{a_+ - b_+ - 1}{b_+(a_+ - c)}\, z(1-z)\,\frac{\mathrm{d}}{\mathrm{dz}} \left[{}_2F_1(a_+, b_+, c; z)\right]\right. \\ &\left. + \left(\frac{1 - a_+ + b_+}{a_+ - c}\, z + 1\right) \times {}_2F_1(a_+, b_+, c; z)\right] \\ &\times {}_2F_1(1 - a_+, 1 - b_+, 2 - c; z)\Bigg\}.\end{aligned} \tag{72}$$

At this point one could (quite justly) argue that we have only succeeded in achieving an even more complicated expression. However, we have been able to reduce the number of hypergeometric functions with different arguments from four to two, which is already a worthy improvement. Moreover, this new horrible-looking expression can be simplified

by making use of the Wronskian of hypergeometric functions. First we write equation (72) with the help of the Wronskian $\mathcal{W}[\cdot,\cdot]$ as

$$\begin{aligned}
1 = |C_{+h}|^2 \Bigg\{ & \frac{a_+ - b_+ - 1}{(1-a_+)(c-b_+-1)}\, z(1-z) \Bigg[{}_2F_1(a_+, b_+, c; z) \\
& \times \frac{\mathrm{d}}{\mathrm{dz}} \Big[{}_2F_1(1-a_+, 1-b_+, 2-c; z) \Big] - {}_2F_1(1-a_+, 1-b_+, 2-c; z) \\
& \times \frac{\mathrm{d}}{\mathrm{dz}} \Big[{}_2F_1(a_+, b_+, c; z) \Big] \Bigg] + {}_2F_1(a_+, b_+, c; z) \Bigg[1 - \frac{b_+(a_+ - c)}{(a_+ - 1)(1 + b_+ - c)} \\
& + \frac{a_+ - b_+ - 1}{1 + b_+ - c} \left(1 + \frac{b_+}{a_+ - 1} \right) z \Bigg] \times {}_2F_1(1-a_+, 1-b_+, 2-c; z) \Bigg\} \\
= |C_{+h}|^2 \Bigg\{ & \frac{a_+ - b_+ - 1}{(1-a_+)(c-b_+-1)}\, z(1-z) \\
& \times \mathcal{W}\Big[{}_2F_1(a_+, b_+, c; z), {}_2F_1(1-a_+, 1-b_+, 2-c; z) \Big] \\
& + {}_2F_1(a_+, b_+, c; z) \Bigg[1 - \frac{b_+(a_+ - c)}{(a_+ - 1)(1 + b_+ - c)} \\
& + \frac{a_+ - b_+ - 1}{1 + b_+ - c} \left(1 + \frac{b_+}{a_+ - 1} \right) z \Bigg] \times {}_2F_1(1-a_+, 1-b_+, 2-c; z) \Bigg\}.
\end{aligned} \tag{73}$$

Then we can make use of Identity 9. Opening the Wronskian in the identity, differentiating the pre-factors in front of the hypergeometric functions, reforming a new Wronskian out of the hypergeometric functions and doing some algebraic manipulations results in the following relation:

$$\begin{aligned}
\mathcal{W}\Big[{}_2F_1(a, b, c; z), {}_2F_1(1-a, 1-b, 2-c; z) \Big] = & \frac{1-c}{z(1-z)} \\
& - {}_2F_1(a, b, c; z) \left(\frac{1-c}{z} + \frac{a+b-c}{1-z} \right) \times {}_2F_1(1-a, 1-b, 2-c; z).
\end{aligned}$$

The Wronskian in the above relation is exactly the one appearing in equation (73) too. Substituting the Wronskian gives rise to an equation with only two kinds of hypergeometric functions and no derivatives nor

$(1-z)^{-1}$-poles:

$$
\begin{aligned}
1 = |C_{+h}|^2 \Bigg\{ & \frac{(a_+ - b_+ - 1)(1-c)}{(1-a_+)(c-b_+-1)} + {}_2F_1(a_+, b_+, c; z) \\
& \times \Bigg[1 - \frac{b_+(a_+ - c)}{(a_+ - 1)(1 + b_+ - c)} + \frac{a_+ - b_+ - 1}{1 + b_+ - c} \left(1 + \frac{b_+}{a_+ - 1} \right) z \\
& - \frac{(a_+ - b_+ - 1)(1-c)}{(1-a_+)(c-b_+-1)}(1-z) - \frac{(a_+ - b_+ - 1)(a_+ + b_+ - c)}{(1-a_+)(c-b_+-1)} z \Bigg] \\
& \times {}_2F_1(1-a_+, 1-b_+, 2-c; z) \Bigg\}.
\end{aligned}
\tag{74}
$$

Now we have arrived at a point where all the hard labor finally bears fruit and a miracle of some sort happens. Carefully calculating the part between the hypergeometric functions in equation (74) above, one finds that this part is identically zero. We are left with a remarkably simple equation:

$$
|C_{+h}|^2 = \frac{(1-a_+)(c-b_+-1)}{(a_+ - b_+ - 1)(1-c)}. \tag{75}
$$

Using the earlier mentioned relations 2) and 5), equation (74) can be expressed as

$$
|C_{+h}|^2 = \frac{\omega_- + m_{1\mathrm{R}} + m_{2\mathrm{R}}}{2\omega_-}. \tag{76}
$$

We have now arrived at the end of the normalization procedure. From equation (76) we choose

$$
C_{+h} = \sqrt{\frac{\omega_- + m_{1\mathrm{R}} + m_{2\mathrm{R}}}{2\omega_-}}. \tag{77}
$$

Equation (67) then dictates the second constant to be

$$
C_{-h} = \frac{\mathrm{i}m_{\mathrm{I}} - h|\vec{k}|}{\sqrt{|\vec{k}|^2 + m_{\mathrm{I}}^2}} \sqrt{\frac{\omega_- - m_{1\mathrm{R}} - m_{2\mathrm{R}}}{2\omega_-}}. \tag{78}
$$

4.5 Solutions

Plugging the afore-obtained constants into equation (59a) gives us two correctly normalized mode functions:

$$\phi_{+h} \doteq \phi^{(1)}_{+h} = \sqrt{\frac{\omega_- + m_{1\mathrm{R}} + m_{2\mathrm{R}}}{2\omega_-}}\, z^{\alpha}(1-z)^{\beta} \times {}_2F_1(a_+, b_+, c; z) \quad (79a)$$

$$\phi_{-h} \doteq \phi^{(1)}_{-h} = \frac{\mathrm{i}m_{\mathrm{I}} - h\left|\vec{k}\right|}{\sqrt{\left|\vec{k}\right|^2 + m_{\mathrm{I}}^2}} \sqrt{\frac{\omega_- - m_{1\mathrm{R}} - m_{2\mathrm{R}}}{2\omega_-}}\, z^{\alpha}(1-z)^{\beta} \times {}_2F_1(a_-, b_-, c; z). \quad (79b)$$

These are called *early-time mode functions* due to the fact that at early times they reduce to positive frequency solutions, cf. equation (60a). A similar normalization procedure would give us the second pair of early-time solutions $\phi^{(2)}_{\pm h}$, the ones reducing to negative frequency solutions at early times (cf. equations (59b) and (60b)). We will not be needing these since we choose our early-time solution to consist of the positive frequency solutions only. The real and imaginary parts of solutions (79a) and (80a) are plotted in Figure 5 for certain parameters to illustrate the nature of the solutions.

Then there are of course the *late-time mode functions* $\widetilde{\phi}^{(1,2)}_{\pm h}$, given in equation (62), which at late times reduce to positive and negative frequency solutions (cf. equation (63)). For completeness we will also give these solutions. At late times we want to have both positive and negative frequency solutions due to the wall, and hence we will keep the solution as general as possible. The solutions $\widetilde{\phi}^{(1,2)}_{\pm h}$ can be normalized following an analogous procedure to the one described in the previous section. As a result one will obtain the following two pairs of normalized late-time solutions:

$$\widetilde{\phi}^{(1)}_{+h} = \sqrt{\frac{\omega_+ + m_{1\mathrm{R}} - m_{2\mathrm{R}}}{2\omega_+}}\, z^{-\alpha}(1-z)^{-\beta} \times {}_2F_1(1-a_+, 1-b_+, 2-\tilde{c}; 1-z), \quad (80a)$$

$$\widetilde{\phi}^{(1)}_{-h} = \frac{\mathrm{i}m_{\mathrm{I}} - h\left|\vec{k}\right|}{\sqrt{\left|\vec{k}\right|^2 + m_{\mathrm{I}}^2}} \sqrt{\frac{\omega_+ - m_{1\mathrm{R}} + m_{2\mathrm{R}}}{2\omega_+}}\, z^{-\alpha}(1-z)^{-\beta} \times {}_2F_1(1-a_-, 1-b_-, 2-\tilde{c}; 1-z), \quad (80b)$$

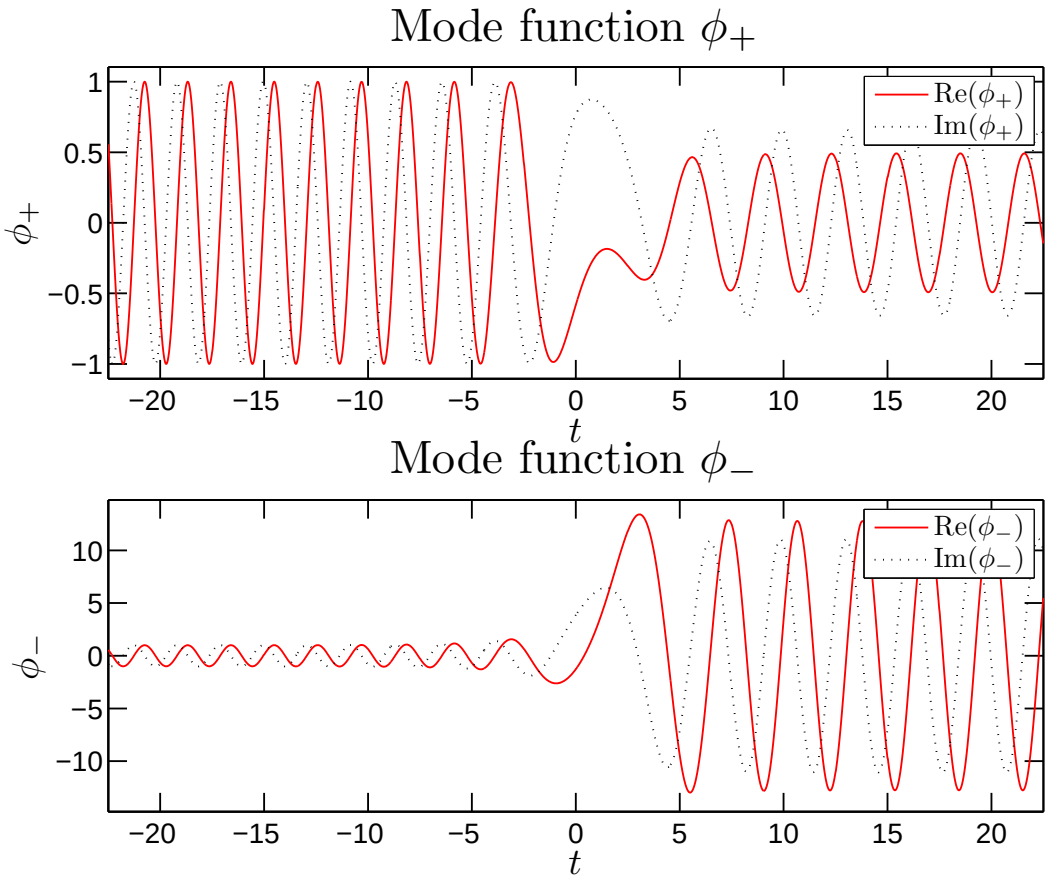

Figure 5: The real and imaginary parts of the mode functions ϕ_+ and ϕ_- of equations (79a) and (79b) near the mass change. Here we have used the following set of parameters: $h = 1$, $|\vec{k}| = 0.4$, $m_{1\mathrm{R}} = 0.5$, $m_{2\mathrm{R}} = 2.5$, $m_{\mathrm{I}} = 0.1$ and $\tau_w = 5$. The oscillating feature of the hypergeometric functions is apparent.

and

$$\widetilde{\phi}^{(2)}_{+h} = \sqrt{\frac{\omega_+ - m_{1\mathrm{R}} + m_{2\mathrm{R}}}{2\omega_+}}\, z^\alpha (1-z)^\beta \times {}_2F_1(a_+, b_+, \tilde{c}; 1-z), \tag{81a}$$

$$\widetilde{\phi}^{(2)}_{-h} = \frac{h|\vec{k}| - \mathrm{i}m_{\mathrm{I}}}{\sqrt{|\vec{k}|^2 + m_{\mathrm{I}}^2}} \sqrt{\frac{\omega_+ + m_{1\mathrm{R}} - m_{2\mathrm{R}}}{2\omega_+}}\, z^\alpha (1-z)^\beta \times {}_2F_1(a_-, b_-, \tilde{c}; 1-z), \tag{81b}$$

where we have for simplicity defined $\tilde{c} \doteq 1 + 2\beta = 1 + a_\pm + b_\pm - c$.

The full late-time solution $\widetilde{\phi}_{\pm h}$ will be a linear combination of equations

(80) and (81):

$$\widetilde{\phi}_{\pm h} = \kappa_{\pm h}\widetilde{\phi}^{(1)}_{\pm h} + \lambda_{\pm h}\widetilde{\phi}^{(2)}_{\pm h},$$

where the coefficients $\kappa_{\pm h}$ and $\lambda_{\pm h}$ are in general $\vec{k}$-dependent. They again obey the normalization condition

$$|\kappa_{\pm h}|^2 + |\lambda_{\pm h}|^2 = 1.$$

These coefficients can be determined using the fact that the early- and late-time solutions have to coincide:

$$\phi_{\pm h} = \widetilde{\phi}_{\pm h} = \kappa_{\pm h}\widetilde{\phi}^{(1)}_{\pm h} + \lambda_{\pm h}\widetilde{\phi}^{(2)}_{\pm h}.$$

Let us look at $\phi_{+h} = \widetilde{\phi}_{+h}$ first. On the left-hand side we have

$$\begin{aligned}
\phi_{+h} &= \sqrt{\frac{\omega_- + m_{1\mathrm{R}} + m_{2\mathrm{R}}}{2\omega_-}}\, z^\alpha (1-z)^\beta \times {}_2F_1(a_+, b_+, c; z) \\
&= \sqrt{\frac{\omega_- + m_{1\mathrm{R}} + m_{2\mathrm{R}}}{2\omega_-}}\, z^\alpha (1-z)^\beta \left[\frac{\Gamma(c)\Gamma(c-a_+-b_+)}{\Gamma(c-a_+)\Gamma(c-b_+)} \right. \\
&\quad \times {}_2F_1(a_+, b_+, \tilde{c}; 1-z) + \frac{\Gamma(c)\Gamma(a_++b_+-c)}{\Gamma(a_+)\Gamma(b_+)} (1-z)^{c-a_+-b_+} \\
&\quad \left. \times {}_2F_1(c-a_+, c-b_+, 1-a_+-b_++c; 1-z) \right],
\end{aligned} \tag{82}$$

where we used Identity 3. The right-hand side can be on the other hand written as

$$\begin{aligned}
\widetilde{\phi}_{+h} &= \kappa_{+h}\sqrt{\frac{\omega_+ + m_{1\mathrm{R}} - m_{2\mathrm{R}}}{2\omega_+}}\, z^{-\alpha}(1-z)^{-\beta} \\
&\quad \times {}_2F_1(1-a_+, 1-b_+, 2-\tilde{c}; 1-z) + \lambda_{+h}\sqrt{\frac{\omega_+ - m_{1\mathrm{R}} + m_{2\mathrm{R}}}{2\omega_+}} \\
&\quad \times z^\alpha (1-z)^\beta \times {}_2F_1(a_+, b_+, \tilde{c}; 1-z) \\
&= z^\alpha (1-z)^\beta \left[\kappa_{+h}\sqrt{\frac{\omega_+ + m_{1\mathrm{R}} - m_{2\mathrm{R}}}{2\omega_+}}\, (1-z)^{c-a_+-b_+} \right. \\
&\quad \times {}_2F_1(c-a_+, c-b_+, 1-a_+-b_++c; 1-z) \\
&\quad \left. + \lambda_{+h}\sqrt{\frac{\omega_+ - m_{1\mathrm{R}} + m_{2\mathrm{R}}}{2\omega_+}} \times {}_2F_1(a_+, b_+, \tilde{c}; 1-z) \right]
\end{aligned} \tag{83}$$

with the help of Identity 2. Expressions (82) and (83) contain now the same hypergeometric functions. Since the expressions have to match for all values of z, we can read off the following relations by comparing the coefficients in front of the hypergeometric functions:

$$\kappa_{+h}\sqrt{\frac{\omega_+ + m_{1R} - m_{2R}}{2\omega_+}} = \sqrt{\frac{\omega_- + m_{1R} + m_{2R}}{2\omega_-}}\,\frac{\Gamma(c)\Gamma(a_+ + b_+ - c)}{\Gamma(a_+)\Gamma(b_+)},$$
$$\lambda_{+h}\sqrt{\frac{\omega_+ - m_{1R} + m_{2R}}{2\omega_+}} = \sqrt{\frac{\omega_- + m_{1R} + m_{2R}}{2\omega_-}}\,\frac{\Gamma(c)\Gamma(c - a_+ - b_+)}{\Gamma(c - a_+)\Gamma(c - b_+)}.$$

The equation $\phi_{-h} = \widetilde{\phi}_{-h}$ can be treated in an exactly same way, and all in all we end up with the following expressions for all the coefficients:

$$\kappa_{\pm h} = \sqrt{\frac{\omega_+[\omega_- \pm (m_{1R} + m_{2R})]}{\omega_-[\omega_+ \pm (m_{1R} - m_{2R})]}}\,\frac{\Gamma(c)\Gamma(a_\pm + b_\pm - c)}{\Gamma(a_\pm)\Gamma(b_\pm)}, \tag{84a}$$

$$\lambda_{\pm h} = \pm\sqrt{\frac{\omega_+[\omega_- \pm (m_{1R} + m_{2R})]}{\omega_-[\omega_+ \mp (m_{1R} - m_{2R})]}}\,\frac{\Gamma(c)\Gamma(c - a_\pm - b_\pm)}{\Gamma(c - a_\pm)\Gamma(c - b_\pm)}. \tag{84b}$$

This is as far as we will go with the Dirac equation. The most important results from this section and the ones that will be used in the following investigations are equations (79). These exact solutions will be used to reveal the phase space structure of the problem.

In Appendix B the Dirac equation of this Chapter is studied in the constant mass limit. The corresponding solutions are given, and they are used to derive another form for the normalization of this time-dependent problem.

5 Phase space structure of the Wigner function

In this chapter we will use the exact mode functions of the Dirac equation studied in Chapter 4 to establish the entire phase space structure of the problem. This will allow us to make comparison with the predictions of cQPA considered in Chapter 3.3.

5.1 Wightman function

Our goal is to somehow construct the Wigner function (10) that was used to reveal the coherence structure in the context of cQPA. We need to however be careful that we really construct an object of correct nature. The exact mode functions resulted from analyzing a *free* problem, while the Wigner function is inherently an object related to *interacting* situations (at least in every sensible physical scenario). This subtlety will be addressed more carefully in the next section, first we will straightforwardly construct the Wightman function appearing inside the Wigner transformation.

The Wigner function is obtained by integrating the 2-point correlator in the average and relative coordinates. Concentrating on $S^<$, we should then compute

$$\mathrm{i}S^<\left(X+\frac{r}{2},X-\frac{r}{2}\right)=\left\langle\Omega\left|\overline{\psi}\left(X-\frac{r}{2}\right)\psi\left(X+\frac{r}{2}\right)\right|\Omega\right\rangle, \tag{85}$$

where we have explicitly included the ground state Ω in the notation. The tricky point here is that our problem actually contains two distinct vacua: the one deep in the symmetric phase (long before the mass change) and the one deep in the broken phase (long after the mass change).[9] However, since we construct the spinors ψ and $\overline{\psi}$ out of the complete exact solutions of the problem, they will operate naturally between the both vacua. Therefore the vacuum expectation value can be treated exactly in the way we are used to.

Now that we understand the nature of the expectation value (85), we can just plug in it the full spinor expansion given in equation (30). This gives

[9]These vacua are related by a Bogoliubov transformation, the coefficients for which are given by $\kappa_{\pm h}$ and $\lambda_{\pm h}$ of equation (84) [26].

(again omitting the ground states from the expectation value) e.g.

$$
\begin{aligned}
\mathrm{i}S^{<}_{\alpha\beta}(u,v) &= \left\langle \overline{\psi}_{\beta}(v)\,\psi_{\alpha}(u) \right\rangle \\
&= \int \frac{\mathrm{d}k_1^3\mathrm{d}k_2^3}{(2\pi)^3(2\pi)^3} \sum_{h_1,h_2} \Big\langle \Big[\hat{a}^{\dagger}_{\vec{k}_2 h_2} \overline{\mu}_{h_2\beta}(v_0,\vec{k}_2)\mathrm{e}^{-\mathrm{i}\vec{k}_2\cdot\vec{v}} \; + \hat{b}_{\vec{k}_2 h_2} \overline{\nu}_{h_2\beta}(v_0,\vec{k}_2)\mathrm{e}^{\mathrm{i}\vec{k}_2\cdot\vec{v}} \Big] \\
&\quad \times \Big[\hat{a}_{\vec{k}_1 h_1} \mu_{h_1\alpha}(u_0,\vec{k}_1)\mathrm{e}^{\mathrm{i}\vec{k}_1\cdot\vec{u}} + \hat{b}^{\dagger}_{\vec{k}_1 h_1} \nu_{h_1\alpha}(u_0,\vec{k}_1)\mathrm{e}^{-\mathrm{i}\vec{k}_1\cdot\vec{u}} \Big] \Big\rangle \\
&= \sum_{h_1,h_2} \int \frac{\mathrm{d}k_1^3\mathrm{d}k_2^3}{(2\pi)^3(2\pi)^3}\, \mathrm{e}^{\mathrm{i}(\vec{k}_1\cdot\vec{u}+\vec{k}_2\cdot\vec{v})} \overline{\nu}_{h_2\beta}(v_0,\vec{k}_2)\nu_{h_1\alpha}(u_0,\vec{k}_1) \left\langle b_{k_2 h_2} b^{\dagger}_{k_1 h_1} \right\rangle \\
&= \sum_{h} \int \frac{\mathrm{d}k^3}{(2\pi)^3}\, \mathrm{e}^{\mathrm{i}\vec{k}\cdot(\vec{v}-\vec{u})} \overline{\nu}_{h\beta}(v_0,\vec{k})\nu_{h\alpha}(u_0,\vec{k}),
\end{aligned}
$$

where we made use of the commutation relations (31) for the creation and annihilation operators. The problem studied in Chapter 4 was spatially homogeneous, and the solutions ended up depending only on the magnitude of the three-momentum and time. Therefore the integral over the three-momentum in the previous equation becomes just a delta function, and we can write

$$
\mathrm{i}S^{<}_{\alpha\beta}(u,v) = \mathrm{i}S^{<}_{\alpha\beta}(u_0,v_0) = \sum_{h} \overline{\nu}_{h\beta}(v_0)\nu_{h\alpha}(u_0). \tag{86}
$$

Following the same steps one can write the other Wightman function as

$$
\mathrm{i}S^{>}_{\alpha\beta}(u,v) = \mathrm{i}S^{>}_{\alpha\beta}(u_0,v_0) = \sum_{h} \mu_{h\alpha}(u_0)\overline{\mu}_{h\beta}(v_0). \tag{87}
$$

The spinor products can be straightforwardly calculated using the decompositions (33):

$$
\overline{\nu}_h\nu_h = \left\{ \begin{bmatrix} \overline{\zeta}^*_h\overline{\zeta}_h & \overline{\zeta}^*_h\overline{\eta}_h \\ \overline{\eta}^*_h\overline{\zeta}_h & \overline{\eta}^*_h\overline{\eta}_h \end{bmatrix} \otimes \xi_h\xi_h^{\dagger} \right\} \gamma^0, \tag{88}
$$

$$
\mu_h\overline{\mu}_h = \left\{ \begin{bmatrix} \eta_h\eta^*_h & \eta_h\zeta^*_h \\ \zeta_h\eta^*_h & \zeta_h\zeta^*_h \end{bmatrix} \otimes \xi_h\xi_h^{\dagger} \right\} \gamma^0. \tag{89}
$$

The interesting (time-dependent) parts of the above objects lie in the functions η_h, ζ_h, $\overline{\eta}_h$ and $\overline{\zeta}_h$, which can be easily written in terms of the exact mode functions through relations (37). In what follows we shall only concentrate on the time-dependent parts, and therefore denote for example

$$
\mathrm{i}S^{>}_{h}\gamma^0 = \begin{bmatrix} \eta_h\eta^*_h & \eta_h\zeta^*_h \\ \zeta_h\eta^*_h & \zeta_h\zeta^*_h \end{bmatrix}. \tag{90}
$$

This just means that we essentially want to consider the time-dependent part of the Wightman function for a specific helicity, and according to the block-diagonal form of equations (88) and (89), the most relevant objects are the ones given in equation (90) (and the similar equation for $S^<$).

5.2 Wigner function

Now it is time to turn our focus on the real object of interest, the Wigner function. As already mentioned, the nature of the object we want to study is a little unsettled. A naïve approach would be to just take the original definition (10), which in our spatially homogeneous case would together with e.g. equation (87) result in

$$\mathrm{i}S^{>}_{\alpha\beta}(k_0, T) = \sum_h \int \mathrm{d}r_0 \, \mathrm{e}^{\mathrm{i}k_0 r_0} \, \mu_{h\alpha}\left(T + \frac{r_0}{2}\right) \overline{\mu}_{h\beta}\left(T - \frac{r_0}{2}\right), \tag{91}$$

where T denotes the time component of the average coordinate X. This expression is however bound to lead to rather unphysical results. To see what is wrong with the above expression and how it should be altered, we shall look first at a simplified case.

5.2.1 Step-function correlator with a finite Fourier transform

Studying the correlator (91) analytically with the full solutions is in practice of no avail due to the complexity of the hypergeometric solutions. An intuitive picture can be obtained by squeezing the time-width of the wall and considering a case where the solutions consist of plane waves immediately before and after the mass change. This way we can neglect the hypergeometric behaviour of the full solutions while still maintaining the correct qualitative picture of the situation. So we say that the mass changes essentially like a step function, and study mode functions of the form

$$\eta_h^{\mathrm{step}}(t) \doteq \theta(-t)\mathrm{e}^{-\mathrm{i}\omega_- t} + \theta(t)\left(\alpha \mathrm{e}^{-\mathrm{i}\omega_+ t} + \beta \mathrm{e}^{\mathrm{i}\omega_+ t}\right), \tag{92}$$

where ω_- and ω_+ are still the early- and late-time forms of the energy, θ is the Heaviside step function and α, $\beta \in \mathbb{C}$.

The problem with the definition (91) for the Wigner function arises essentially from the integration over the relative coordinate r_0. This integration

picks correlations between the mode function and its complex conjugate, and when the integration is performed from minus infinity to infinity, there are correlations coming from *separate sides of the wall with arbitrarily large time distances*. Such large-distance correlations are however not sensible, in the sense that in a physical setting interactions will diminish the large-scale correlations. The first step towards understanding this problem is to consider a Fourier transform performed in a finite-sized box, i.e. limit the relative coordinate correlations by imposing a cut-off distance to the integration. To this end we define the Wigner function in a box[10] as

$$S_L^{<,>}(k_0, T) \doteq \frac{1}{2L} \int_{-L}^{L} \mathrm{d}r_0 \, \mathrm{e}^{\mathrm{i}k_0 r_0} \, S^{<,>}\left(T + \frac{r_0}{2}, T - \frac{r_0}{2}\right). \tag{93}$$

The Wightman function can of course be computed exactly similarly as before resulting in an expression similar to (91), the only difference being in the integration limits and the normalization $1/2L$.

Let us now see what information our new definition gives for the step function correlator. Looking at e.g. the $(1,1)$-component of $\mathrm{i}S^{>}\gamma^0$, we have

$$\left[\mathrm{i}S_L^{>}\gamma^0\right]_{11} = \frac{1}{2L} \int_{-L}^{L} \mathrm{d}r_0 \, \mathrm{e}^{\mathrm{i}k_0 r_0} \, \eta^{\mathrm{step}}\left(T + \frac{r_0}{2}\right) \eta^{\mathrm{step}*}\left(T - \frac{r_0}{2}\right),$$

where we have ignored the helicity-part. Plugging in the mode functions and being careful with the Heaviside step functions the integral can be straightforwardly computed, resulting in

$$\left[\mathrm{i}S_L^{>}\gamma^0\right]_{11} = \frac{1}{L}\left(\mathcal{J}_1 + \mathcal{J}_2 + \mathcal{J}_3\right), \tag{94}$$

where

$$\begin{aligned}
\mathcal{J}_1 &\doteq \frac{\sin(2|T|(k_0 - \omega_-))}{k_0 - \omega_-}\theta(-T), \\
\mathcal{J}_2 &\doteq |\alpha|^2 \frac{\sin(2|T|(k_0 - \omega_+))}{k_0 - \omega_+}\theta(T) + |\beta|^2 \frac{\sin(2|T|(k_0 + \omega_+))}{k_0 + \omega_+}\theta(T) \\
&\quad + 2\mathbb{R}\mathrm{e}\left(\alpha\beta^* \mathrm{e}^{-2\mathrm{i}\omega_+ T}\right) \frac{\sin(2|T|k_0)}{k_0}\theta(T),
\end{aligned}$$

[10] In our spatially homogeneous case this is just a Fourier transformation on an interval. The definition generalizes readily to higher dimensions.

$$\mathcal{J}_3 \doteq \mathbb{R}\mathrm{e}\left\{ \frac{\mathrm{i}\alpha \mathrm{e}^{\mathrm{i}T(\omega_- - \omega_+)}}{k_0 - \frac{\omega_- + \omega_+}{2}} \left[\mathrm{e}^{\mathrm{i}2|T|\left(k_0 - \frac{\omega_- + \omega_+}{2}\right)} - \mathrm{e}^{\mathrm{i}L\left(k_0 - \frac{\omega_- + \omega_+}{2}\right)} \right] \right.$$
$$\left. + \frac{\mathrm{i}\beta \mathrm{e}^{\mathrm{i}T(\omega_- + \omega_+)}}{k_0 - \frac{\omega_- - \omega_+}{2}} \left[\mathrm{e}^{\mathrm{i}2|T|\left(k_0 - \frac{\omega_- - \omega_+}{2}\right)} - \mathrm{e}^{\mathrm{i}L\left(k_0 - \frac{\omega_- - \omega_+}{2}\right)} \right] \right\} \theta(L - 2|T|).$$

We have purposely split the result in three different parts due to their distinct nature. $\mathcal{J}_1$ and $\mathcal{J}_2$ correspond to the early- and late-time solutions, respectively, while $\mathcal{J}_3$ contains structure depending on the size of the box L.

The essential properties of these different correlations can be neatly revealed with the help of the following formal[11] representation of the Dirac delta function

$$\delta(x) = \lim_{\varepsilon \to 0} \left[\frac{\sin(x/\varepsilon)}{\pi x} \right]. \tag{95}$$

In the limit $T \to -\infty$ of equation (94) only $\mathcal{J}_1$ remains due to the step functions, and with the help of equation (95) we can write

$$\lim_{T \to -\infty} \left[\mathrm{i}S_L^{>} \gamma^0 \right]_{11} = \frac{\pi}{L} \delta(k_0 - \omega_-).$$

So at early times we only expect to see spectral structure at the $k_0 = \omega_-$ -shell, which is sensible since our initial condition includes just a particle with energy ω_-. In the late time limit on the other hand we have

$$\lim_{T \to \infty} \left[\mathrm{i}S_L^{>} \gamma^0 \right]_{11} = \frac{\pi}{L} |\alpha|^2 \, \delta(k_0 - \omega_+) + \frac{\pi}{L} |\beta|^2 \, \delta(k_0 + \omega_+)$$
$$+ \frac{\pi}{L} \times \text{OSCILLATION} \times \delta(k_0).$$

This triumphant result contains exactly the structure predicted by cQPA. First, we see that at late times the phase space has the expected structure corresponding to particles ($k_0 = \omega_+$) and antiparticles ($k_0 = -\omega_+$). In addition, there is spectral structure at the $k_0 = 0$ -shell, which according to cQPA describes coherence between the particle- and antiparticle-solutions. The nature of this structure is oscillatory, which is also seen from cQPA when one solves the shell-functions parametrizing the spectral structures.

[11] Formal in the sense that the right hand side of equation (95) (which does not converge on its own) acts as the delta distribution when integrated against sensible functions.

The results above give us the correct qualitative picture of the phase space structure at early and late times. However, there is also the peculiar term $\mathcal{J}_3$. As indicated by the step function, the existence of this term is restricted by the size of the Fourier transform L. Nevertheless, for large values of L this structure exists long before and after the mass change. At those times, the term can give rise to spectral-like structure corresponding to shells

$$k_0 = \frac{\omega_- + \omega_+}{2} \qquad \text{and} \qquad k_0 = \frac{\omega_- - \omega_+}{2}.$$

These structures are immediately recognized as *correlations coming from different sides of the mass wall*. They are mixtures of the early-time particle-solution with the late time particle- and antiparticle-solutions. The larger the Fourier transform range L, the larger the distance between the furthest correlations. These kinds of coherences are not predicted by cQPA, or by any other approach to our knowledge. This does however not render cQPA erroneous. cQPA is essentially a *local* approximation, so these kinds of nonlocal beyond-the-wall coherences *should* be outside its scope. One of the approximations made in cQPA was the gradient approximation, which requires that the background changes at a relatively slow pace and can be treated classically. This approximation does not hold now near the mass change, because the mass changes infinitely rapidly at the step wall. Of course this kind of a mass change is not very physical, and the results with the kink-potential will be of more interest. This step wall however allows us to study the situation qualitatively.

Before returning to the exact solutions of the kink-potential, we shall look at the step-wall from another point of view. Even though the beyond-the-wall coherences identified above can and do exist, there should not be correlations coming from arbitrarily large distances from separate sides of the wall. This is because in a physical setting interactions would not permit such large scale coherences. In the previous approach these correlations where limited by the size of the Fourier transform L, but this is in no way a proper way to limit the correlations. In principle, we should be able to make the Fourier transform as large as we want; a priori it should be infinite. The limit $L \to \infty$ is not meaningful in the earlier expressions, since the finite Fourier transform we defined is not related to the full Fourier transform in such a continuous way. Instead, we should start out with a Wigner function that takes into account all possible correlations, but in a physically meaningful way.

This is where the free nature of our solutions steps in. The problematic

correlations arise because we are just plugging the free-particle solutions blindly into the Wigner function. The correct way to do this is to introduce the mean free path Γ of the particles, and damp the large scale correlations with it. This is what is done in the next section.

5.2.2 Step-function correlator with a damped Fourier transform

Instead of limiting the size of the Fourier transform, we define the following damped Wigner transform:

$$S_\Gamma^{<,>}(k_0, T) \doteq \int_{-\infty}^{\infty} \mathrm{d}r_0 \, \mathrm{e}^{\mathrm{i}k_0 r_0 - \Gamma|r_0|} \, S^{<,>}\left(T + \frac{r_0}{2}, T - \frac{r_0}{2}\right). \tag{96}$$

Here $\Gamma > 0$, the mean free path of the particles, suppresses the correlations coming from large time distances from separate sides of the mass wall. A large mean free path Γ corresponds to weak interactions, and a small one to strong interactions.

We can use this to analyze the step function correlator similarly as with the finite-sized Wigner transform of the previous section. Concentrating again on one component, the Wigner function splits into three pieces:

$$\begin{aligned}\left[\mathrm{i}S_\Gamma^{>}\gamma^0\right]_{11} &= \int_{-\infty}^{\infty} \mathrm{d}r_0 \, \mathrm{e}^{\mathrm{i}k_0 r_0 - \Gamma|r_0|} \, \eta^{\mathrm{step}}\left(T + \frac{r_0}{2}\right) \eta^{\mathrm{step}*}\left(T - \frac{r_0}{2}\right) \\ &= \mathcal{J}_{\Gamma 1} + \mathcal{J}_{\Gamma 2} + \mathcal{J}_{\Gamma 3},\end{aligned}$$

where now

$$\begin{aligned}\mathcal{J}_{\Gamma 1} \doteq \frac{2}{(k_0 - \omega_-)^2 + \Gamma^2} \Big[&\Gamma + (k_0 - \omega_-)\mathrm{e}^{-2\Gamma|T|} \sin(2|T|(k_0 - \omega_-)) \\ &- \Gamma \mathrm{e}^{-2\Gamma|T|} \cos(2|T|(k_0 - \omega_-))\Big] \, \theta(-T),\end{aligned}$$

$$\begin{aligned}\mathcal{J}_{\Gamma 2} \doteq \frac{2|\alpha|^2}{(k_0 - \omega_+)^2 + \Gamma^2} \Big[&\Gamma + (k_0 - \omega_+)\mathrm{e}^{-2\Gamma|T|} \sin(2|T|(k_0 - \omega_+)) \\ &- \Gamma \mathrm{e}^{-2\Gamma|T|} \cos(2|T|(k_0 - \omega_+))\Big] \, \theta(T) \\ + \frac{2|\beta|^2}{(k_0 + \omega_+)^2 + \Gamma^2} \Big[&\Gamma + (k_0 + \omega_+)\mathrm{e}^{-2\Gamma|T|} \sin(2|T|(k_0 + \omega_+))\end{aligned}$$

$$
\begin{aligned}
&-\Gamma \mathrm{e}^{-2\Gamma|T|}\cos(2|T|(k_0+\omega_+))\Big]\,\theta(T)\\
&+\frac{4\mathbb{R}\mathrm{e}\left(\alpha\beta^*\mathrm{e}^{-2\mathrm{i}\omega_+ T}\right)}{k_0^2+\Gamma^2}\Big[\Gamma+k_0\mathrm{e}^{-2\Gamma|T|}\sin(2|T|k_0)\\
&-\Gamma \mathrm{e}^{-2\Gamma|T|}\cos(2|T|k_0)\Big]\,\theta(T),
\end{aligned}
$$

$$
\begin{aligned}
\mathcal{J}_{\Gamma 3} \doteq 2\mathbb{R}\mathrm{e}\Bigg\{ &\frac{-\alpha \mathrm{e}^{\mathrm{i}T(\omega_- - \omega_+)}}{\mathrm{i}\left(k_0-\frac{\omega_-+\omega_+}{2}\right)-\Gamma}\,\mathrm{e}^{2|T|\left[\mathrm{i}\left(k_0-\frac{\omega_-+\omega_+}{2}\right)-\Gamma\right]}\\
-&\frac{\beta \mathrm{e}^{\mathrm{i}T(\omega_- + \omega_+)}}{\mathrm{i}\left(k_0-\frac{\omega_--\omega_+}{2}\right)-\Gamma}\,\mathrm{e}^{2|T|\left[\mathrm{i}\left(k_0-\frac{\omega_--\omega_+}{2}\right)-\Gamma\right]}\Bigg\}.
\end{aligned}
$$

Let us now look first at this mysterious term $\mathcal{J}_{\Gamma 3}$. Again we see the rise of spectral-like structure at $k_0 = \frac{\omega_- \pm \omega_+}{2}$. However, if we move away from the mass wall in time, these solution die off due to the damping factor $\mathrm{e}^{-2|T|\Gamma}$. The definition (96) of the Wigner function gives us the correct qualitative picture, and allows us to get rid of the box-artifacts apparent in the L-dependent Wigner function (93).

Then the other terms. First note that in the limit of weak interactions one has

$$
\begin{aligned}
\mathcal{J}_{\Gamma 1} &\xrightarrow{\Gamma\to 0} \frac{2\sin(2|T|(k_0-\omega_-))}{k_0-\omega_-}\theta(-T),\\
\mathcal{J}_{\Gamma 2} &\xrightarrow{\Gamma\to 0} 2|\alpha|^2\,\frac{\sin(2|T|(k_0-\omega_+))}{k_0-\omega_+}\theta(T)+2|\beta|^2\,\frac{\sin(2|T|(k_0+\omega_+))}{k_0+\omega_+}\theta(T)\\
&\quad+4\mathbb{R}\mathrm{e}\left(\alpha\beta^*\mathrm{e}^{-2\mathrm{i}\omega_+ T}\right)\frac{\sin(2|T|k_0)}{k_0}\theta(T),
\end{aligned}
$$

so that in this limit the expressions reduce at early and late times to the expected spectral solutions:

$$
\begin{aligned}
\mathcal{J}_{\Gamma\to 0,1} &\xrightarrow{T\to-\infty} 2\pi\delta(k_0-\omega_-),\\
\mathcal{J}_{\Gamma\to 0,2} &\xrightarrow{T\to\infty} 2\pi|\alpha|^2\delta(k_0-\omega_+)+2\pi|\beta|^2\delta(k_0+\omega_+)\\
&\qquad+\text{OSCILLATION}\times 4\pi\delta(k_0).
\end{aligned}
$$

Of course $\mathcal{J}_{\Gamma 3}$ too gives a long-living spectral structure in the weak interaction limit. However, if we fix Γ, the only early-time structure is

$$
\lim_{T\to-\infty}\left[\mathrm{i}S^{>}_{\Gamma}\gamma^0\right]_{11} = \lim_{T\to-\infty}\mathcal{J}_{\Gamma 1} = \frac{2\Gamma}{(k_0-\omega_-)^2+\Gamma^2}.
$$

So instead of a delta function we get a Breit–Wigner type of distribution, which is exactly what we should now that we have added the interaction strength to the integration. At early times there is a *resonance* in the phase space at $k_0 = \omega_-$. At late times the structure becomes

$$\lim_{T\to\infty}\left[\mathrm{i}S^{>}_{\Gamma}\gamma^0\right]_{11} = \lim_{T\to\infty}\mathcal{J}_{\Gamma 2} = \frac{2|\alpha|^2\Gamma}{(k_0-\omega_+)^2+\Gamma^2} + \frac{2|\beta|^2\Gamma}{(k_0+\omega_+)^2+\Gamma^2} + \text{OSCILLATION}\times\frac{\Gamma}{k_0^2+\Gamma^2},$$

i.e. we have three Breit–Wigner type of distributions. The resonances correspond to particles ($k_0 = \omega_+$), antiparticles ($k_0 = -\omega_+$) and coherence ($k_0 = 0$) which has again the oscillating feature, as it should.

At this point it should be quite clear that the damped Wigner function (96) is a reasonable object to study. Now that we have also obtained a qualitative picture of the emerging phase space structure, we are ready to get back to our original calculation with the more physical kink-potential.

5.2.3 Wigner function for the kink-potential

As with the step function, we shall for simplicity only consider one of the Wightman functions. To be more precise, we will be interested in the object

$$W(k_0,t) \doteq \mathrm{i}S^{>}_{\Gamma h}(k_0,t)\gamma^0 = \int_{-\infty}^{\infty}\mathrm{d}r_0\,\mathrm{e}^{\mathrm{i}k_0r_0-\Gamma|r_0|}\,\mathrm{i}S^{>}\left(t+\frac{r_0}{2},t-\frac{r_0}{2}\right)\gamma^0$$
$$= \int_{-\infty}^{\infty}\mathrm{d}r_0\,\mathrm{e}^{\mathrm{i}k_0r_0-\Gamma|r_0|}\begin{bmatrix}\eta_h\left(t+\frac{r_0}{2}\right)\eta_h^*\left(t-\frac{r_0}{2}\right) & \eta_h\left(t+\frac{r_0}{2}\right)\zeta_h^*\left(t-\frac{r_0}{2}\right)\\ \zeta_h\left(t+\frac{r_0}{2}\right)\eta_h^*\left(t-\frac{r_0}{2}\right) & \zeta_h\left(t+\frac{r_0}{2}\right)\zeta_h^*\left(t-\frac{r_0}{2}\right)\end{bmatrix},$$

since it should establish the full phase space structure (note that for clarity we named the time coordinate t, although it still refers to the average coordinate). The computation of this Wightman function from the exact mode functions is a non-trivial numerical problem. The results of this computation for different parameter sets, performed using MATLAB, are shown in Figures 6 - 16. We shall now analyze these figures in detail.

Figure 7a has the absolute value of the Wigner function W for one set of parameters. For clarity we have also plotted the (k_0,t)-projection of

it in Figure 7b. Already in Figure 7a we see that the phase space structure behaves exactly as we anticipated it to. At early times there is one Breit–Wigner-peak, whereas at late times there are three different peaks; particles, antiparticles and coherence. The complete structure becomes particularly clear when one looks at the Wigner function from a bird's-eye view, as is done in Figure 7b. The early-time particle-solution transforms at the mass change into the three solutions predicted by cQPA. In this case the parameters have been chosen so that the total energy of the particle decreases, as can be seen in the figures. The energy function

$$\omega(t) = \sqrt{\left|\vec{k}\right|^2 + |m(t)|^2}$$

for these parameters is shown in Figure 6. It is clear that the particle-shell in Figure 7b follows exactly this energy function.

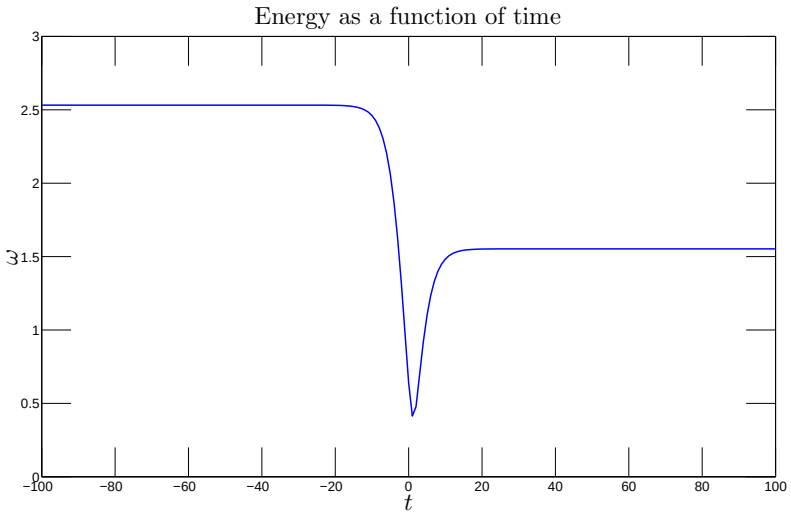

Figure 6: The energy function $\omega(t)$ for parameters $\left|\vec{k}\right| = 0.4$, $m_{1\mathrm{R}} = 0.5$, $m_{2\mathrm{R}} = 2$, $m_{\mathrm{I}} = -0.005$ and $\tau_w = 5$.

The essential parameters characterizing the properties of the possible phase space structure are the magnitude of the mass of the particle $|m|$, the time-width of the wall τ_w and the interaction strength Γ. How does altering these parameters and their relative magnitudes change the possible structure?

Figure 9 has the absolute value of the Wigner function W with the same parameters as Figure 7, except that now the time-width of the wall τ_w is substantially larger. This corresponds to a smoother mass change. The

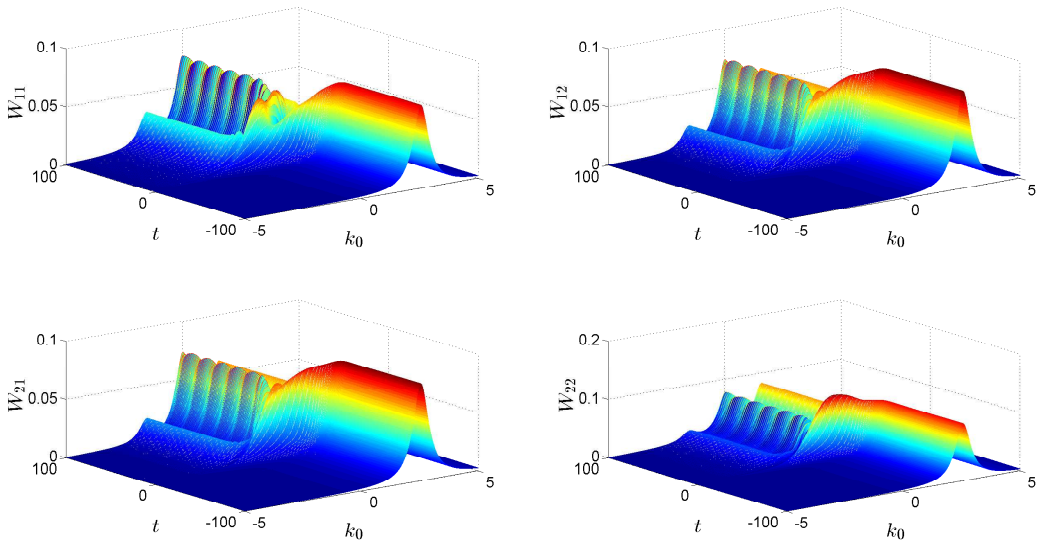

(a) The absolute value of W.

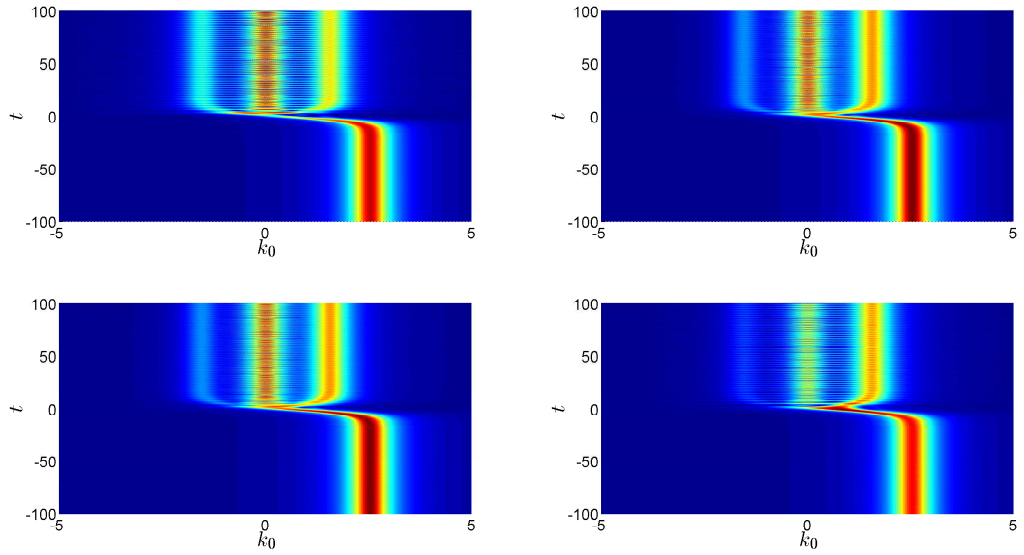

(b) The absolute value of W projected onto the (k_0, t)-plane.

Figure 7: The Wigner function W for parameters $h = 1$, $\left|\vec{k}\right| = 0.4$, $m_{1\mathrm{R}} = 0.5$, $m_{2\mathrm{R}} = 2$, $m_{\mathrm{I}} = -0.005$, $\tau_w = 5$ and $\Gamma = 2$.

change in the phase space structure is clear; the shells are sharper and the coherence- and antiparticle-solutions have diminished. The antiparticle-solution has basically vanished, and the coherence shell is very low too. This is sensible; a smooth mass change does not generate much structure in the phase space. The particle solution on the other hand is clear as opposed to the smeared shell of Figure 7. The interaction strength Γ and mass $|m|$ are now much larger compared to the characteristic time scale of the mass wall, given by τ_w^{-1}. The particle solution holds together, since the smooth mass wall does not have time to smear it out. The energy function $\omega(t)$ in this case is shown in Figure 8, and comparison with the energy function of Figure 6 confirms the less abrupt nature of the mass change.

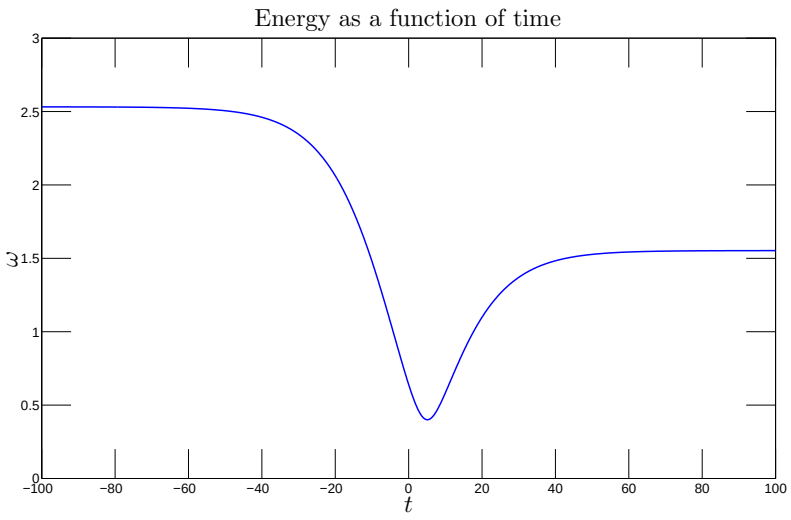

Figure 8: The energy function $\omega(t)$ for parameters $\left|\vec{k}\right| = 0.4$, $m_{1\mathrm{R}} = 0.5$, $m_{2\mathrm{R}} = 2$, $m_{\mathrm{I}} = -0.005$ and $\tau_w = 20$.

An interesting question is: what will happen if the interaction strength Γ is taken to be smaller? According to the analysis performed with the step-function correlator in the previous section, one would expect that in such a weakly interacting system the long-range correlations mixing the early- and late-time solutions should play a role near the mass wall.

In Figure 10 we have again plotted the absolute value of the Wigner function W with the parameters of Figure 7, except that we have reduced the interaction strength by a factor of 20. A first note is that the shells are much more peaked. This is once more an expected feature, since in

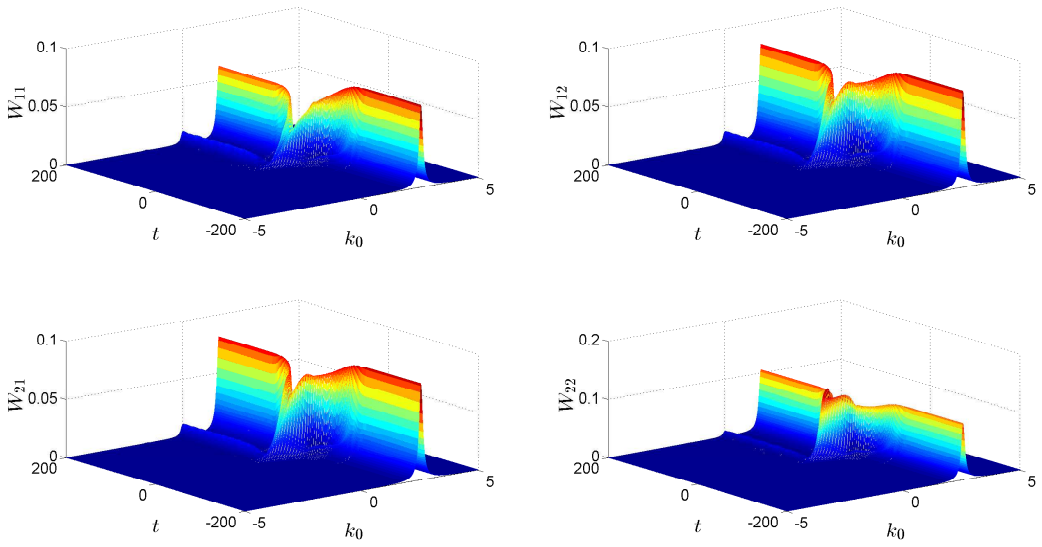

(a) The absolute value of W.

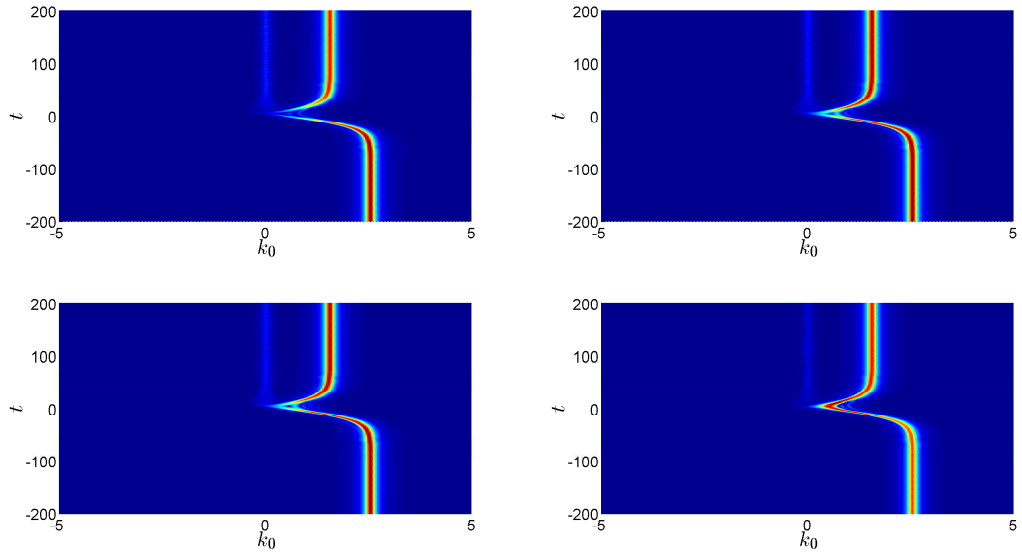

(b) The absolute value of W projected onto the (k_0, t)-plane.

Figure 9: The absolute value of the Wigner function W for parameters $h = 1$, $\left|\vec{k}\right| = 0.4$, $m_{1\mathrm{R}} = 0.5$, $m_{2\mathrm{R}} = 2$, $m_{\mathrm{I}} = -0.005$, $\tau_w = 20$ and $\Gamma = 2$.

the previous section we noted that in the limit $\Gamma \to 0$ the Breit–Wigner-distributions approach delta functions.

A more interesting phenomenon is the rise of new structure at the mass change. In the early- and late-time limits the phase space structure is the one predicted by cQPA and seen in Figure 7. In the vicinity of $t = 0$ there are however spectral structures that do not correspond to standard particles nor antiparticles. Instead, they are exactly the mixture solutions we encountered with the step-function correlator. In the (k_0, t)-plane they are positioned at

$$k_0 = \frac{\omega_- \pm \omega_+}{2},$$

meaning that they constitute of contributions from the particle- and anti-particle-solutions from separate sides of the wall. For large values of $|t|$ they however die out, which is again consistent with our previous analysis. When one goes enough far from the mass wall, the large scale correlations are suppressed by the damping factor even in this weakly interacting system. Near the wall they can however give a dominant contribution to the phase space structure. This can be seen in the figures, where the mixture shells rise, albeit for a short time, above the other structure. They peak at $t = 0$, and then shrink again while the particle-, antiparticle- and coherence-solutions return to be the governing structure.

At this point it is worth mentioning that Figures 7, 9 and 10 fulfil the ultimate goal of this thesis. They provide a clear picture of the phase space structure of the system under consideration, and are in excellent agreement with cQPA. Moreover, the novel structure emerging in Figure 10 is well understood in the light of the step-function correlator analysis, completing the full qualitative picture of the situation.

It is still worthwhile to produce a few more pictures, just to see how altering the parameters affects the solutions. In Figure 11 we have a parameter set with a relatively large $|\vec{k}|$. Since in this situation the energy is quite larger compared to the mass change, there should not be much new structure emerging in the phase space. This is seen manifestly in the figure, where we have essentially nothing but the particle solution. The relatively small change in the energy is also especially clear in the projected figure. Figure 12 contains the actual energy function.

In Figure 14 we have chosen the mass parameters so that the mass (energy) is increasing. We have also used relatively small values for the

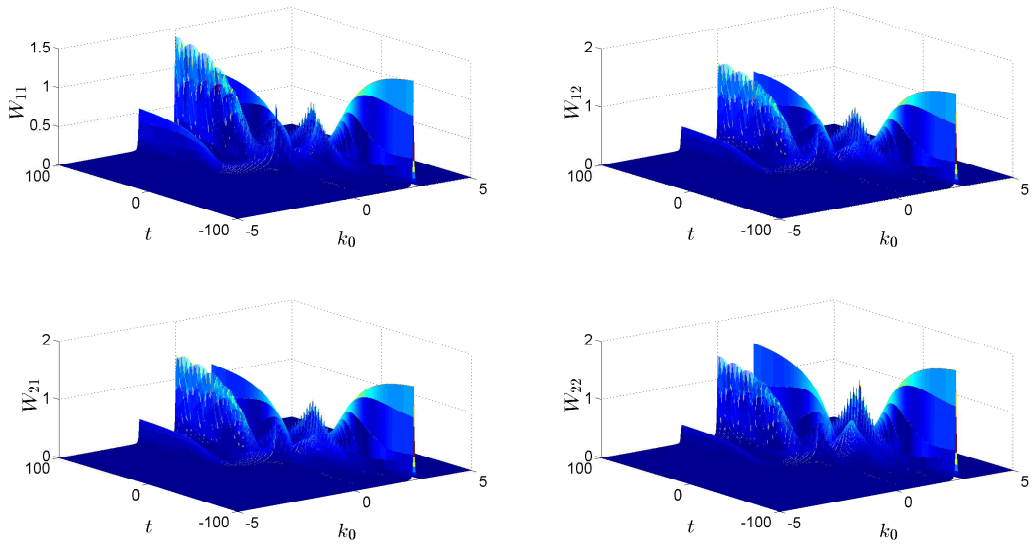

(a) The absolute value of W.

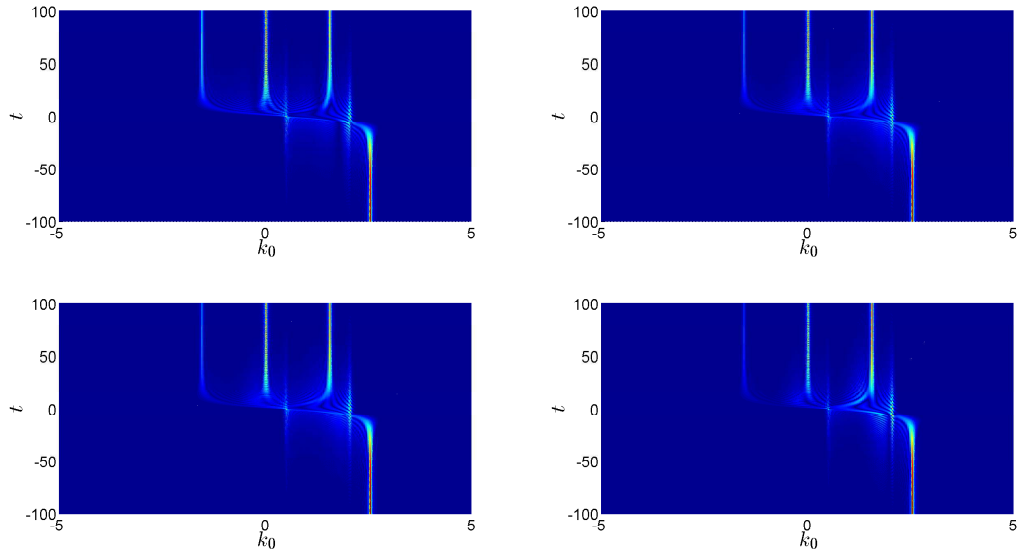

(b) The absolute value of W projected onto the (k_0, t)-plane.

Figure 10: The absolute value of the Wigner function W for parameters $h = 1$, $\left|\vec{k}\right| = 0.4$, $m_{1\mathrm{R}} = 0.5$, $m_{2\mathrm{R}} = 2$, $m_{\mathrm{I}} = -0.005$, $\tau_w = 5$ and $\Gamma = 0.1$.

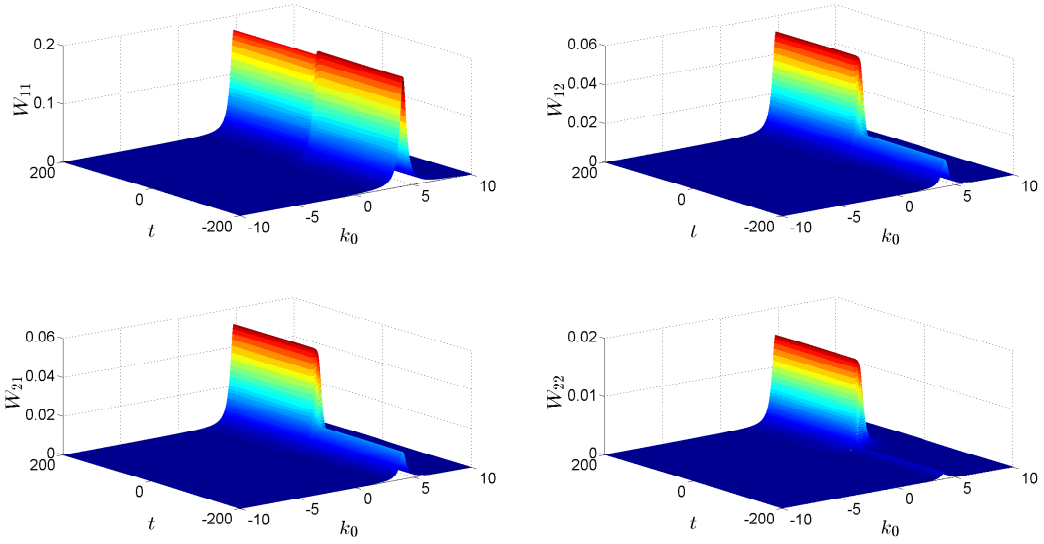

(a) The absolute value of W.

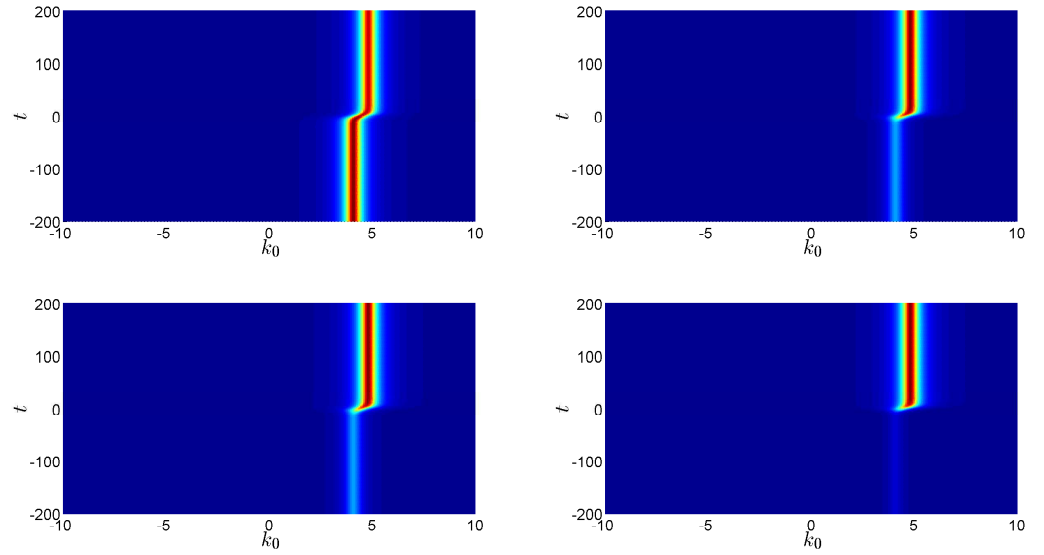

(b) The absolute value of W projected onto the (k_0, t)-plane.

Figure 11: The absolute value of the Wigner function W for parameters $h = -1$, $\left|\vec{k}\right| = 4$, $m_{1\mathrm{R}} = 1.6$, $m_{2\mathrm{R}} = -1$, $m_{\mathrm{I}} = 0.1$, $\tau_w = 6$ and $\Gamma = 2$.

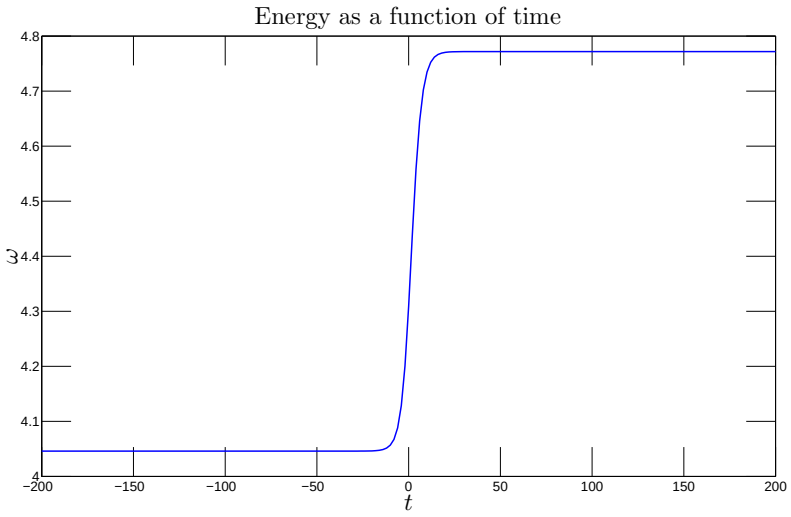

Figure 12: The energy function $\omega(t)$ for parameters $\left|\vec{k}\right| = 4$, $m_{1\mathrm{R}} = 1.6$, $m_{2\mathrm{R}} = -1$, $m_{\mathrm{I}} = 0.1$ and $\tau_w = 6$.

parameters, especially for the interaction strength. This leads again to the emergence of mixture shells near the mass wall, as can be seen in the figure. The energy profile, shown in Figure 13, is also again seen to fit nicely into the particle solution in the phase space.

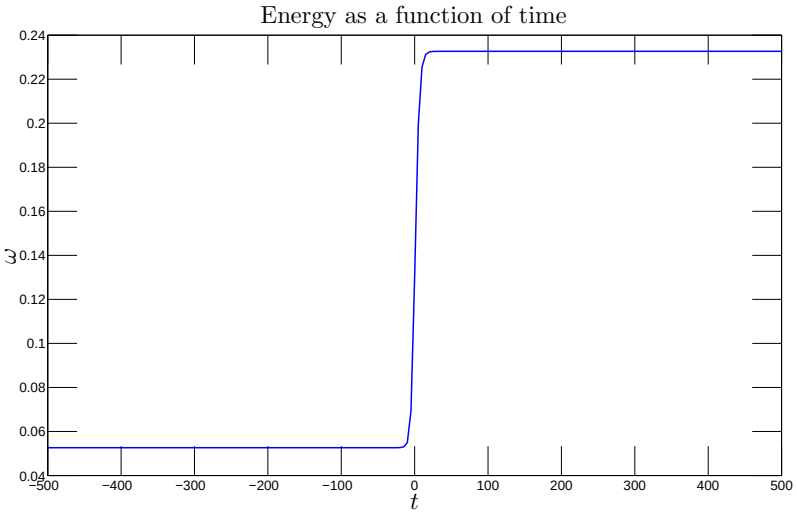

Figure 13: The energy function $\omega(t)$ for parameters $\left|\vec{k}\right| = 0.05$, $m_{1\mathrm{R}} = 0.12$, $m_{2\mathrm{R}} = -0.107$, $m_{\mathrm{I}} = 0.01$ and $\tau_w = 6$.

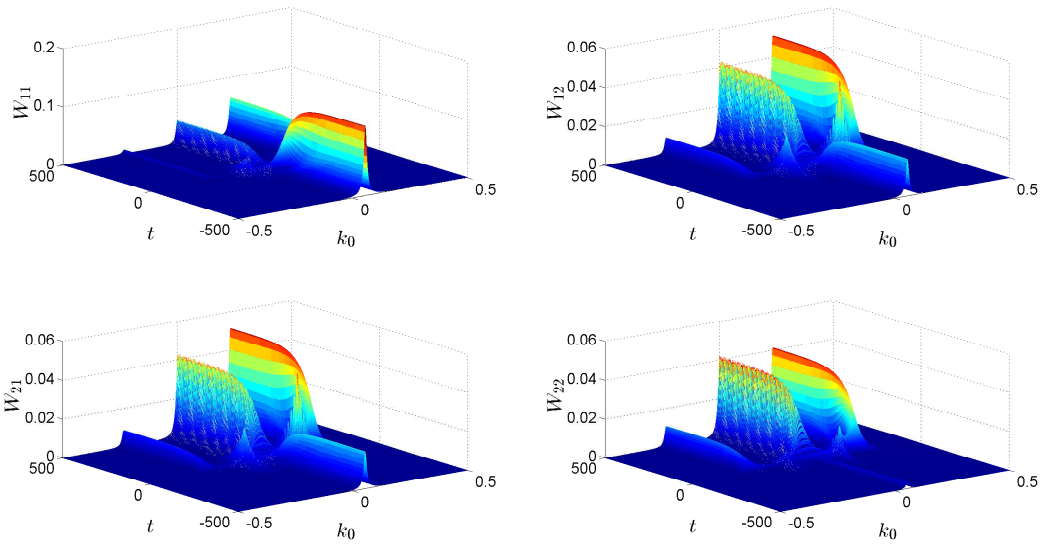

(a) The absolute value of W.

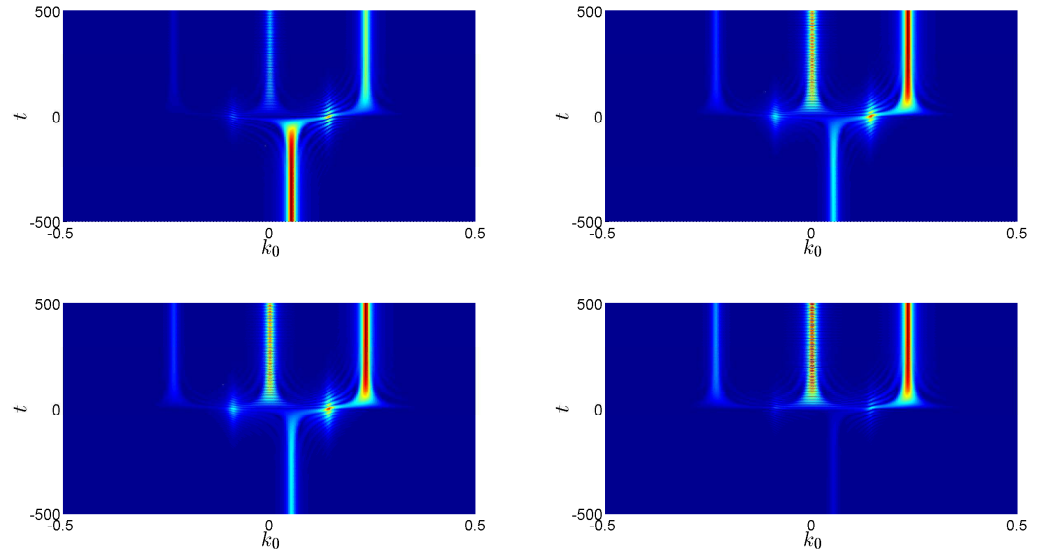

(b) The absolute value of W projected onto the (k_0, t)-plane.

Figure 14: The absolute value of the Wigner function W for parameters $h = -1$, $\left|\vec{k}\right| = 0.05$, $m_{1\mathrm{R}} = 0.12$, $m_{2\mathrm{R}} = -0.107$, $m_{\mathrm{I}} = 0.01$, $\tau_w = 6$ and $\Gamma = 0.05$.

In Figure 16 we have a somewhat more physical set of parameters, in the sense that the wall is rather smooth and the interaction strength is larger than the time scale of the wall. Once more we see exactly what we are expecting to. There is a clear particle-solution, a definite coherence-solution and a faint yet visible antiparticle-solution. The mixture shells are absent, because the rather large interaction strength cuts correlations coming from large time distances from different sides of the mass wall. The energy profile for these parameters is shown in Figure 15.

It is worthwhile to note, that the amount of structure corresponding to antiparticles depends strongly on the mass parameters and the time-width of the wall. A general feature is that a smoother mass change generates less antiparticle-solution. This is natural, since making the wall thinner enhances the quantum nature of the process and produces possibly more antiparticle-solution.

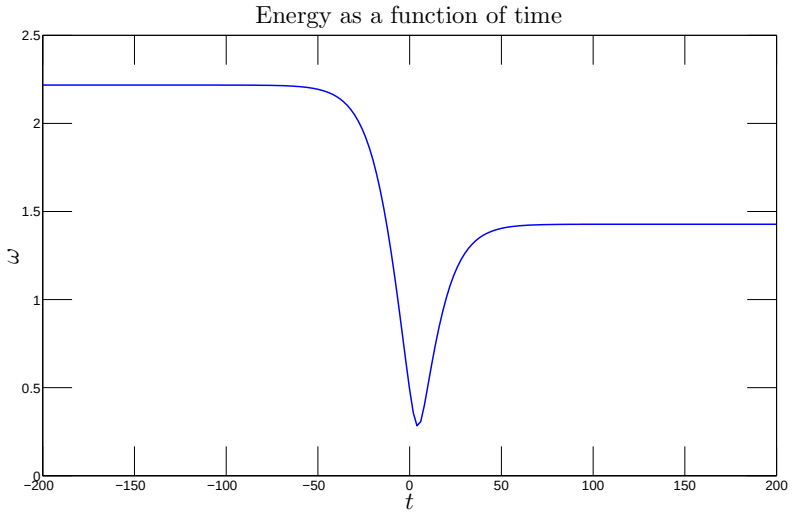

Figure 15: The energy function $\omega(t)$ for parameters $\left|\vec{k}\right| = 0.28$, $m_{1\mathrm{R}} = 0.4$, $m_{2\mathrm{R}} = 1.8$, $m_{\mathrm{I}} = -0.005$ and $\tau_w = 20$.

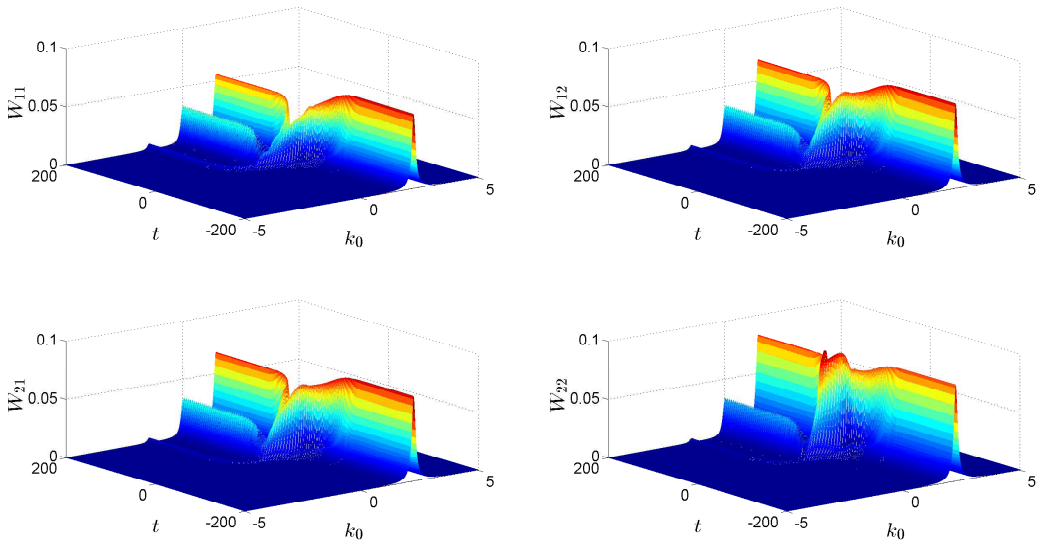

(a) The absolute value of W.

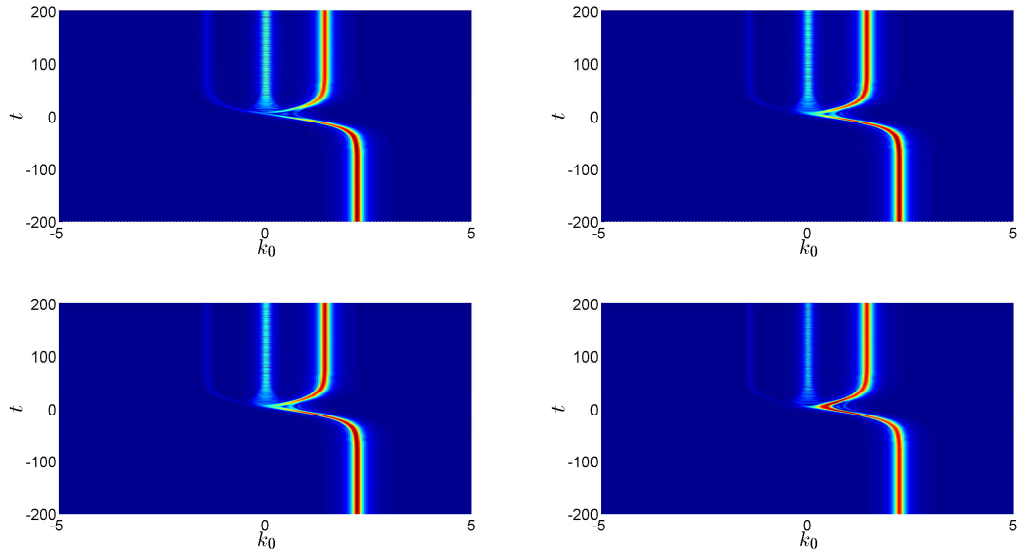

(b) The absolute value of W projected onto the (k_0, t)-plane.

Figure 16: The absolute value of the Wigner function W for parameters $h = 1$, $\left|\vec{k}\right| = 0.28$, $m_{1\mathrm{R}} = 0.4$, $m_{2\mathrm{R}} = 1.8$, $m_{\mathrm{I}} = -0.005$, $\tau_w = 20$ and $\Gamma = 2$.

6 Conclusions

In this thesis we have studied the phase space structure of the Wightman function of the Schwinger–Keldysh formalism in a non-trivial background, and connected the results to the coherent quasiparticle approximation (cQPA). We started out by introducing electroweak baryogenesis (EWBG), a model trying to explain the particle-antiparticle asymmetry of the universe. This served as a motivation to study non-equilibrium quantum phenomena. We then went on to study the basics of the cQPA-formalism, most importantly revealing the novel coherence structure predicted by it in the phase space of non-translation invariant systems.

After reviewing cQPA we left it aside, and picked up a problem where the coherence structure should be visible. This problem was a Dirac equation with a time-dependent complex-valued mass profile, motivated by mass-altering CP-violating phase transitions. We proceeded to solve this equation with analytic means, arriving finally at a set of exact mode function solutions for the problem.

The obtained exact solutions were used to construct the Wigner-transformed Wightman function (i.e. the Wigner function) of the problem. This function was used to study the phase space structure of the problem, both in its full glory using numerical techniques and analytically in a certain limit, namely that of a mass changing in time as a step function. Already the analytic study of the Wigner function revealed that the Wightman function exhibits the full cQPA-structure; the phase space consists of solutions related to particles, antiparticles and quantum coherence between them. This step function analysis also suggested that for weakly interacting systems the phase space structure near the mass change may be more complicated than expected. New coherence solutions corresponding to correlations coming from different sides of the mass wall were found to exist. In physical situations these large-scale correlations are of course suppressed by interactions, and this led us to redefine the Wigner function so that it takes into account the mean free path of particles when computing the correlations. It was also noted that these correlations coming from separate sides of the mass wall should be (as they are) absent in the cQPA-formalism, since cQPA is essentially a local approximation.

The numerical analysis was made in light of the information obtained

with the step function correlator. Several plots of the redefined Wigner function with the full exact solutions were produced, and the phase space structure was analyzed for different sets of parameters. The results were in perfect agreement with cQPA, showing a clear coherence structure in the phase space in addition to the ordinary particle- and antiparticle-solutions. The mixed coherence shells, coming from large-scale correlations, were also found to emerge when the interaction strength of the system was taken to be rather weak. These mixture shells exist only in vicinity of the mass wall, and farther away from the wall only the cQPA-structure remains.

The significance of these results lies in the fact that we arrived at them without using any cQPA-techniques. The Wightman functions were constructed out of exact solutions, ruling out all possible ambiguities which could be present in approximative studies of the phase space. This unquestionably affirms that the phase space of quantum systems that are not translation invariant has in general structure besides the traditional particle- and antiparticle-shells, namely that corresponding to quantum coherence. These coherence solutions are entirely absent in standard approaches to non-equilibrium quantum field theory. The coherent quasiparticle approximation provides a comprehensive tool capable of revealing them and studying them with rigorous quantum transport equations.

The main goal of this thesis was to verify the cQPA-structure with the help of the exact solutions. This task was successfully completed, and in addition we found out about the existence of the novel mixing shells, whose nature was also studied and understood. The investigations performed in this thesis leave also room for further studies. An immediate follow-up would be to generalize the analysis from a time-dependent mass profile to a mass depending on one spatial coordinate. This would essentially be a quantum reflection problem, and it would have direct applications in EWBG-scenarios. It would also be interesting to see what kind of a role the mixing large-scale coherences would play in the space-dependent case. Another potential future application would be to seek for possible ways to improve the cQPA-formalism with the help of the exact mode functions.

References

[1] K. A. Olive et al. (Particle Data Group Collaboration), *Review of Particle Physics*, Chinese Physics C **38** (2014) 090001.

[2] A. D. Sakharov, *Violation of CP Invariance, C Asymmetry, and Baryon Asymmetry of the Universe*, Journal of Experimental and Theoretical Physics Letters **5** (1967).

[3] M. D. Schwartz, *Quantum Field Theory and the Standard Model*, Cambridge University Press, New York, 2014.

[4] K. Kajantie, M. Laine, K. Rummukainen and M. Shaposhnikov, *Is There a Hot Electroweak Phase Transition at $m_H \gtrsim m_W$?*, Physical Review Letters **77** (1996).

[5] M. L. Bellac, *Thermal Field Theory*, Cambridge University Press, Cambridge, 2000.

[6] C. Gale and J. I. Kapusta, *Finite-Temperature Field Theory: Principles and Applications*, *2nd Edition*, Cambridge University Press, New York, 2006.

[7] F. C. Khanna, A. P. C. Malbouisson, J. M. C. Malbouisson and A. E. Santana, *Thermal Quantum Field Theory: Algebraic Aspects and Applications*, World Scientific, Singapore, 2009.

[8] J. S. Schwinger, *Brownian Motion of a Quantum Oscillator*, Journal of Mathematical Physics **2**, (1961).

[9] L. V. Keldysh, *Diagram technique for nonequilibrium processes*, Zhurnal Eksperimental'noi i Teoreticheskoi Fiziki **47** (1964).

[10] *The New Encyclopædia Britannica Volume 9: Micropædia, Ready Reference*, *15th Edition*, s.v. "Quasiparticle", Encyclopædia Britannica, Chicago, 2002.

[11] R. D. Mattuck, *A Guide to Feynman Diagrams in the Many-Body Problem*, *2nd Edition*, Dover Publications, New York, 1992.

[12] M. E. Peskin and D. V. Schroeder, *An Introduction to Quantum Field Theory*, Westview Press, 1995.

[13] E. Kaxiras, *Atomic and Electronic Structure of Solids*, Cambridge University Press, Cambridge, 2003.

[14] E. A. Calzetta and A. B. Hu, *Nonequilibrium Quantum Field Theory*, Cambridge University Press, Cambridge, 2008.

[15] M. Herranen, *Quantum Kinetic Theory with Nonlocal Coherence*, Dissertation, University of Jyväskylä, Research Report No. 3/2009, arXiv:0906.3136 [hep-ph].

[16] M. Herranen, K. Kainulainen and P. M. Rahkila, *Towards a kinetic theory for fermions with quantum coherence*, Nuclear Physics B **810** (2008), arXiv:0807.1415 [hep-ph].

[17] M. Herranen, K. Kainulainen and P. M. Rahkila, *Quantum kinetic theory for fermions in temporally varying backgrounds*, Journal of High Energy Physics **0809** (2008), arXiv:0807.1435 [hep-ph].

[18] M. Herranen, K. Kainulainen and P. M. Rahkila, *Kinetic transport theory with quantum coherence*, Nuclear Physics A **820** (2008), arXiv:0811.0936 [hep-ph].

[19] M. Herranen, K. Kainulainen and P. M. Rahkila, *Kinetic theory for scalar fields with nonlocal quantum coherence*, Journal of High Energy Physics **0905** (2008), arXiv:0812.4029 [hep-ph].

[20] M. Herranen, K. Kainulainen and P. M. Rahkila, *Coherent quasiparticle approximation (cQPA) and nonlocal coherence*, Journal of Physics: Conference Series **220** (2009), arXiv:0912.2490 [hep-ph].

[21] M. Herranen, K. Kainulainen and P. M. Rahkila, *Coherent quantum Boltzmann equations from cQPA*, Journal of High Energy Physics **1012** (2010), arXiv:1006.1929 [hep-ph].

[22] M. Herranen, K. Kainulainen and P. M. Rahkila, *Flavour-coherent propagators and Feynman rules: Covariant cQPA formulation*, Journal of High Energy Physics **1202** (2011), arXiv:1108.2371 [hep-ph].

[23] C. Fidler, M. Herranen, K. Kainulainen and P. M. Rahkila, *Flavoured quantum Boltzmann equations from cQPA*, Journal of High Energy Physics **1202** (2011), arXiv:1108.2309 [hep-ph].

[24] G. Baym and L. P. Kadanoff, *Quantum Statistical Mechanics*, W. A. Benjamin, New York, 1962.

[25] T. Prokopec, M. G. Schmidt and S. Weinstock, *Transport equations for chiral fermions to order ħ and electroweak baryogenesis: Part I*, Annals of Physics **314** (2004), arXiv:hep-ph/0312110v2.

[26] T. Prokopec, M. G. Schmidt and J. Weenink, *An exact solution of the Dirac equation with CP violation*, Physical Review D **87** (2013) 083508, arXiv:1301.4132 [hep-th].

[27] A. Ayala, J. Jalilian-Marian, L. McLerran and A. P. Vischer, *Scattering in the presence of the electroweak phase transition bubble walls*, Physical Review D **49** (1994), arXiv:hep-ph/9311296.

[28] K. Funakubo, A. Kakuto, S. Otsuki, K. Takenaga and F. Toyoda, *Fermion scattering off a CP-violating electroweak bubble wall*, Physical Review D **50** (1994), arXiv:hep-ph/9402204.

[29] I. S. Gradshteyn and I. M. Ryzhik, *Table of Integrals, Series, and Products*, 7^{th} *Edition*, Academic Press, San Diego, 2007.

[30] G. B. Arfken and H. J. Weber, *Mathematical Methods for Physicists*, 6^{th} *Edition*, Academic Press, San Diego, 2005.

[31] The Wolfram Functions Site, *functions.wolfram.com/*, visited November 26, 2015.

Appendix A Conventions

Throughout the thesis we will be using natural units, in which

$$c = \hbar = 1.$$

A space-time four-vector will in general be denoted as

$$x = (t, \vec{x}) = (x_0, \vec{x})$$

and the four-momentum similarly

$$k = (k_0, \vec{k}).$$

Deviations from these notation should be clear from the context. For example for the average coordinate appearing in the Wigner transformation we write $X = (T, \vec{X})$. The space-time metric is chosen to be the one often used in particle physics:

$$g_{\mu\nu} = g^{\mu\nu} = \mathrm{diag}(1, -1, -1, -1).$$

The Dirac gamma matrices will be represented in the chiral (Weyl) basis, in which

$$\gamma^0 = \begin{bmatrix} 0 & \mathbb{1} \\ \mathbb{1} & 0 \end{bmatrix} = \sigma^1 \otimes \mathbb{1}, \quad \gamma^i = \begin{bmatrix} 0 & \sigma^i \\ -\mathrm{i}\sigma^i & 0 \end{bmatrix} = \mathrm{i}\sigma^2 \otimes \sigma^i$$

where i runs from 1 to 3 and σ^i are the Pauli sigma matrices. The fifth gamma matrix is defined as

$$\gamma^5 \doteq \mathrm{i}\gamma^0\gamma^1\gamma^2\gamma^3.$$

Appendix B Constant mass solutions

In this appendix we consider solutions for the Dirac equation (29) in the limit of constant mass. We also use these solutions to derive another expression for the normalization of the mode functions.

For simplicity we will only consider the particle spinor μ_h. This will be sufficient to determine the normalization, since we choose our initial state to consist only of a particle solution, whereas the late-time solution will be a mixture of particle- and antiparticle-solutions. The equations for the mode functions appearing in μ_h are

$$\begin{cases} \mathrm{i}\partial_t \eta_h + h\left|\vec{k}\right|\eta_h = m\zeta_h & \text{(97a)} \\ \mathrm{i}\partial_t \zeta_h - h\left|\vec{k}\right|\zeta_h = m^*\eta_h. & \text{(97b)} \end{cases}$$

In the limit of a constant mass our solutions can be written in terms of plane waves, $\mu_h(t,\vec{k}) \sim u_h(k)\mathrm{e}^{-\mathrm{i}k\cdot x}$, and therefore equations (97) reduce to

$$\begin{cases} k_0\eta_h + h\left|\vec{k}\right|\eta_h = m\zeta_h & \text{(98a)} \\ k_0\zeta_h - h\left|\vec{k}\right|\zeta_h = m^*\eta_h. & \text{(98b)} \end{cases}$$

These are just the basic component equations of the Dirac equation in the chiral basis with the exception of a complex mass. Solving the above equations with positive energy $k_0 = E > 0$ gives us a spinor solution

$$\mu_h(t,\vec{k}) = \begin{bmatrix} \eta_h(t,\vec{k}) \\ \zeta_h(t,\vec{k}) \end{bmatrix} \otimes \xi_h(\vec{k}) = \left\{ N \begin{bmatrix} \sqrt{E - h\left|\vec{k}\right|} \\ \sqrt{E + h\left|\vec{k}\right|}\mathrm{e}^{-\mathrm{i}\theta} \end{bmatrix} \otimes \xi_h(\vec{k}) \right\} \mathrm{e}^{-\mathrm{i}k\cdot x}, \tag{99}$$

where N is a normalization constant and θ is the phase of the mass. We will choose the constant mass to correspond to that of the early-time particle-solution deep in the unbroken phase in the case with varying mass. This accounts to (cf. equation (50))

$$\theta = \arctan\left(\frac{m_{1\mathrm{I}}}{m_{1\mathrm{R}} + m_{2\mathrm{R}}}\right).$$

To fulfil the normalization condition (32) we set

$$N = \frac{1}{\sqrt{2E}}.$$

Note that this also normalizes accordingly the full spinor ψ to unity, since we have not included the usual factor of $(2E)^{-1/2}$ in the expansion (30).

Let us now use solution (99) to normalize the solutions of the problem with a time-dependent mass. We start with the mode functions from equation (59a)

$$\phi_{\pm h} = D_{\pm h} z^{\alpha} (1-z)^{\beta} \times {}_2F_1(a_{\pm}, b_{\pm}, c; z),$$

which at early times reduce to the positive frequency solution:

$$\phi_{\pm h} \xrightarrow{t \to -\infty} D_{\pm h}\, \mathrm{e}^{-\mathrm{i}t\omega_-}.$$

Then we require that at early times the mode function is normalized to the constant mass solution. Together with equations (37a) and (99) this gives us the relation

$$D_{\pm h} = \frac{1}{2}\left(\sqrt{1 - \frac{h|\vec{k}|}{\omega_-}} \pm \sqrt{1 + \frac{h|\vec{k}|}{\omega_-}}\, \mathrm{e}^{-\mathrm{i}\theta} \right), \tag{100}$$

where we have identified the energy E of the incoming particle as the early-time limit ω_- of the varying energy. Even though at first sight these normalization constants look rather different from the ones presented in equations (77) and (78), they should nevertheless correspond to each other. One can verify this quite easily by first writing

$$\mathrm{e}^{-\mathrm{i}\theta} = \sqrt{\frac{m_{1\mathrm{R}} + m_{2\mathrm{R}} - \mathrm{i}m_{1\mathrm{I}}}{m_{1\mathrm{R}} + m_{2\mathrm{R}} + \mathrm{i}m_{1\mathrm{I}}}}$$

with the use of the logarithmic form of the arctan-function, and then computing the ratios C_+/C_- and D_+/D_-. These ratios are found to be inverses of each other, which guarantees that the normalizations are essentially the same indeed.